Lyα Blobs

and the relationship with AGN and sub-mm sources

Toru Yamada (Tohoku University)

Lyα Blobs

Large Extended Lyα Emitters

radio quiet

d~30-150kpc, L~10+42-44 erg/s, δv ~ 500-2000 km/s

Size defined by

- isophotal area in Lyα emission
- half-light radius / FWHM

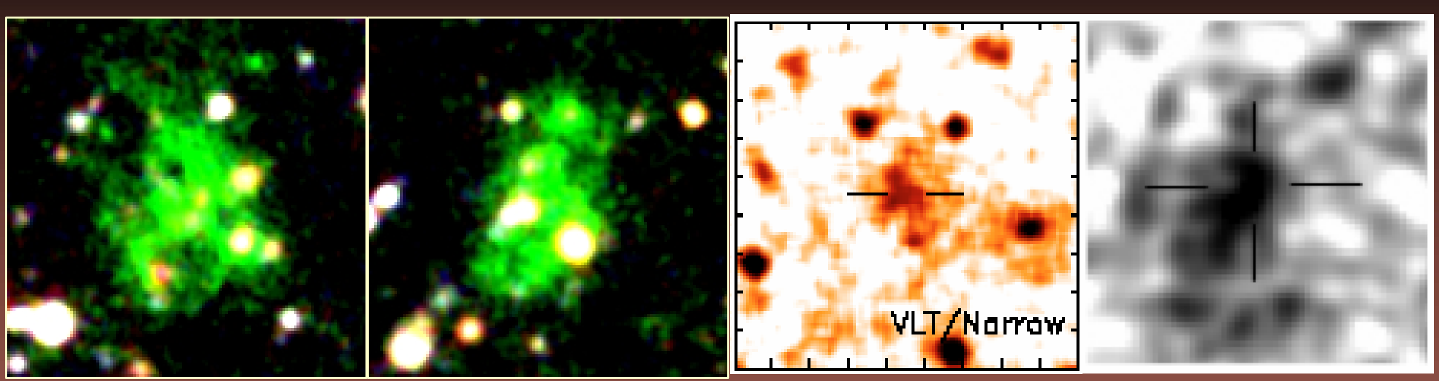

References see below

High-Redshift Lyα Haloes

Lyα Halo assoc. w/

Powerful Radio Galaxies

- Typically ~30-150kpc, log L(LyA)~44 erg/s
- a good fraction (~30%) size > 100 kpc
- alignment effects / jet-activity related ?

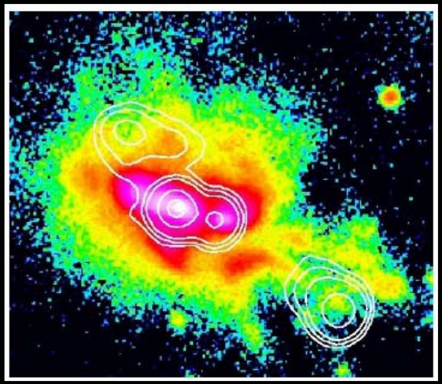

4C41.17
z=3.8
from van Breugel+ 2006

McCarthy 1993 ARAA for earlier results
Van Ojik et al. 1997
Venemans et al. 2007

Radio-Loud Quasars

-Typically ~50-100 kpc, logL=44-45 erg/s
- radio-jet related? / ~PRG halos ?
- dense environment?

Heckman et al. 1991
Hu et al. 1991
Lehnelt and Becker 1998

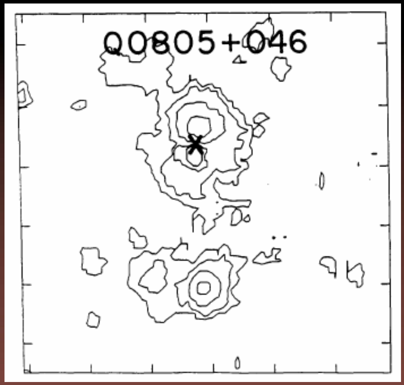

Weidinger et al. 2004
Christensen et al. 2006

Radio-Quiet Quasars

-Typically ~10-50 kpc
-logL~43-44 erg/s < RLQs

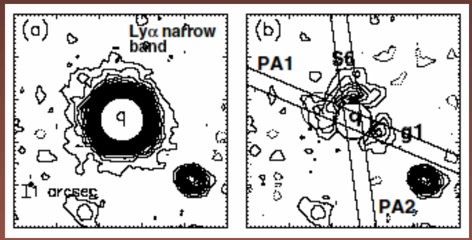

High-Redshift Lyα Halo

Lyα Halos assoc. w/

Sub-mm Galaxies

(overlap with Lyα Blobs, PRGs)

Ivison et al. 1998
Greve et al. 2007
Geach et al. 2006

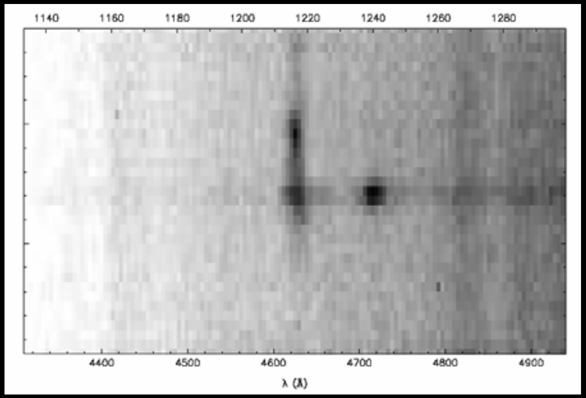

Lyman-Break Galaxies

Hayashino et al. 2005

Motivation to Search/Study Lyα Blobs

Gaseous Environment of High-Redshift Galaxies

- Gas Bounded in Collapsed Halo
- Infall / Accretion
- Ourflow [SNe / AGN feedback]

Gas Bounded in Collapsed Halo

- Size ➔ Lower limit of their Mass
  (assuming spherical collapse model)

$$M_{vir} = 4/3\pi R_{vir}^3 \rho_{crit}(z)\, \Delta_c(z) > 4\times10^{10} (R_{Ly\alpha} / 25\mathrm{kpc})^3 M_{sun}$$

(at z~3)

- Size, Velocity width ➔ Dynamical Mass

$$M_{dyn} = R\,\Box(\Delta V)^2 / G$$
$$\sim 5\times10^{11} (R_{Ly\alpha} / 25\mathrm{kpc})(\Delta V / 300\ \mathrm{km/s})^2 M_{sun}$$

Cooling Accretion in Collapsing Halo

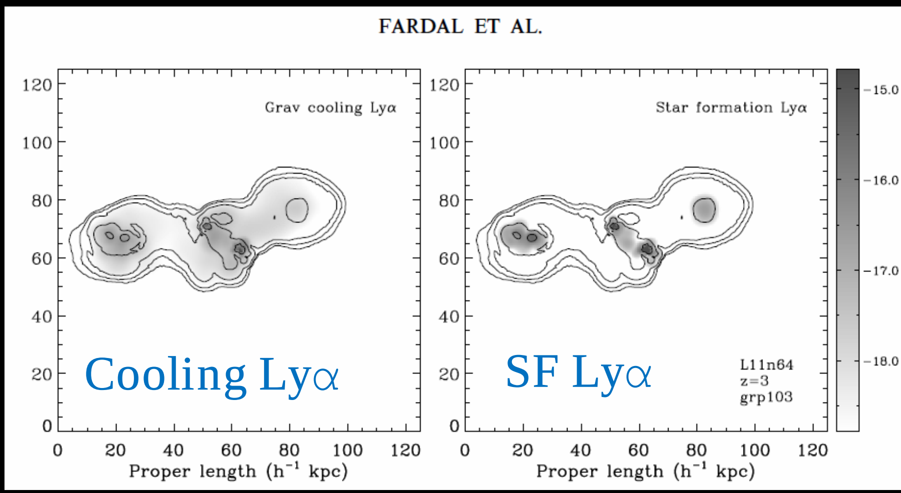

Simulation by Fardel et al. 2001

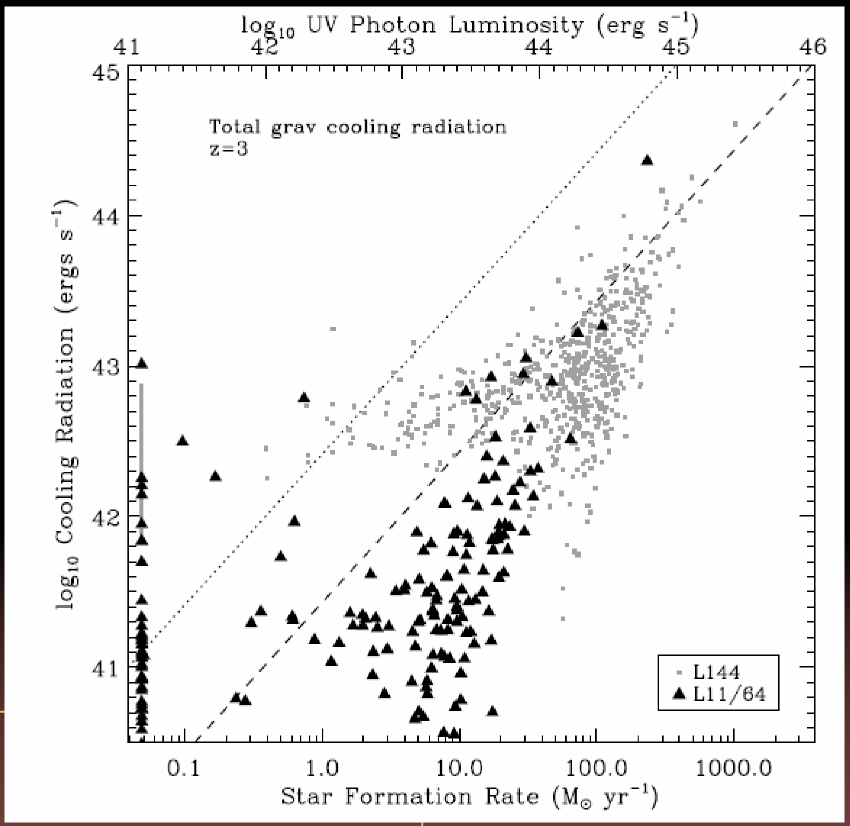

Gas heated by virial shock
in the collapsing halos
cools and accretes radiating Lyα emission

Cold Gas Infall

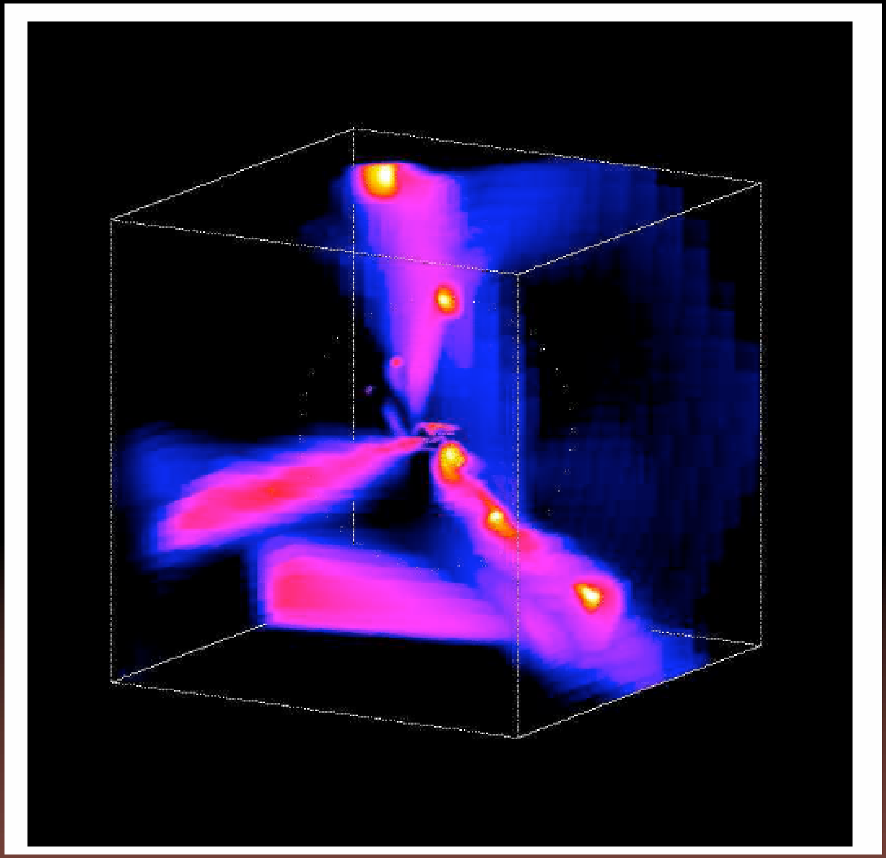

“radial flux of the cold gas stream”
Dekel et al. 2009

320kpc

Cold gas stream penetrating hot halo of massive forming galaxies which results in SF

T~0.01-0.1 Tvir

Keres et al. 2004, 2009

Galactic Superwind

Taniguchi and Shioya (2000)

$$r_{\rm shell} \sim 110 L_{\rm mech,43}^{1/5} n_{\rm H,-5}^{-1/5} t_8^{3/5} \ \ {\rm kpc},$$

$$v_{\rm shell} \sim 650 L_{\rm mech,43}^{1/5} n_{\rm H,-5}^{-1/5} t_8^{-2/5} {\rm km\ s^{-1}},$$

$$L_{\rm mech} \sim \eta \ E_{\rm SN} \ N_{\rm SN}/t_{\rm GW} \sim 10^{43} \ {\rm erg\ s^{-1}}$$

For massive starburst

$$n_{\rm LAB} \simeq 3.4 \times 10^{-5} h^3 \ {\rm Mpc^{-3}}.$$

Galactic Superwinds

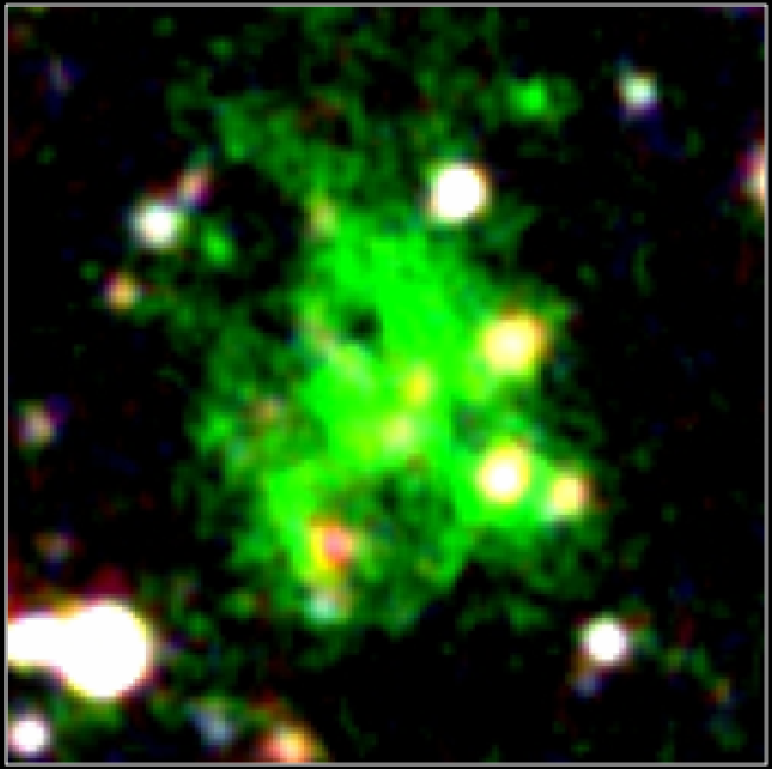

SSA22 Steidel's Blob1 z=3.1
Subaru Suprime Cam Image
(Matsuda et al. 2004)

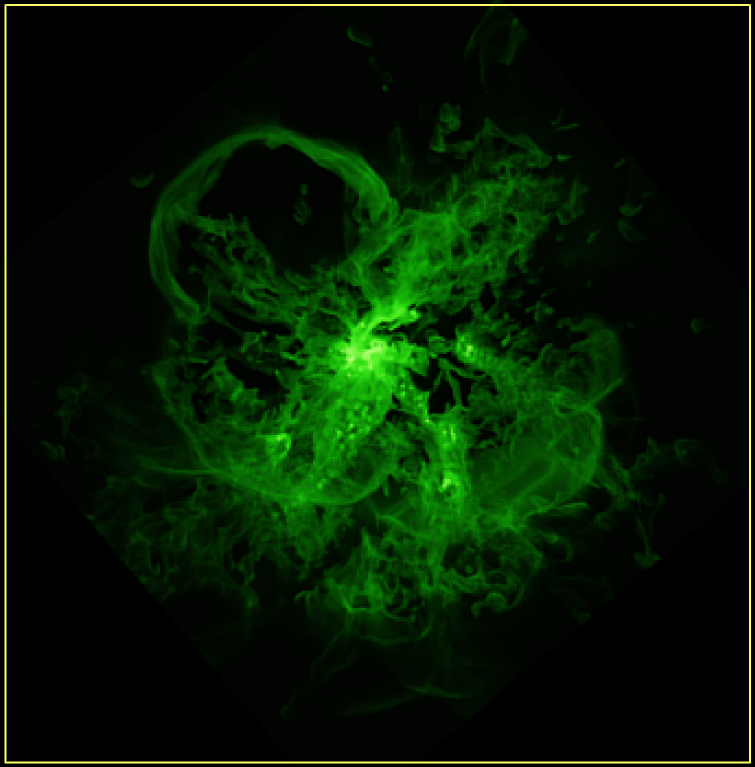

Mori and Umemura 2006
Simulation
SNe shock heating

AGN feedback/outflow

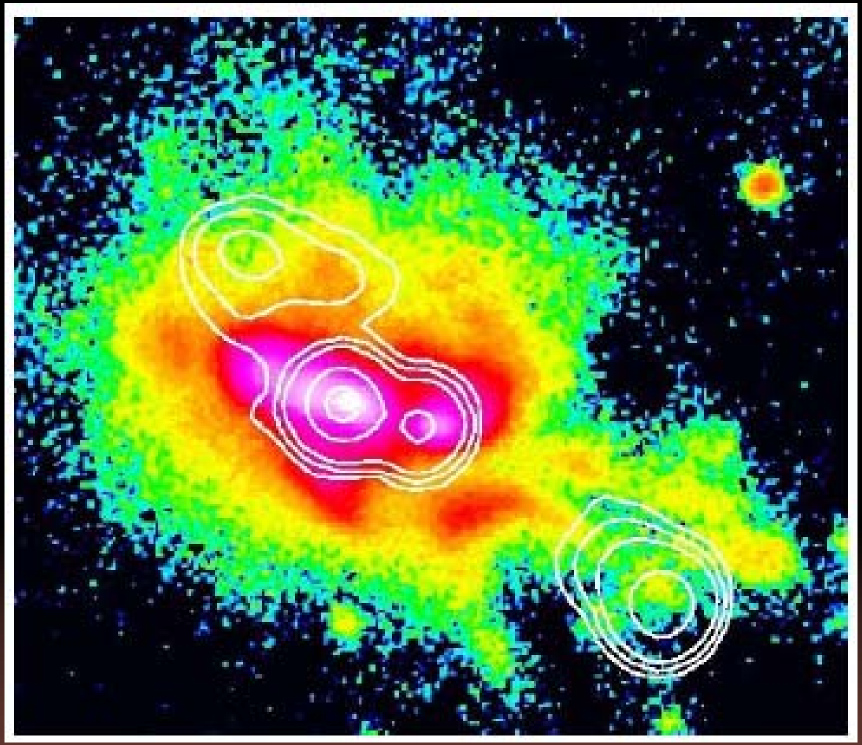

"AGN feedback"

Ciotti and Ostriker 1997,2007,2009
Silk and Rees 1998, Fabian 1999
Wythe and Loeb 2005
Hopkins et al. 2006 ......etc., etc.

AGN activity heats ISM

Radio Jet

Gas Motions: Can you tell Inflow/Outflow?

Dijkstra et al. 2006
Infalling gas clouds

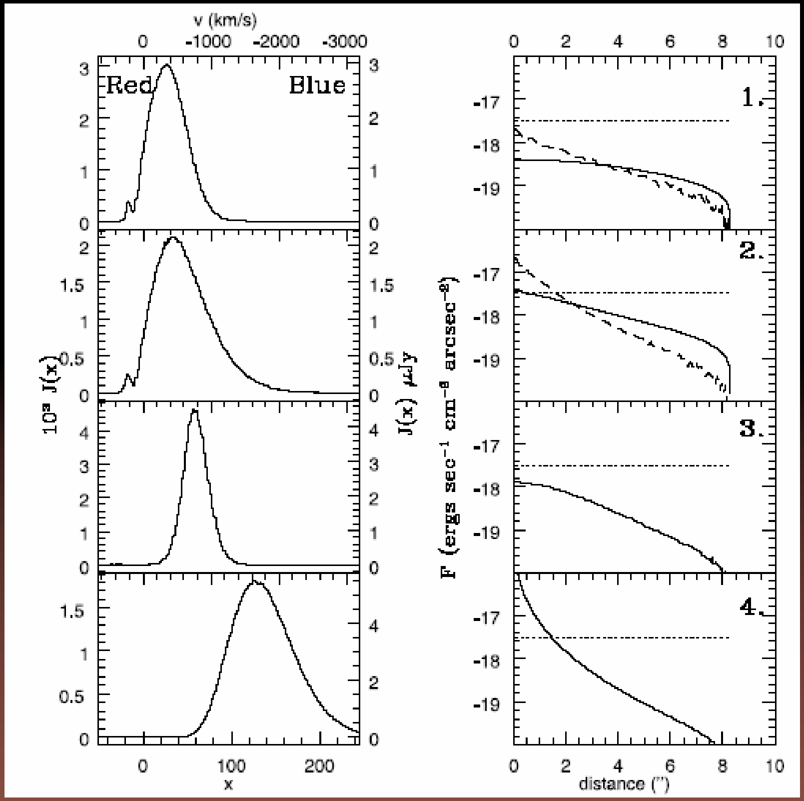

Verhamme et al. 2008
Expanding shell for LBG/LAE

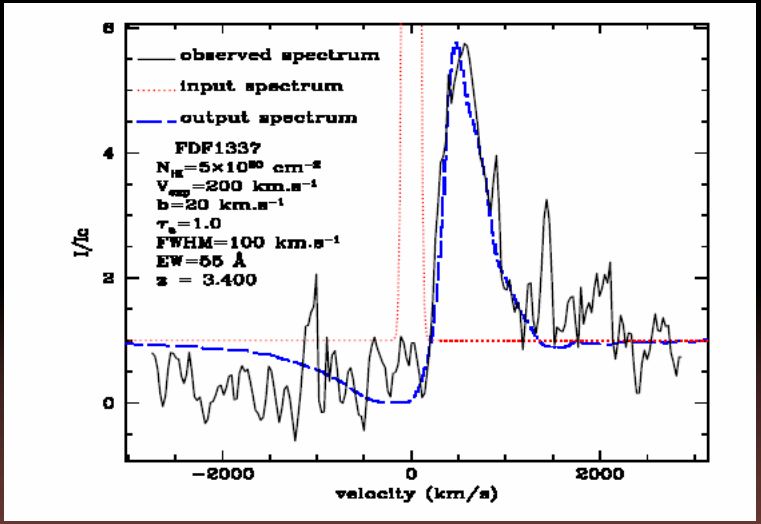

Gas Motion, Scattering, Observed Profiles

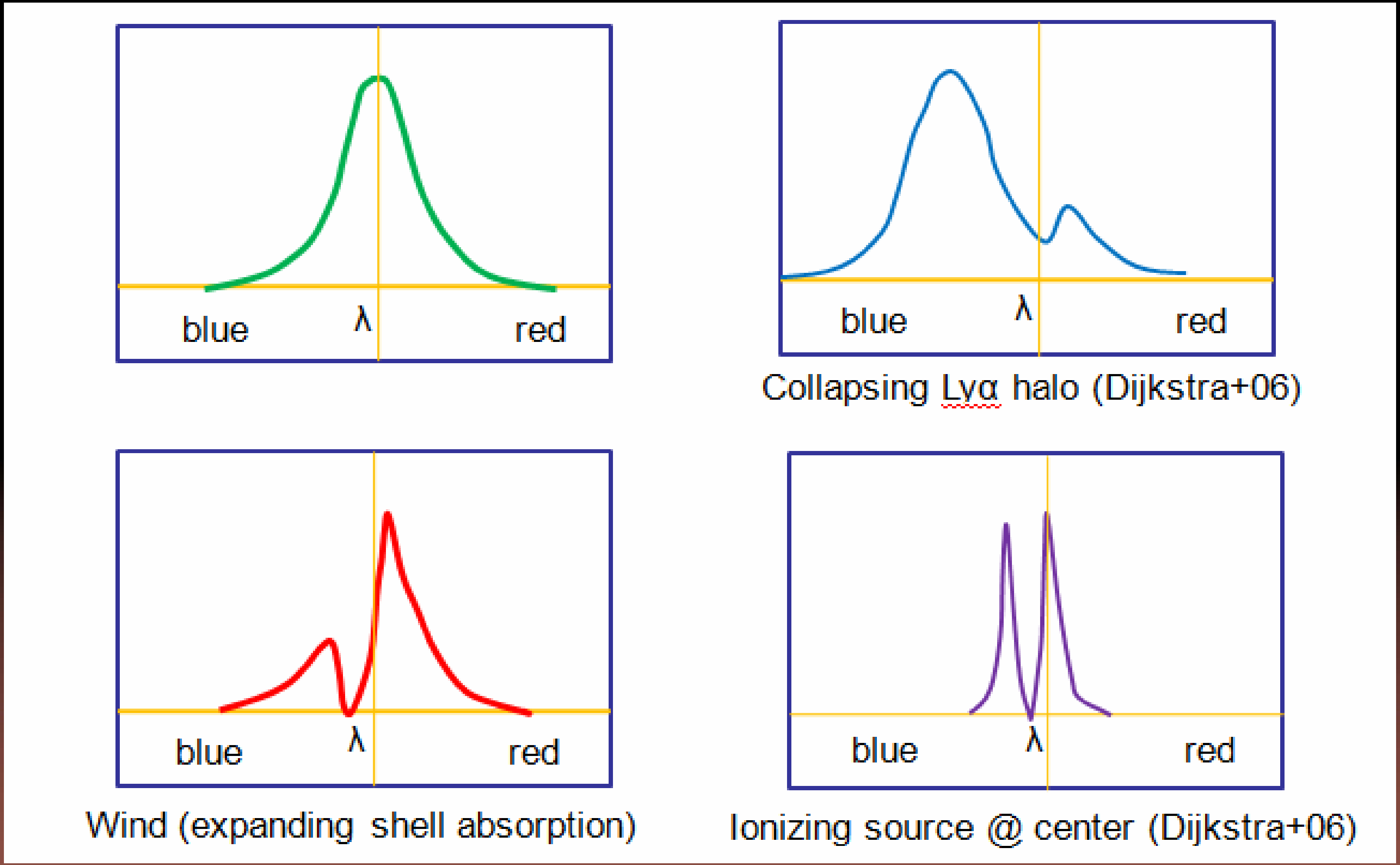

1. Observations
Of
Lyα Blobs

Prototypical Gigantic Lyα Blobs

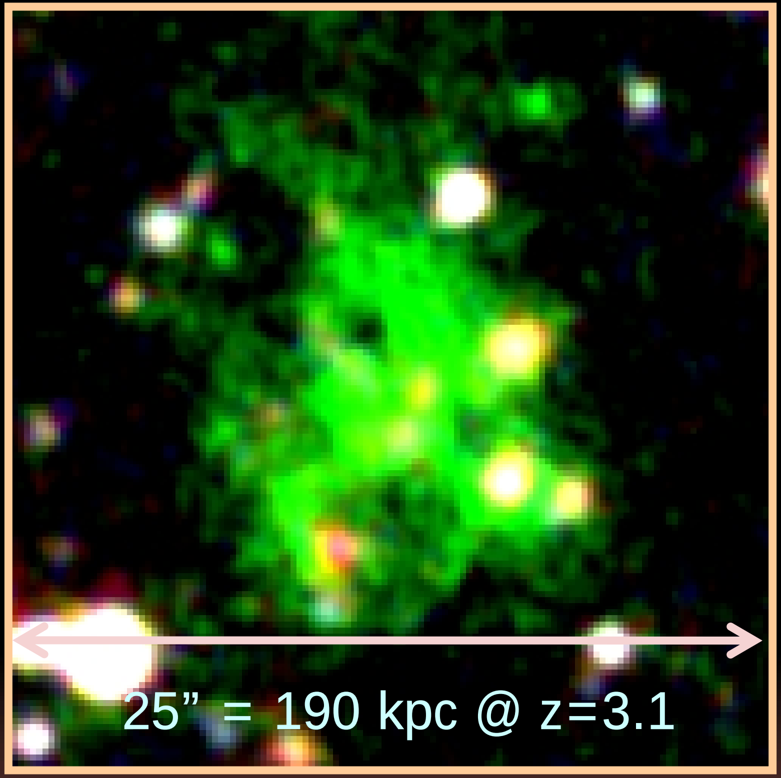

Steidel et al. 2000 SSA22 Blob1

Sub-mm source reported, not recovered
X-ray source is NOT detected

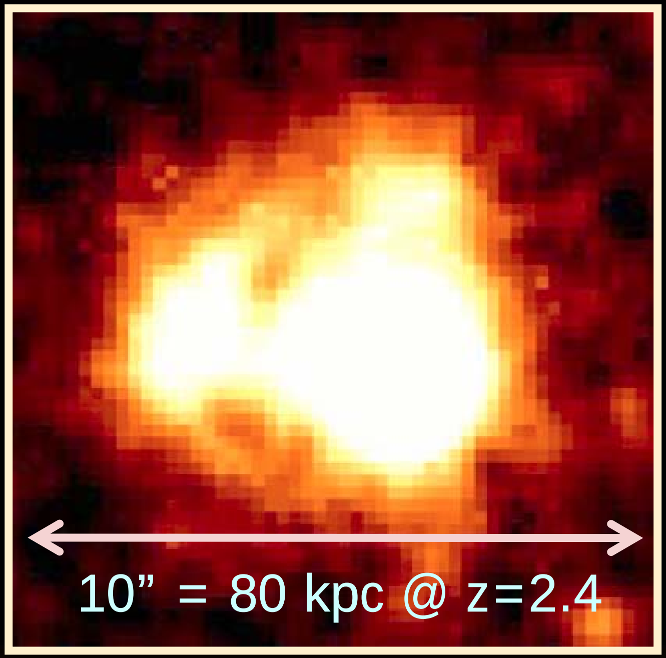

Keel et al. 1999 53W002 field No.18

SCUBA Sub-mm Source
X-ray AGN, obscured
(narrow-line, low excitation)

Both Subaru Images (Matsuda+04, Nakamura+0905)

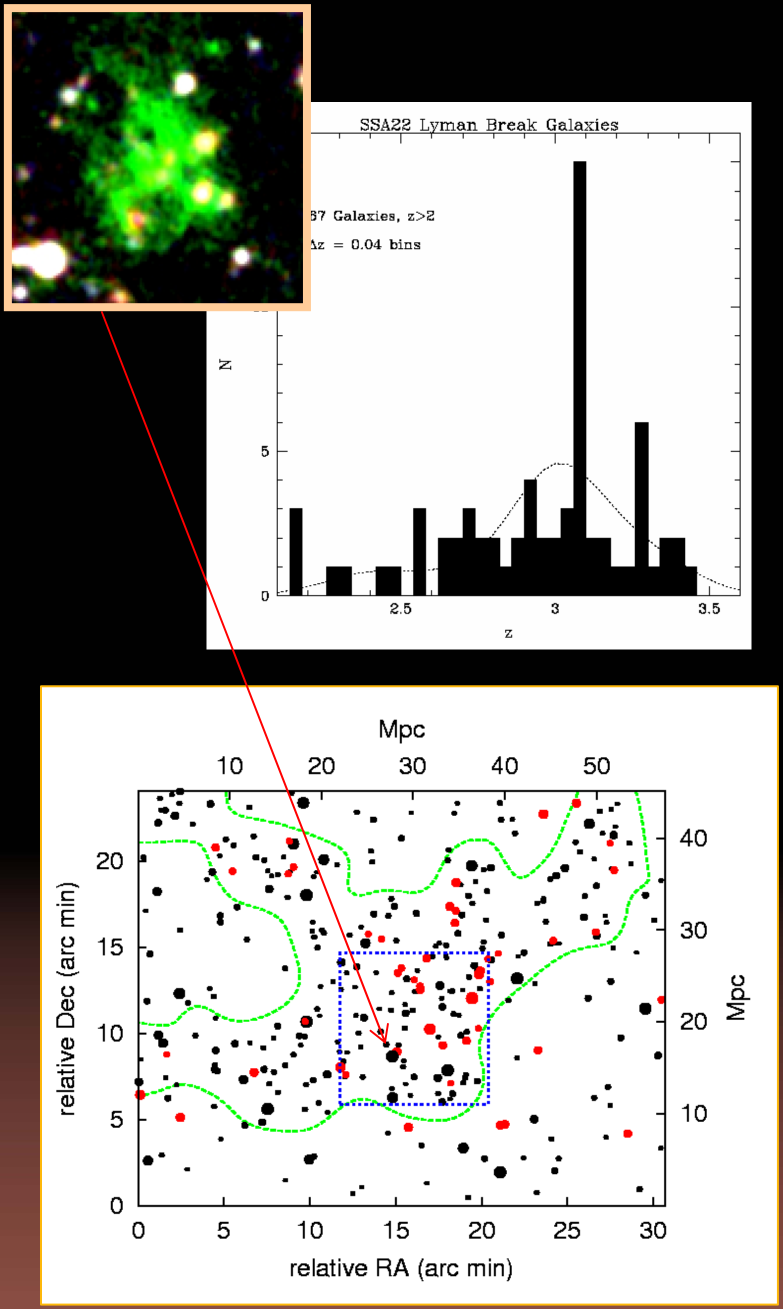

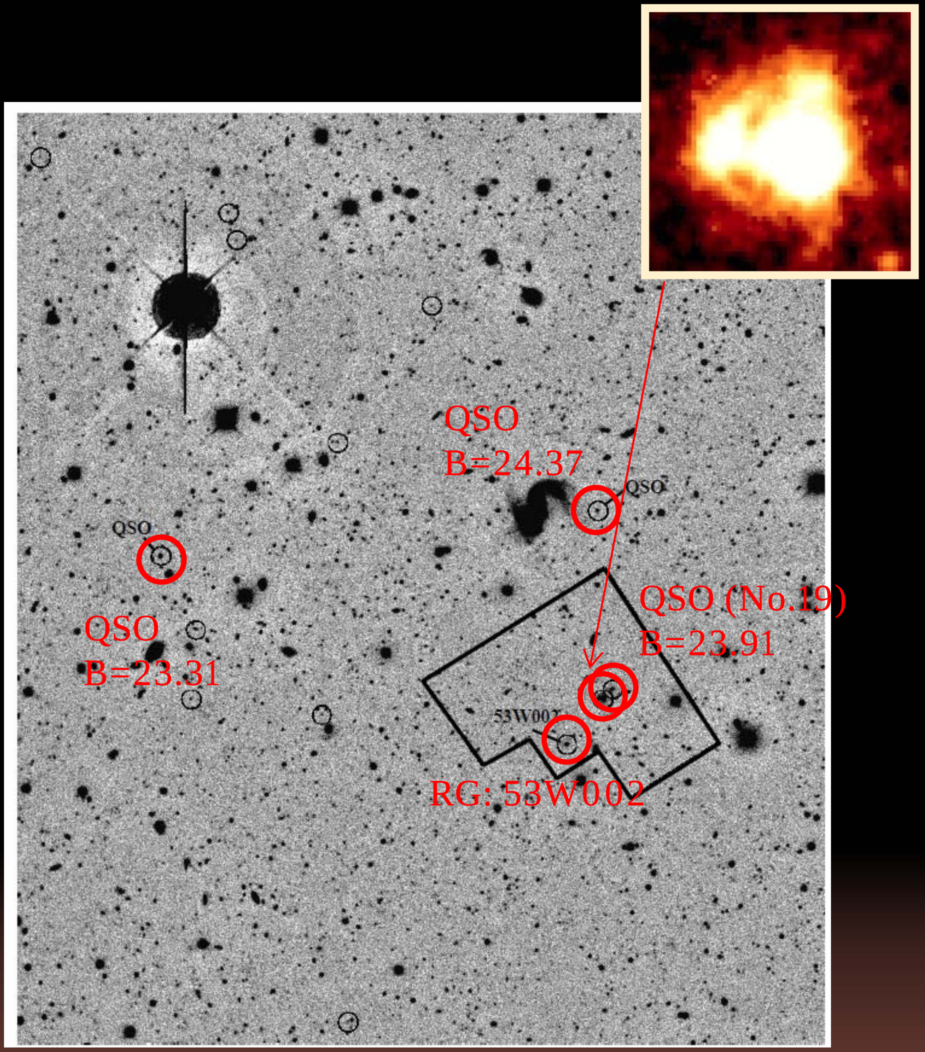

53W002 ‘AGN cluster’ @ z=2.39

SSA22 Proto-cluster / superstructure @ z=3.09

Matsuda-Blobs z=3.1 >30kpc

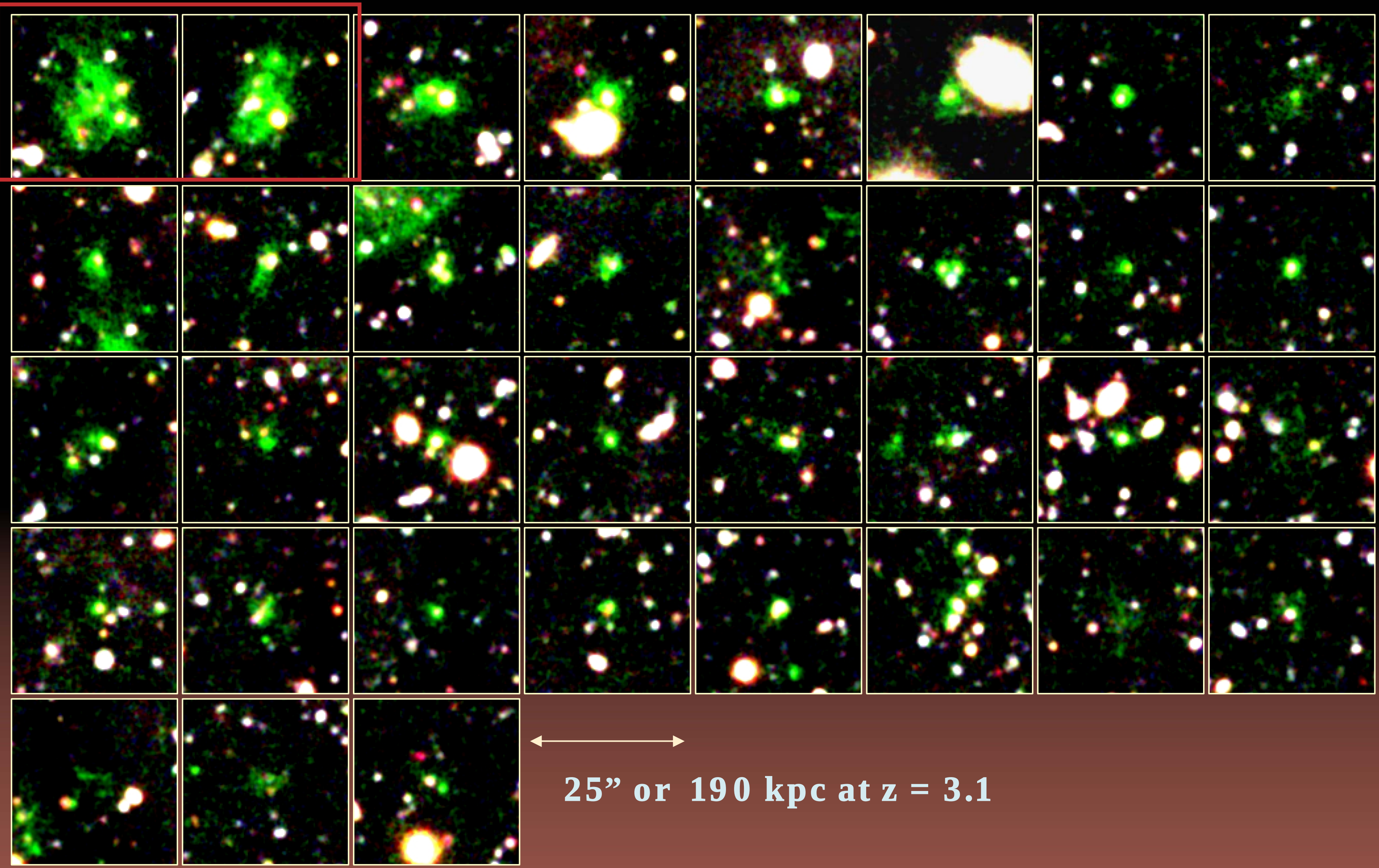

25” or 190 kpc at z = 3.1

Known LABs (>20kpc, by 'their' definition, radio quiet)

references	z	N	Size * (kpc)	L(LyA) (erg/s)
Keel et al. 1999	2.39	1	100	1.e44
Steidel et al. 2000	3.09	2	150	1.e44
Matsuda et al. 2004	3.09	33	30-120	1.e43-44
Palnus et al. 2004	2.38	4	~50	1.e43-44
Dey et al. 2005	2.66	1	160	1.7e44
Nilsson et al. 2006	3.16	1	60	1.e43
Smith et al. 2007	2.83	1	95	2.1e44
Saito et al. 2008	3.7	1+	70	
Yang et al. 2009	2.3	4	30-50	1.e43-44
Matsuda et al.	3.09	76	30-70	1.e43-44
Ouchi et al. 2009	6.6	1	20	4.e43
Prescott et al. 2009	1.69	1	45	4.e43
Smith et al. 2008	2.83	17	20-100	1.e43-44
Ivison et al. 1998	2.8	1	~100	
Greve et al. 2007	2.67	1	110	

‘Detection’ of Lyα Blobs by isophotal area

Z=3.1 Matsuda et al. 2004
SB threshold ~ 2 x 10^{-18} erg/s/cm^2

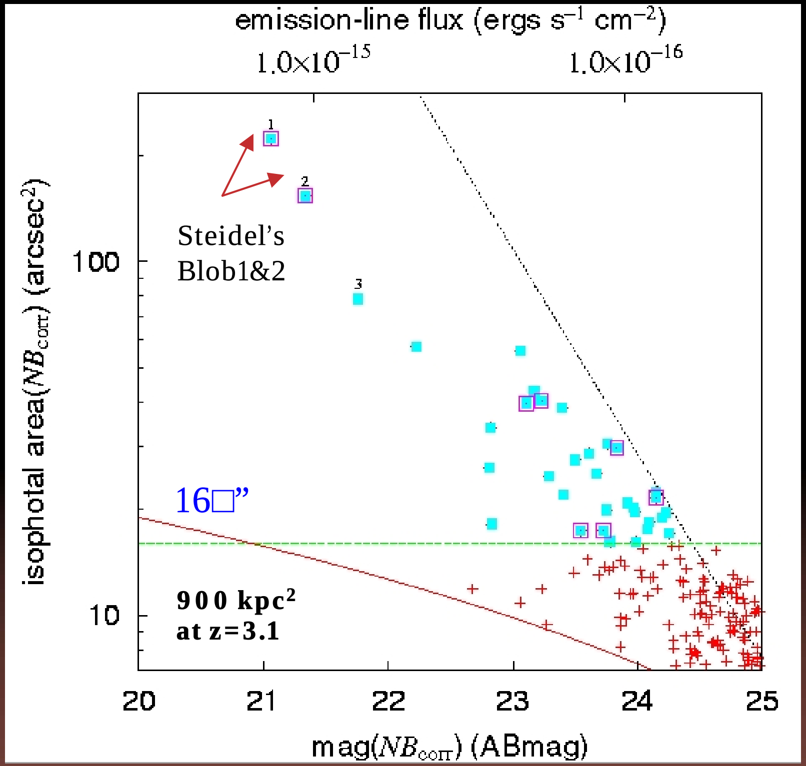

Z=2.3 Yang et al. 2009
SB threshold ~ 5 x 10^{-18} erg/s/cm^2

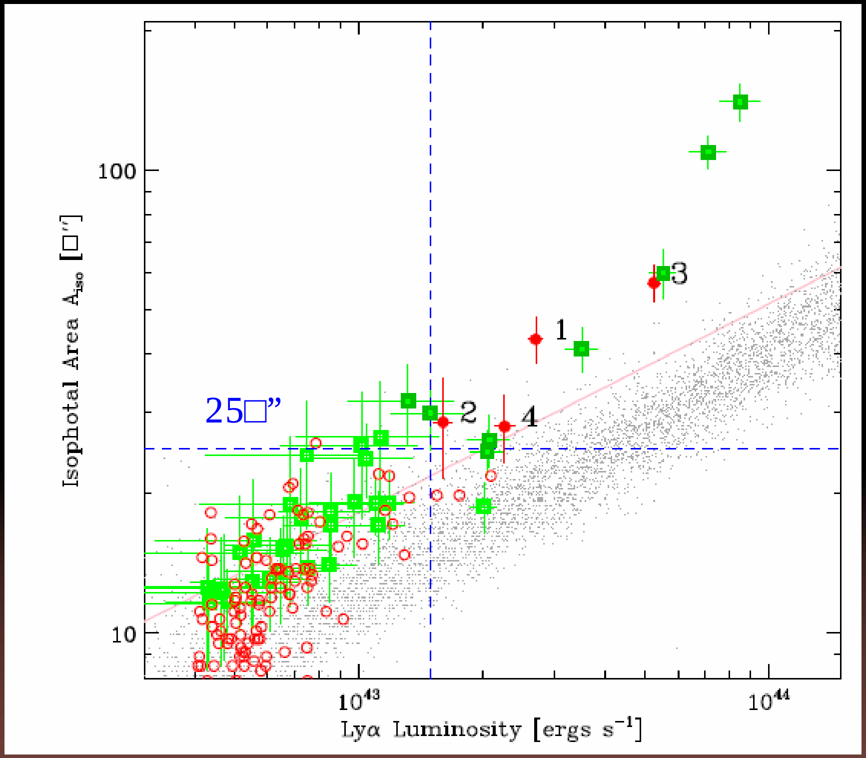

~ NOT (very much) discrete population from other Lyα Emitters in Size, Luminosity, SB, but the LARGEST, more LUMINOUS

Number Density

Yang et al. 2009

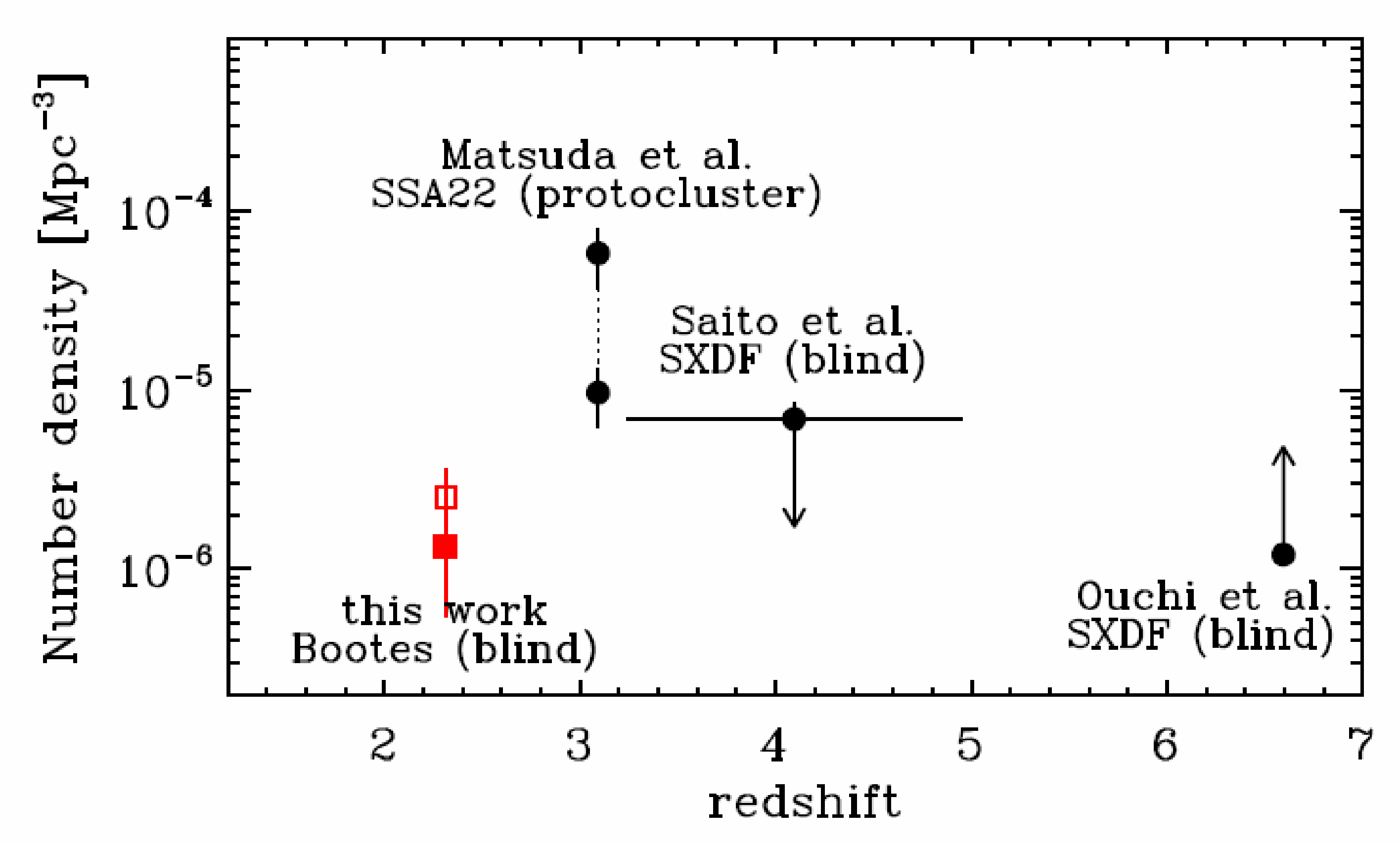

Rare, ~ 10^{-5} – 10^{-6} / Mpc^3

Clustering

Lyα Blobs preferentially observed in the high-density regions

Lyα Blobs themselves are strongly clustered population

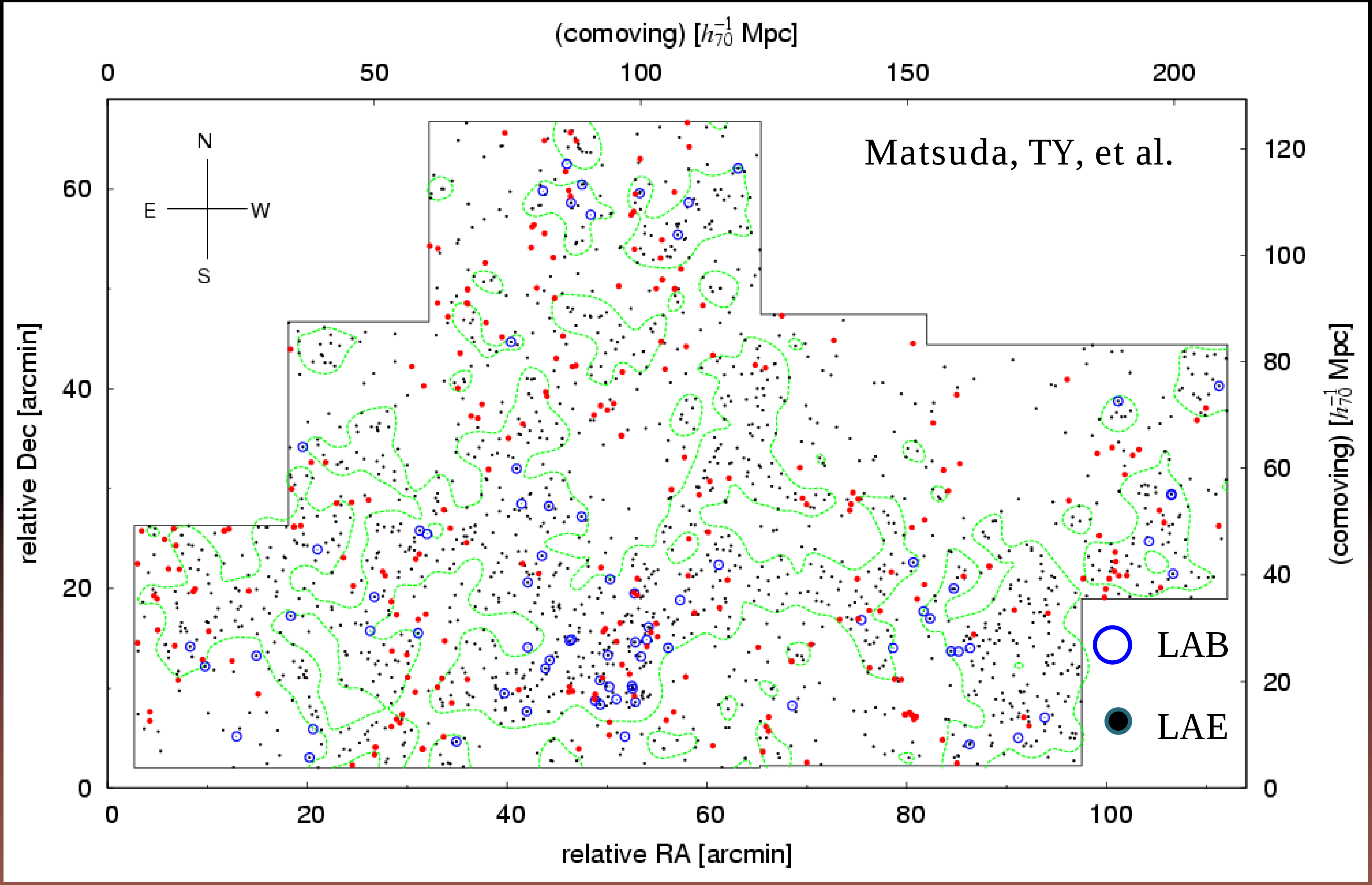

Large gas motion Δv~500-2000km/s

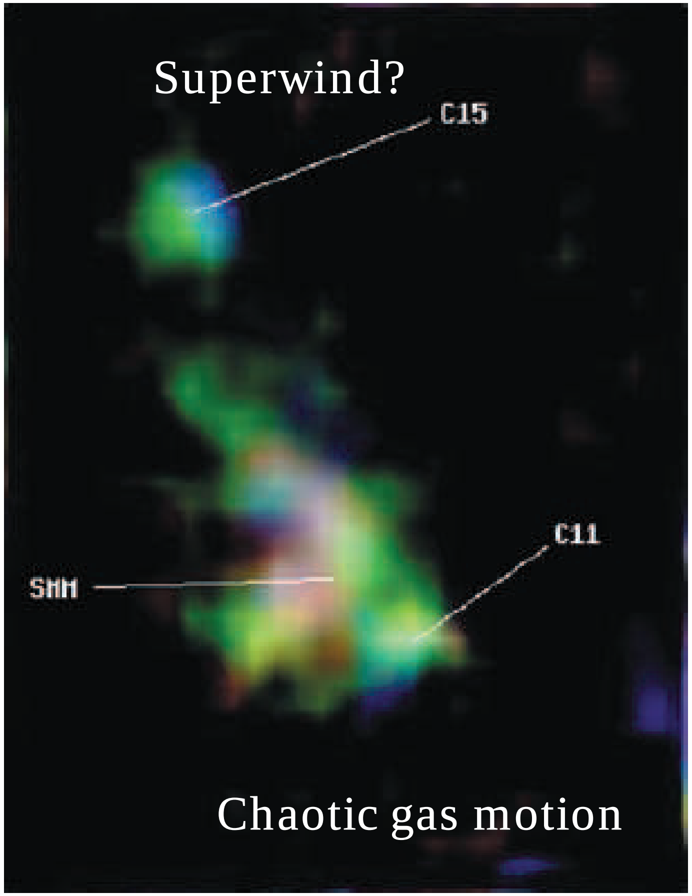

Bower et al. 2004 SAURON

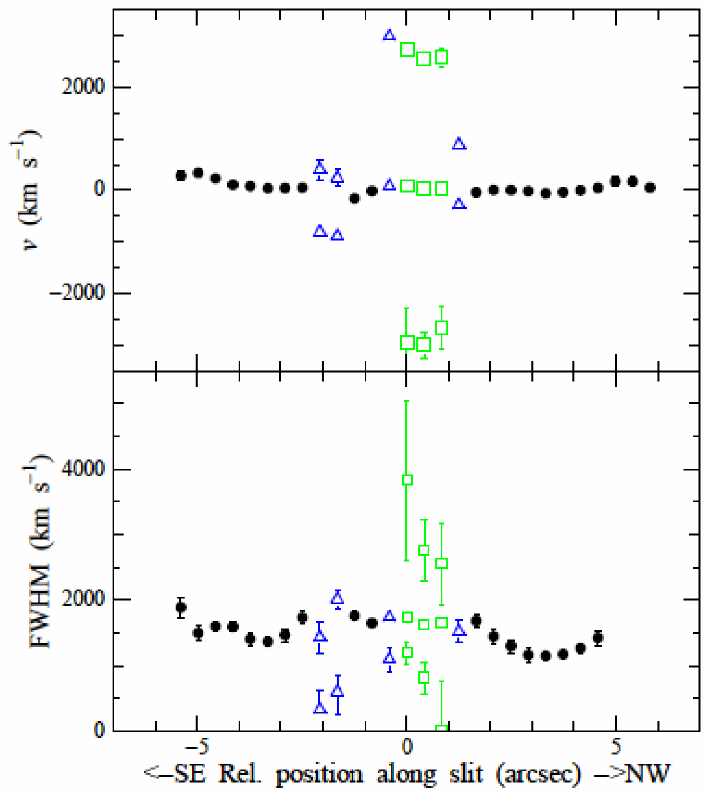

Fig. 4.— The spatial variations of the peak velocities of the Lyα nebula (upper panel) and the FWHMs corrected for the instrumental resolution (lower panel). Data for the triple-peaked regions and the double-peaked regions are shown by open squares and open triangles, respectively. Those for the single-peaked regions are shown by filled circles. Measurement errors are shown by vertical bars.

Ohyama et al. 2003 longslit FOCAS

Giant expanding shell?

SSA22 z=3.1 Blob2 Wilman et al.

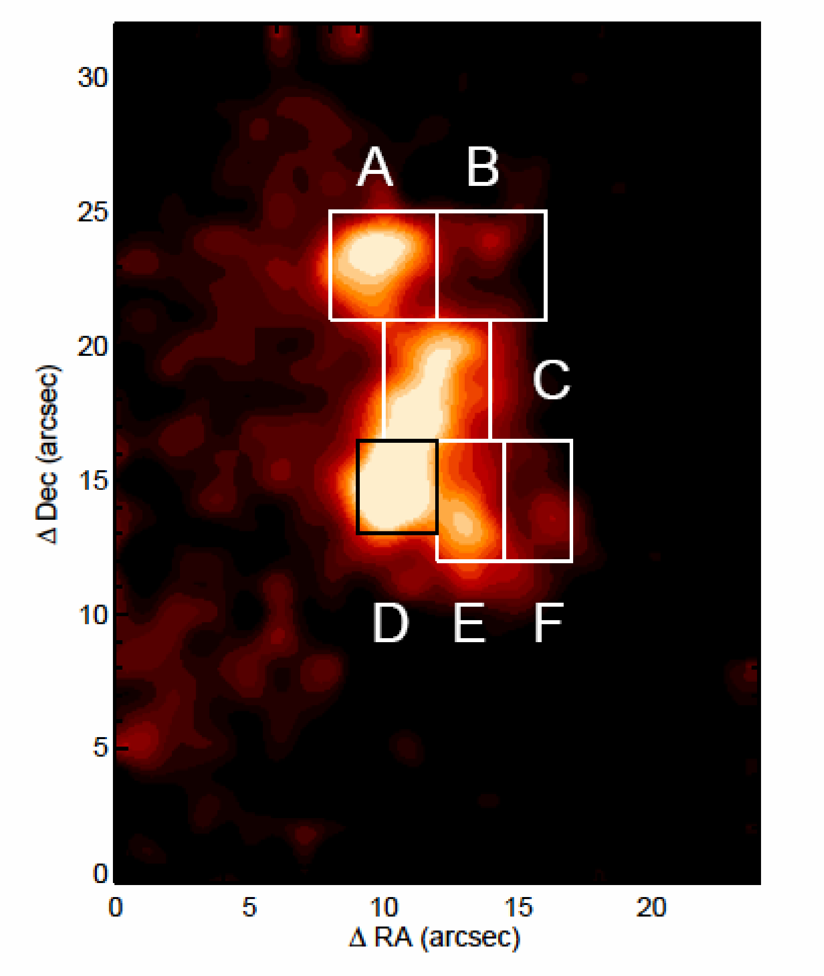

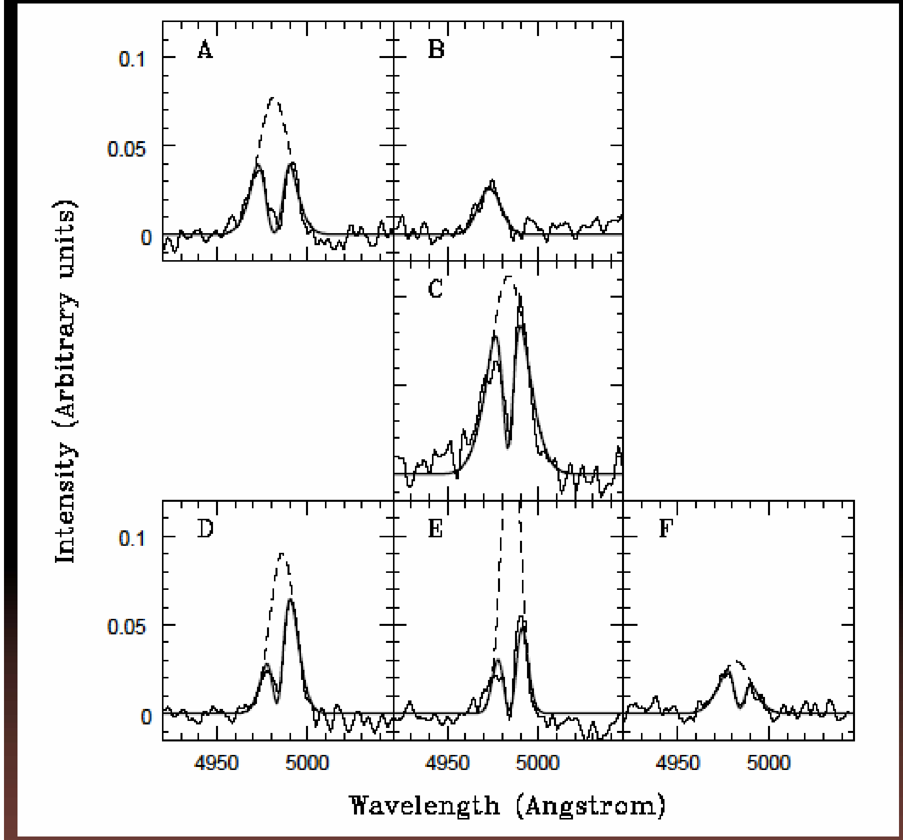

Δv~1000 km/s

Abs➔ HI expanding shell?

Lyα Profiles of Lyα Emitters

Matsuda et al. 2006

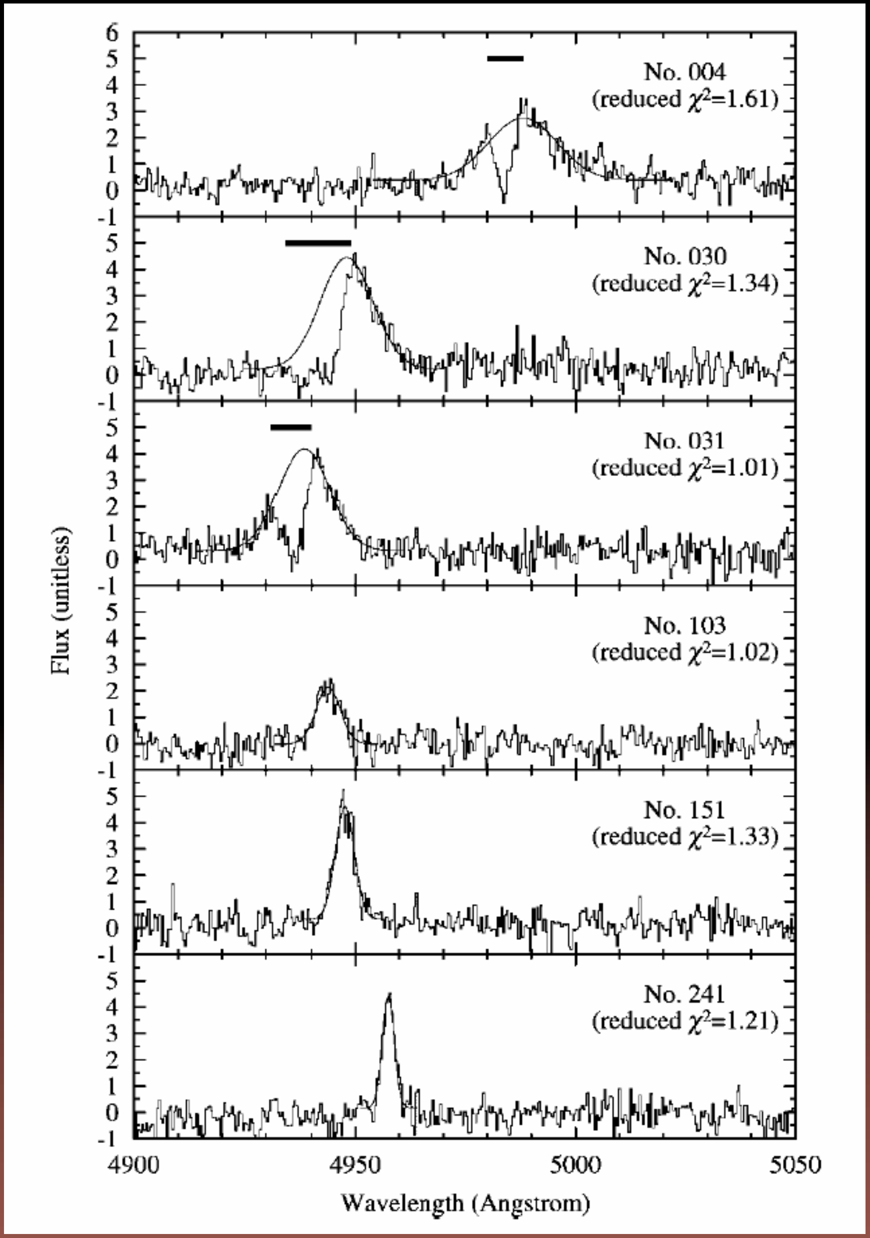

Lyα Blobs (SSA22 z=3.1)

More compact
Lyα Emitters

Line Width

Matsuda, TY, et al. 2006

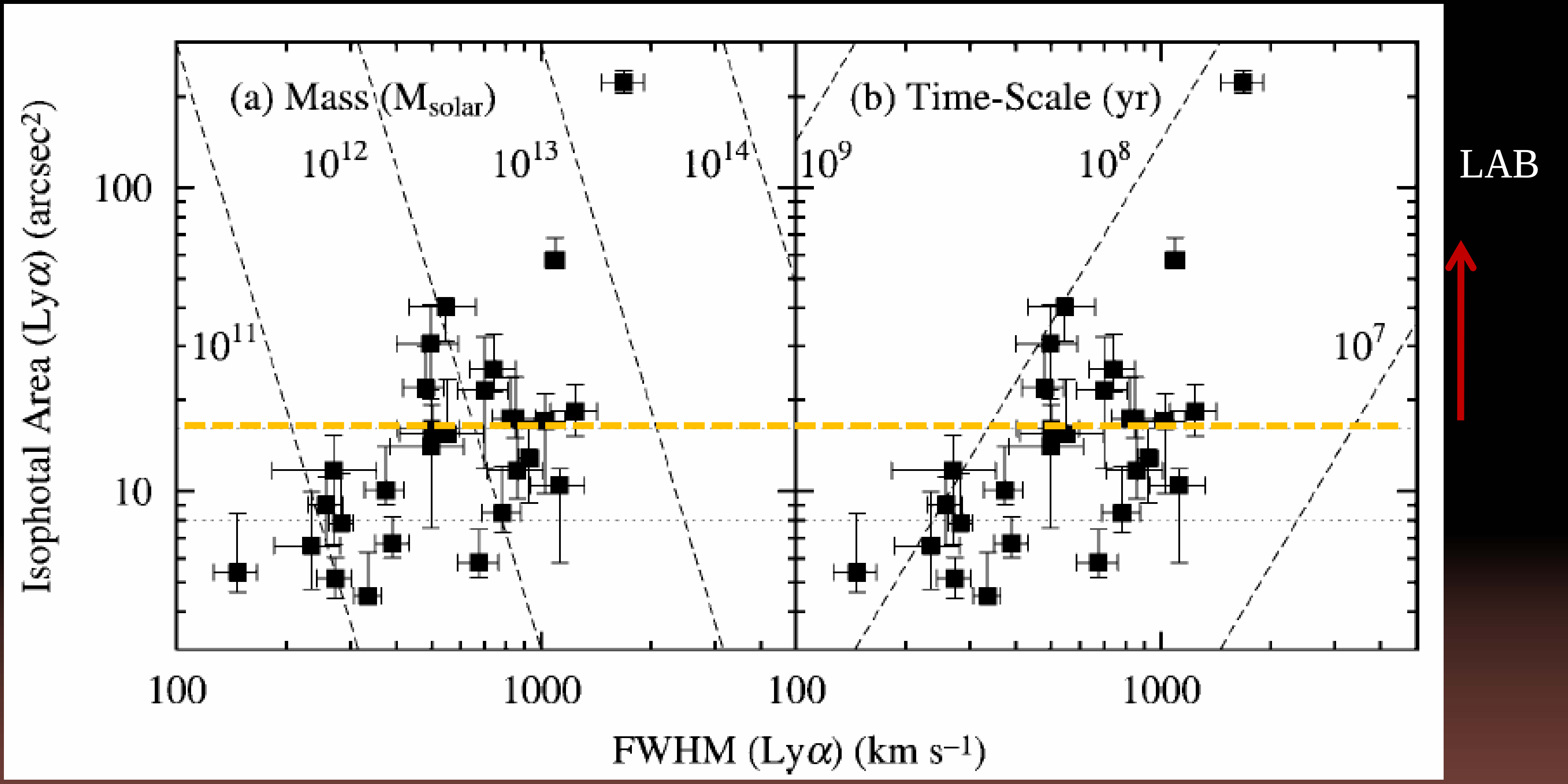

$M_{dyn} \sim 3\sigma^2 R/G$

If superwind;
SF time scale (age) ~ 2*r / σ

Stellar Mass

DRGs **LBGs**

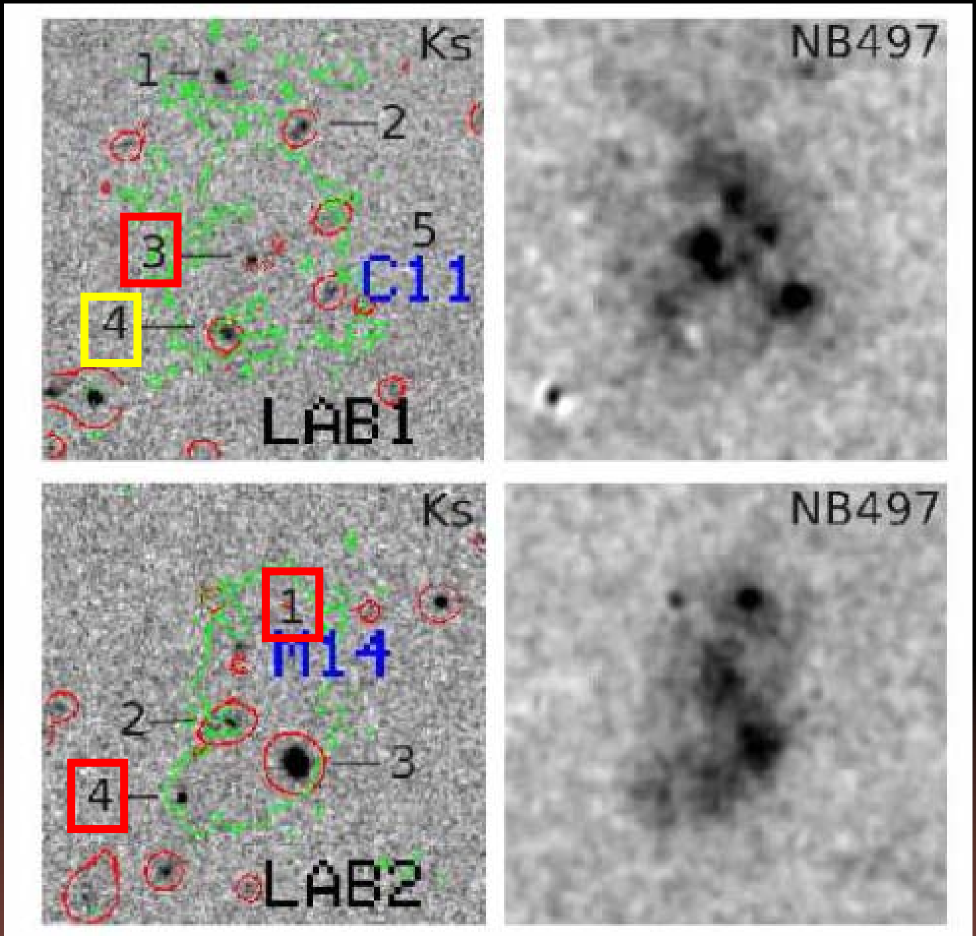

MOIRCS Ks

Uchimoto, TY, et al. 2008

60% of the counterparts of LAB are LBG with R<25.5 (Matsuda, TY, et al. 2004)

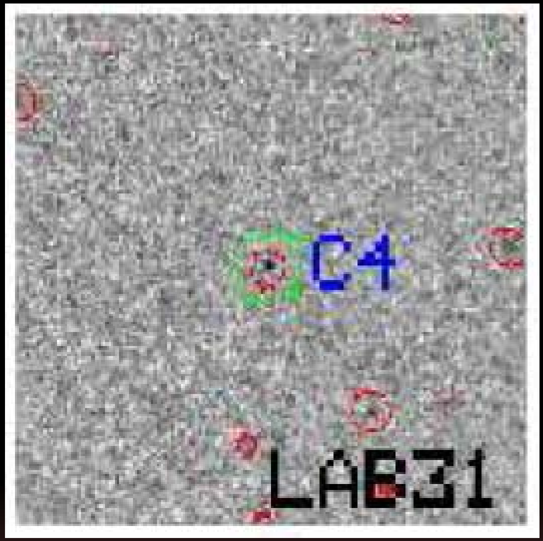

MOIRCS Ks

Stellar Mass of (Plausible) the Galaxy Counterparts of LABs

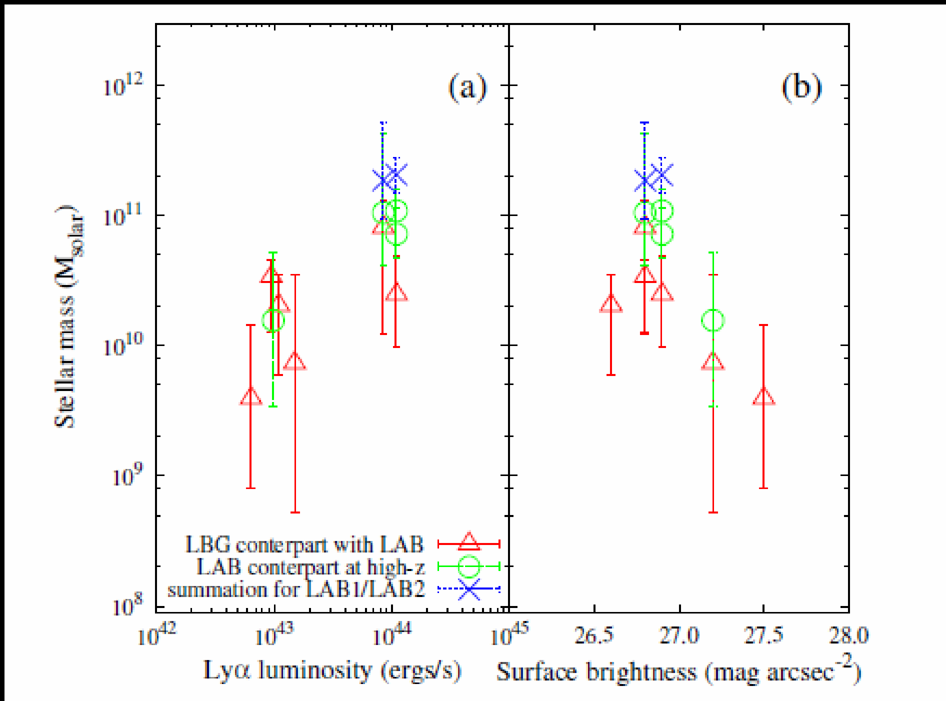

Uchimoto, TY, + 2008

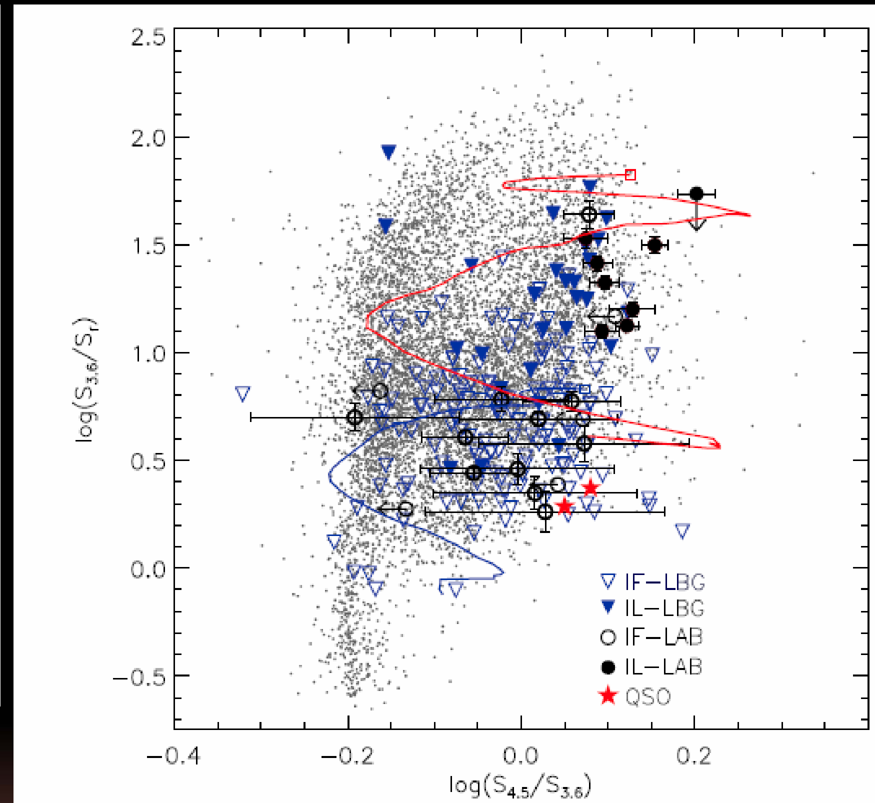

Webb, TY, et al. 2009

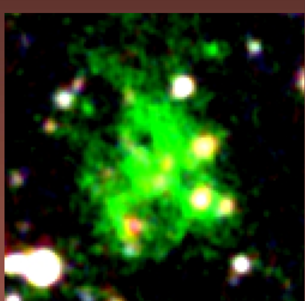

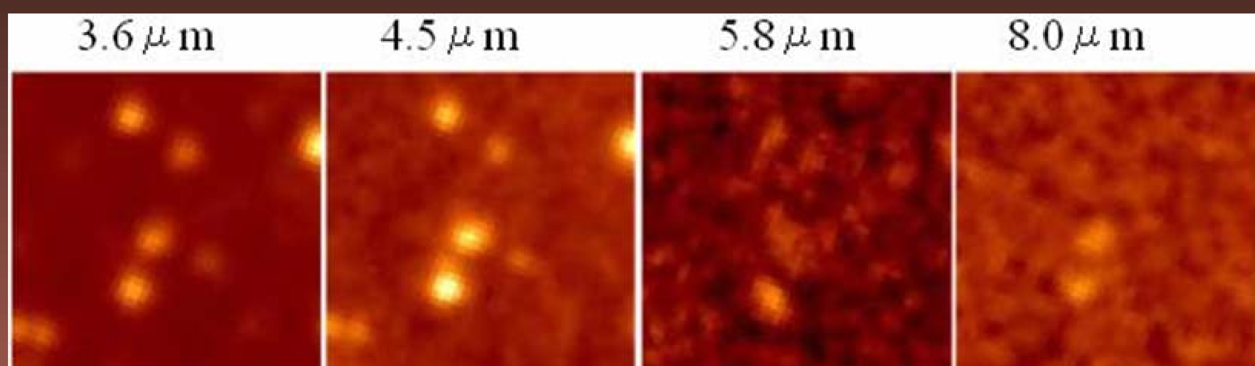

Size, Velocity width, Stellar mass, clustering

→ Lyα Blobs are associated with massive objects

$\sim 10^{11}$-10^{12} M_{sun}

FYI,

Appendix: Lyα Blobs ZOO

A Lyα Blob at z=6.6

Ouchi et al. 2009

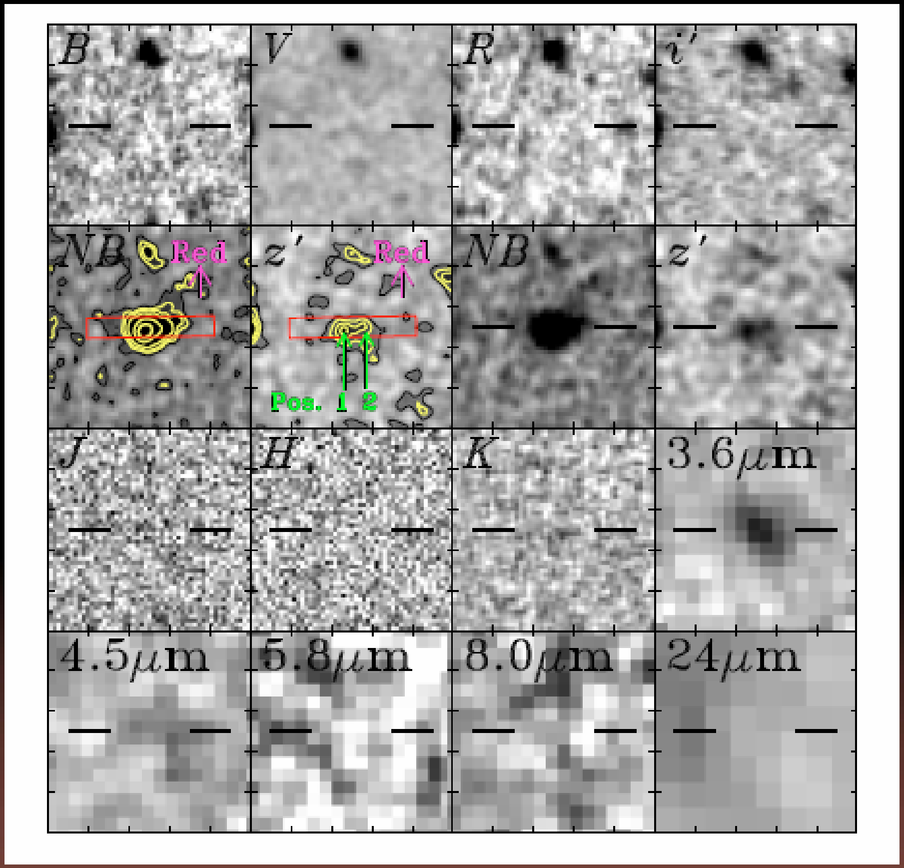

D~ 20kpc

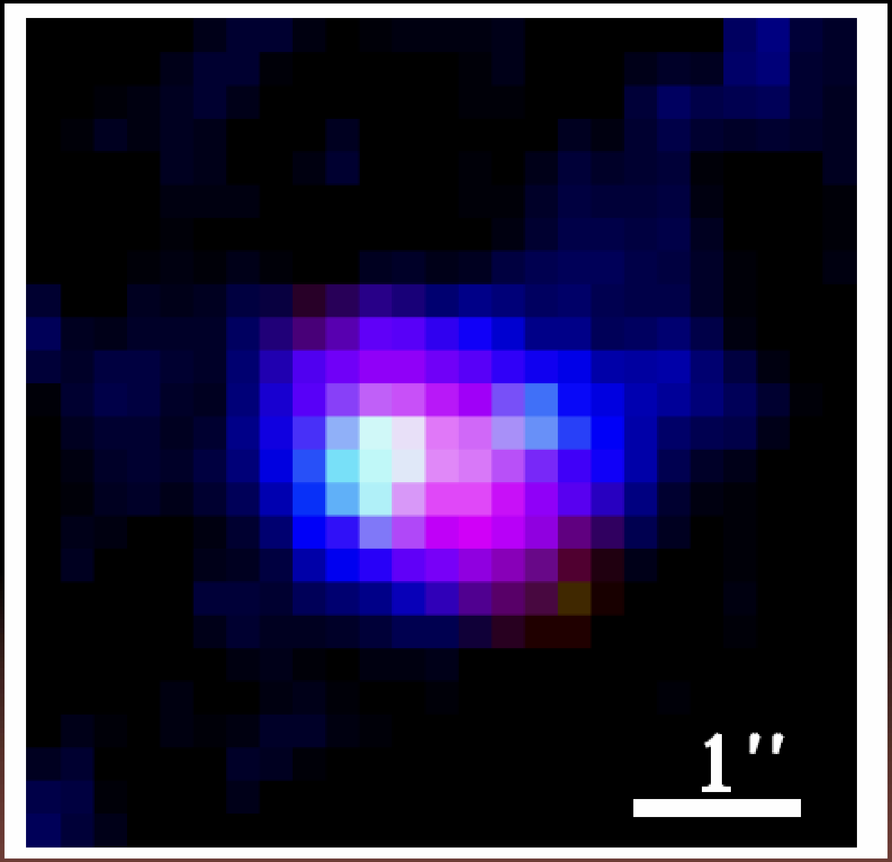

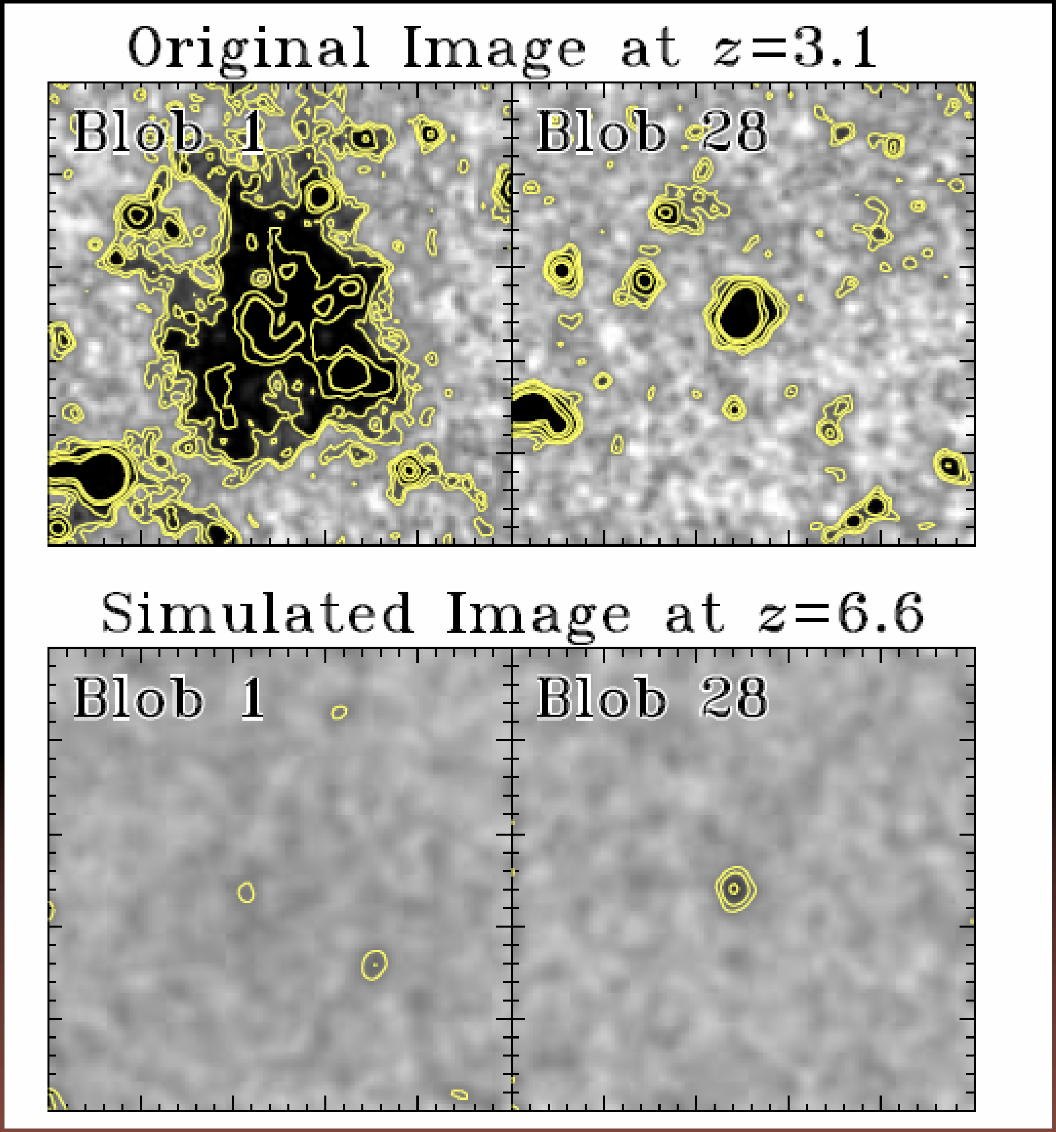
Original Image at z=3.1
Blob 1
Blob 28
Simulated Image at z=6.6
Blob 1
Blob 28

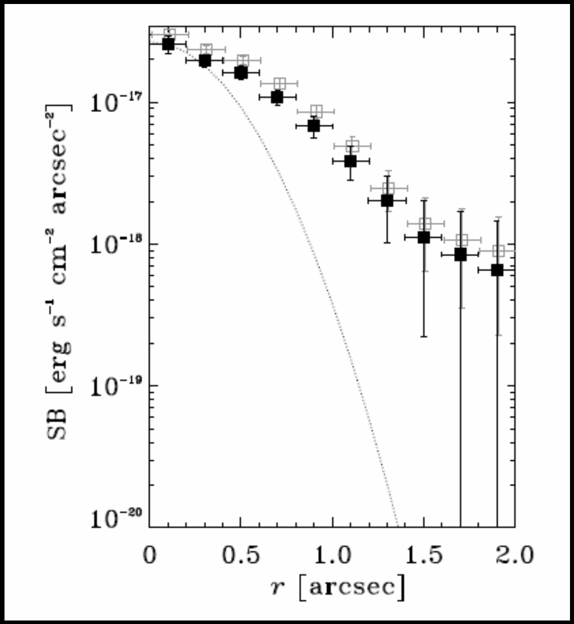
SB [erg s⁻¹ cm⁻² arcsec⁻²]
10⁻¹⁷
10⁻¹⁸
10⁻¹⁹
10⁻²⁰
0
0.5
1.0
1.5
2.0
r [arcsec]

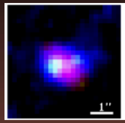
1"

Origins of the Extended LyA Emission

(what powers LABs?)

- Galactic Superwinds / AGN feedback

- Photoionization

  by (hidden) massive stars

  by (hidden) AGN

- Cooling Collapse

  (LyA radiation from the gas heated in the collapse of DM haloes)

signatures of ‘cooing collapse’?

- Large EW
  No counterpart in any other wavelength
  Nilsson et al. 2006
- Relatively flat surface-brightness distribution
  Dijkstra et al. 2006 Nilsson et al. 2006, Smith et al. 2008
- Red sharp cut off in profile
  Dijkstra et al. 2006 Smith et al. 2008
- Diffuse HeII (for hot, T~10^5 gas) ? Yang et al. 2006

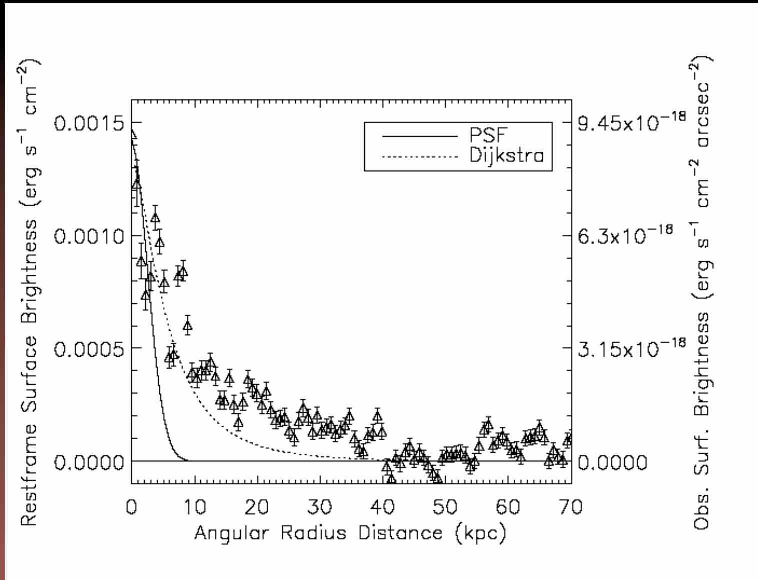

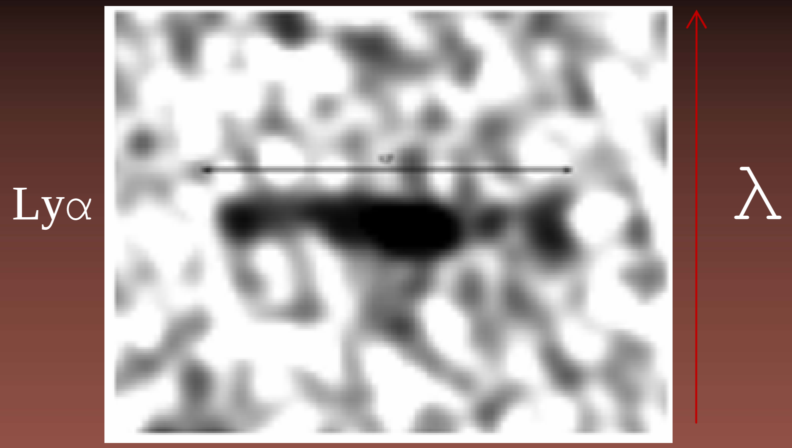

Nilsson et al.'s Blob z=3.16

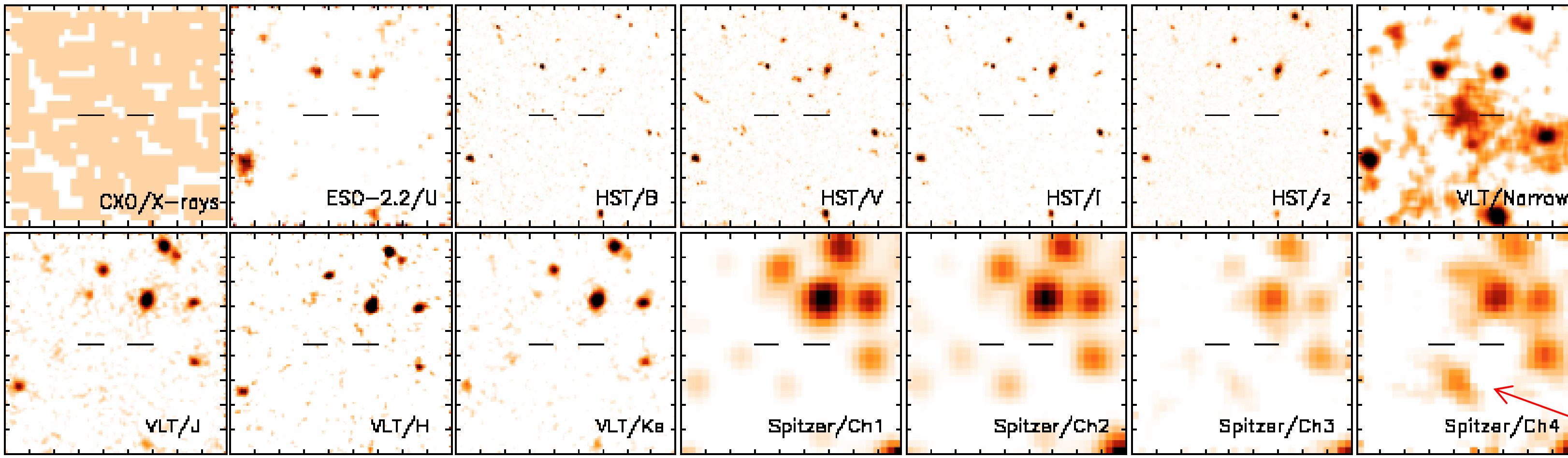

Fig. 2. Thumbnail images of all available multi-wavelength data in the GOODS South field, centred on the Lyα blob. All images are 18″ × 18″.

18”

Red Object?

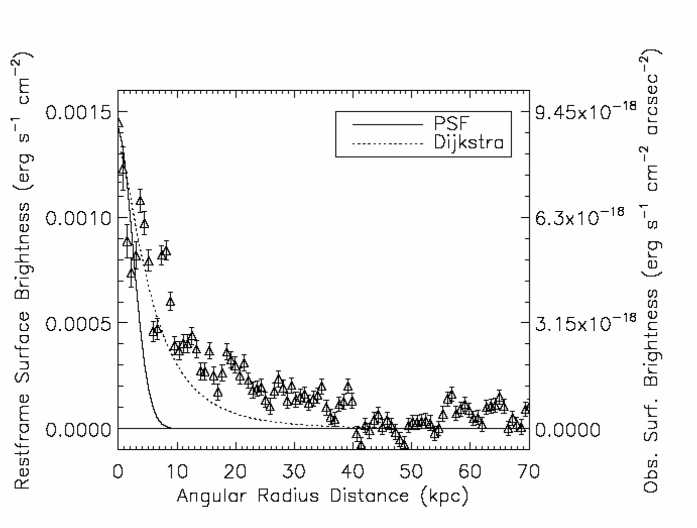

Not detected
in any other wavelength
… cooling collapsing object?

Smith et al.'s Blob z=2.83

26"

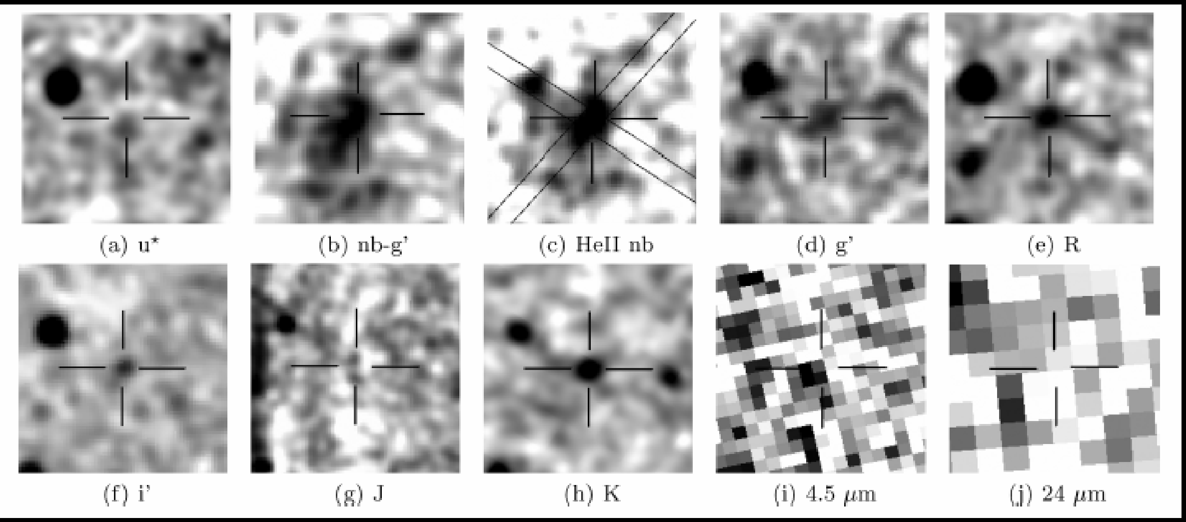

MIPS detected

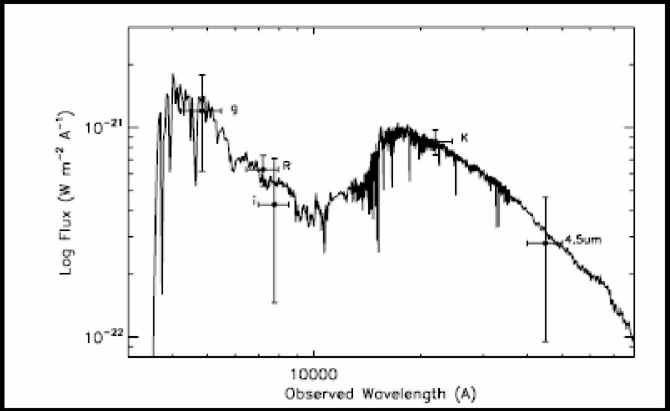

First confirmed LAB in ~15 deg^2
NB survey w/ INT

Cold gas accretion ?
(~Fardel+01, Dijkstra+06)
- SFR(UV,LyA[4"]) ~ 20 M/yr
-Red sharp cut off(?)
AGN/SF not sufficient to power entire Lyα

Lyα

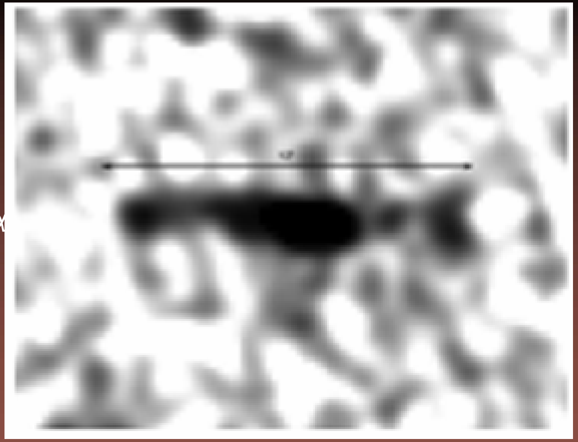

λ

signatures of 'galactic superwind'?

- Large velocity width

  Ohyama et al., Steidel et al., Dey et al., Matsuda et al.

- Line profile for expantion Wilman et a
- Diffuse metal emission??
- Shell morphology Matsuda et al.2004

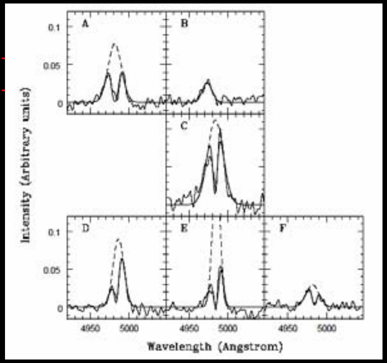

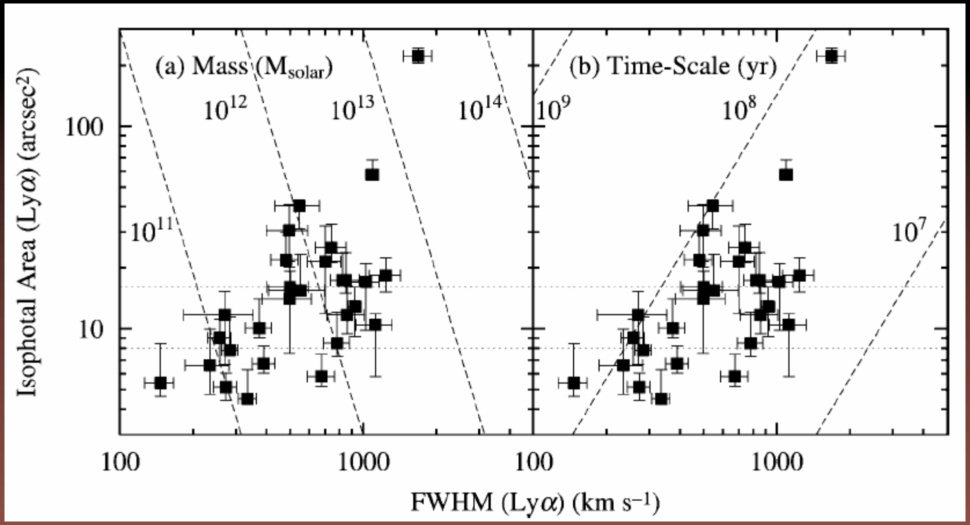

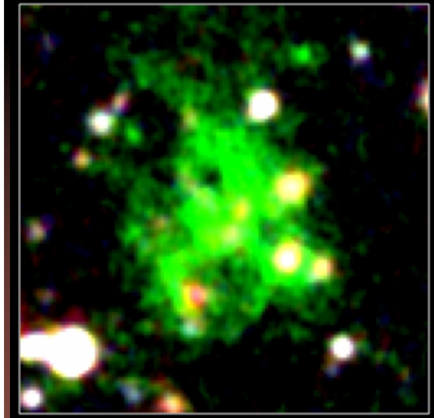

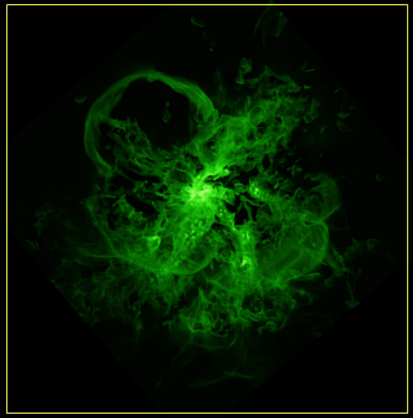

signatures of ‘Starburst/AGN’?

- MIR/Sub-mm Detection

Dey et al., Geach et al., Ivison et al.
Webb et al. (2009)

-PAH Colbert et al.

- X-ray Detection

Geach et al.

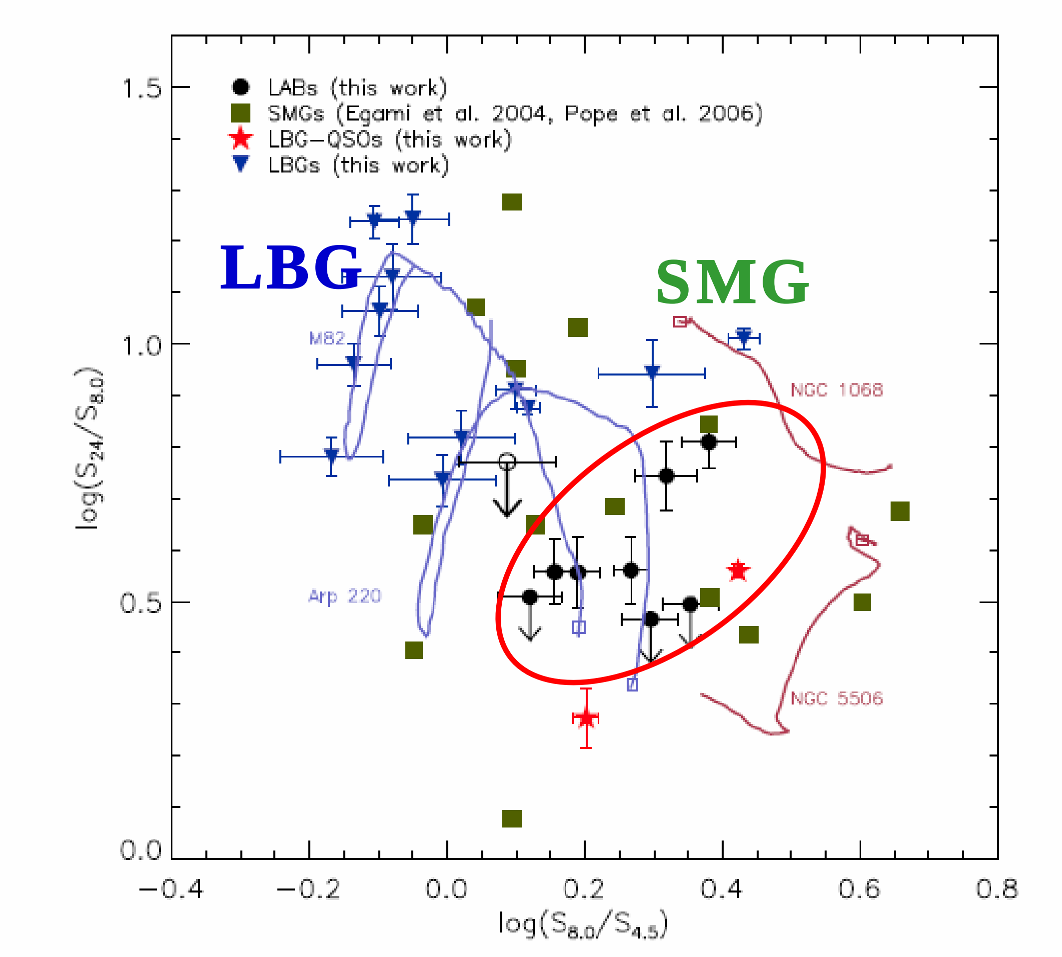

8um counterparts of 6 LABs

Webb, et al.

2. Lyα Blobs and Sub-mm Sources

Sub-mm Properties of Lyα Blobs

SCUBA SMM 02399-0136 (z=2.8)
Ivison et al. 1998

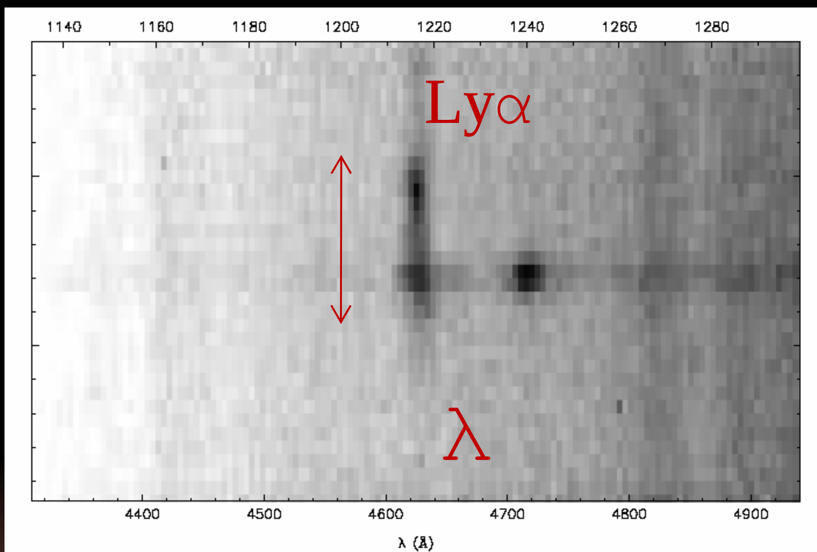

53W002 No.18
LAB … Keel et al. (1999)

Detected in
Sub-mm observation
(Smail et al. 2003)

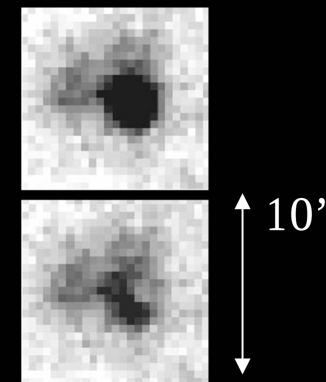

Greve et al. 2007
J065045.4 z=2.672

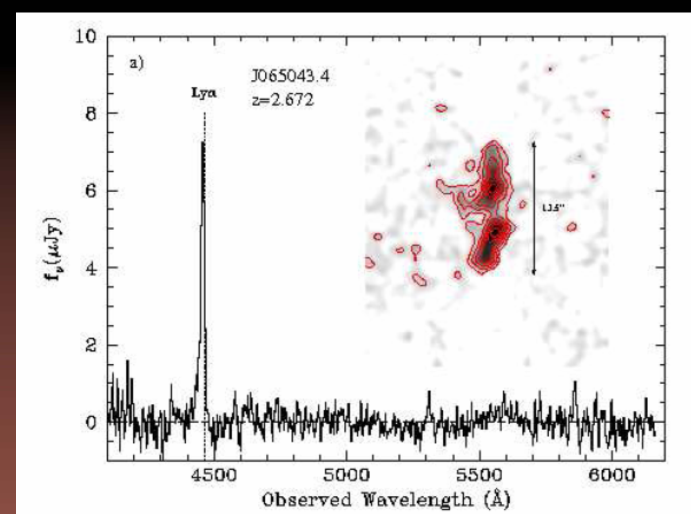

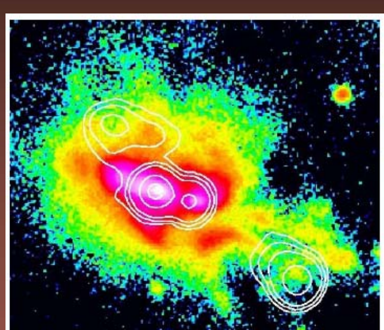

HzPRG many are
sub-mm detected

Sub-mm Properties of Lyα Blobs

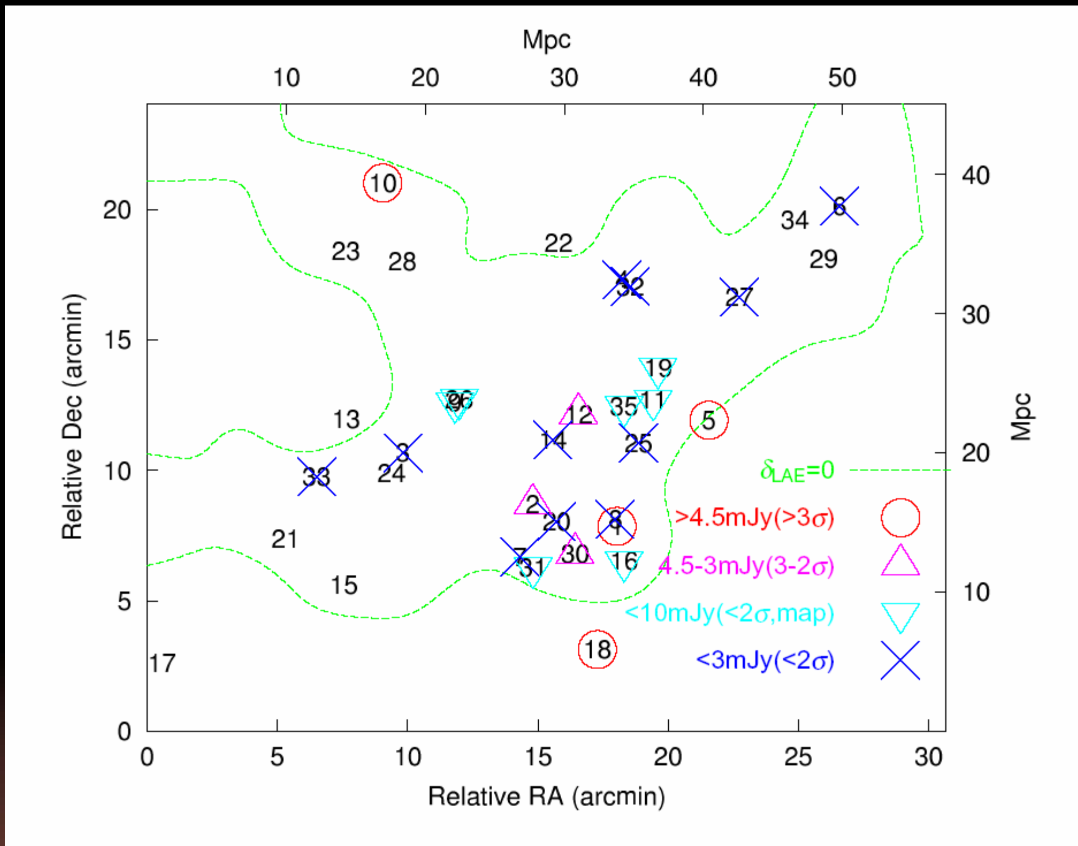

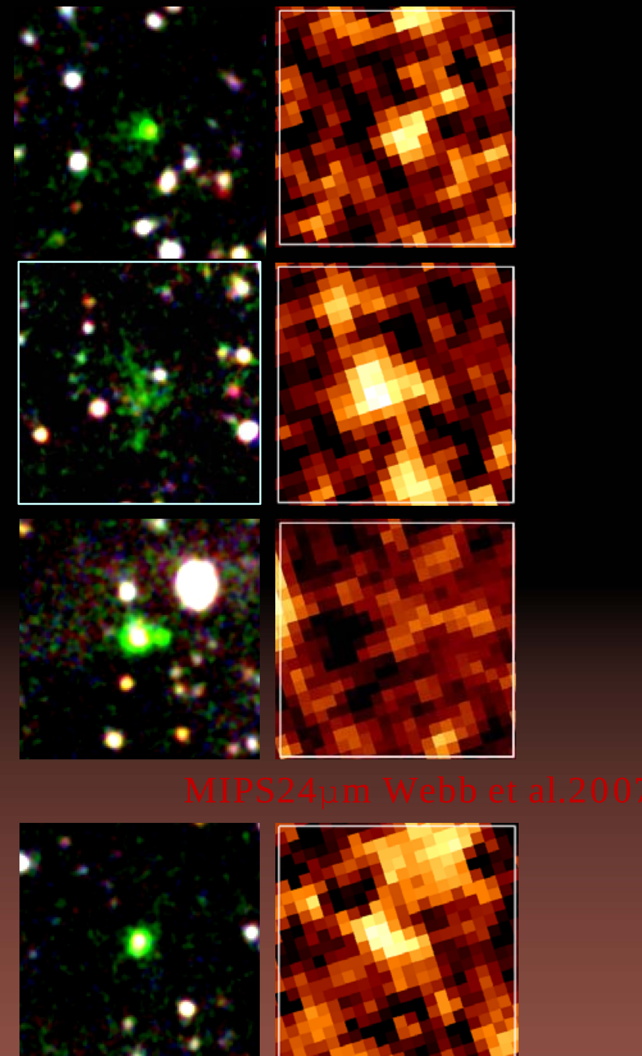

Geach, et al. 2006

5 / 23 detected at >4.5mJy
SFR ~ 1000 M_{sun}/yr
+ statistical detection
~3.0 (±0.9) mJy

SSA22 Blob1 sub-mm observations

SCUBA ~18mJy (Chapman et al. 2004)

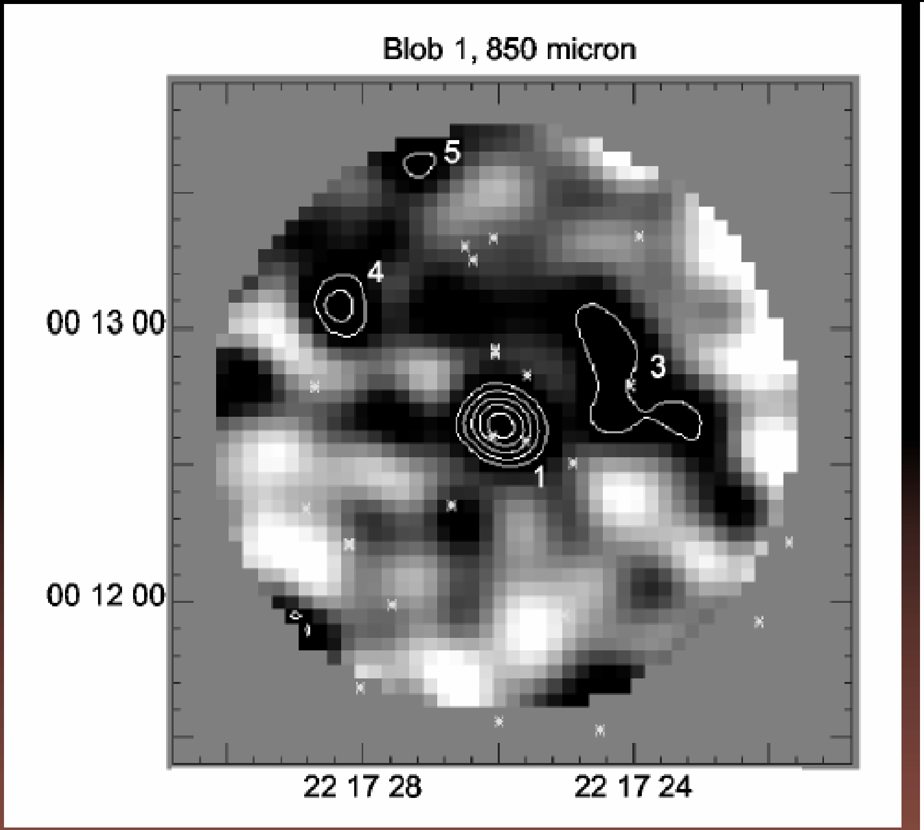

Extended? Θ > 4-5” if Gaussian

SMA < 4mJy/beam
(Matsuda et al. 2007)

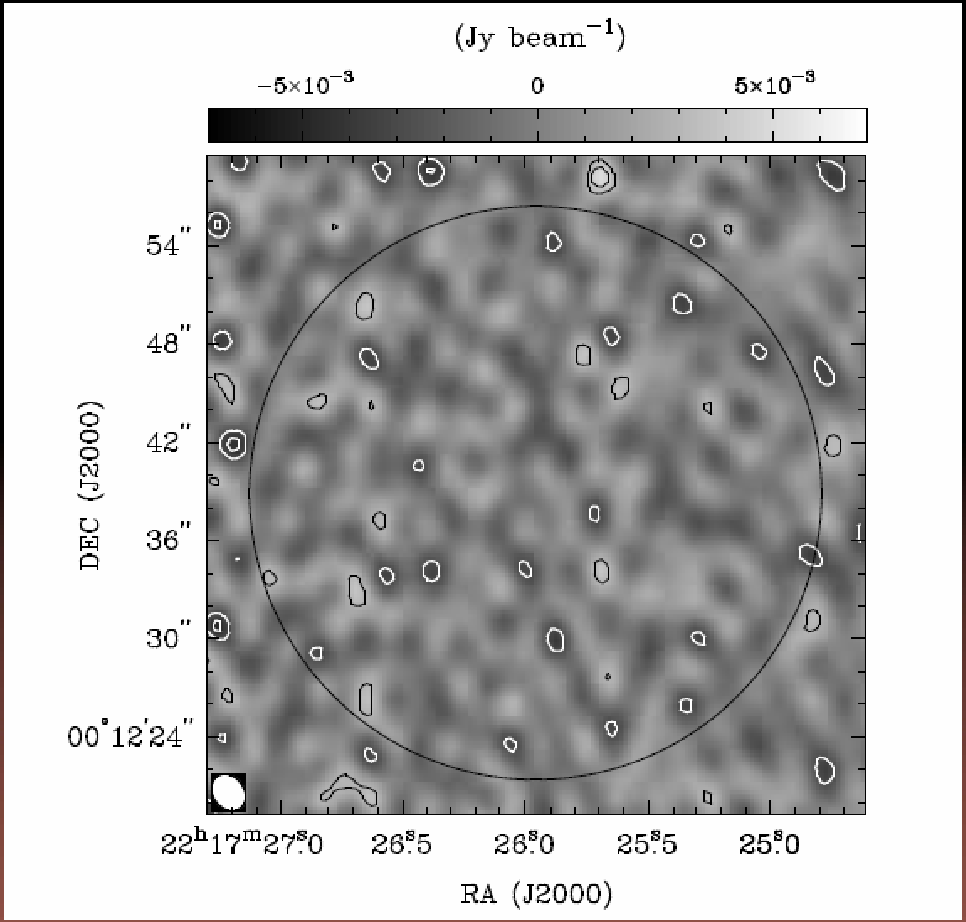

ASTE+AzTEK Observations of SSA22 protocluster

Tamura et al. 2009

Overdensity of sub-mm sources in Lyα overdensity at ~50Mpc scale
Z=3.1

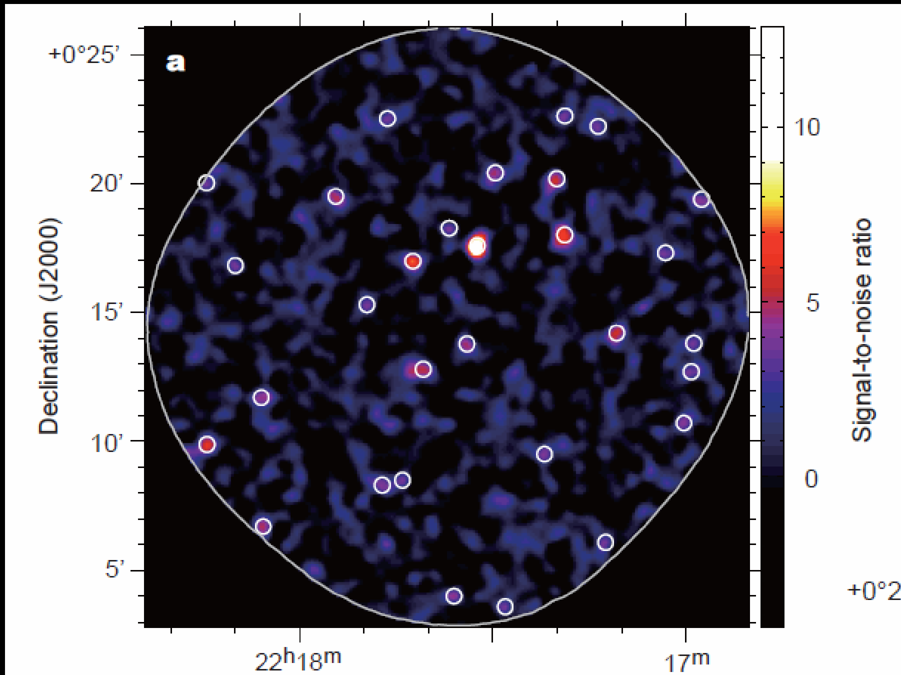

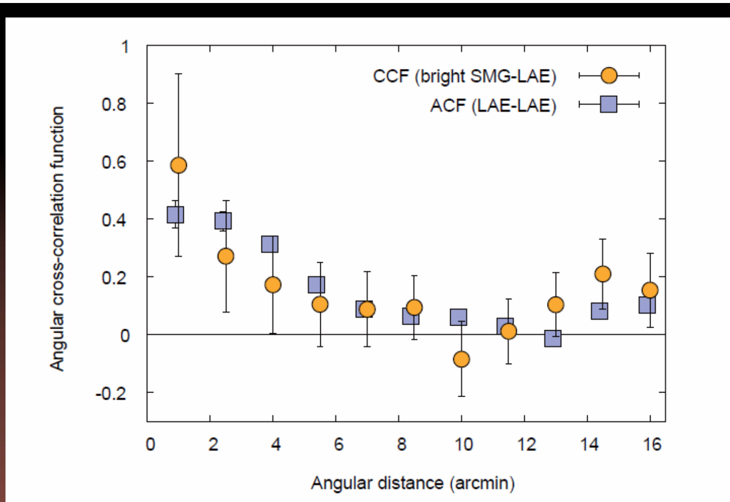

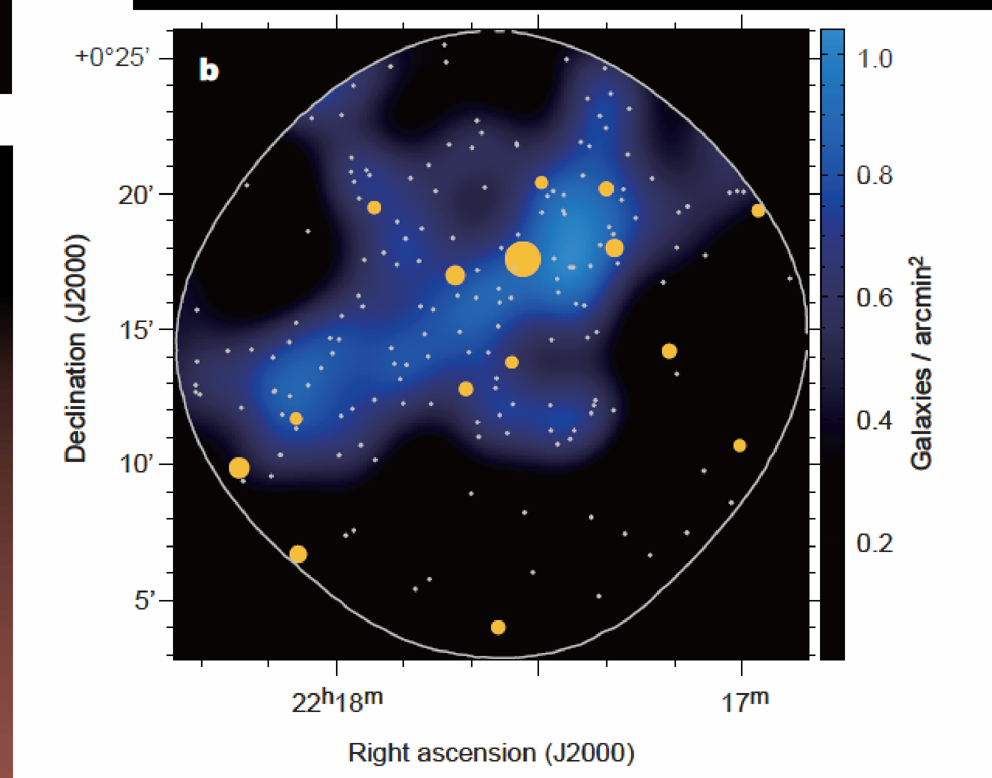

A fraction of Lyα Blobs are bright sub-mm sources

➔ massive starburst galaxies

- for SSA22, 5(4)/23 are detected by SCUBA
- some large Blobs are MIPS sources

What is the difference between
Lyα Blobs detected and NOT detected in sub-mm?

Superwinds?

➔ sensitive search for metal lines is badly needed!

3. Lyα Blobs and Active Galactic Nuclei

3-1. AGN in Lyα Blobs

3-2. Extended Lyα Haloes associated with
Quasars / Powerful-Radio Galaxies

3-2. AGN in Lyα Blobs

A large fraction of giant (~50-150kpc) Lyα Blobs show evidence of AGN

Geach et al. (2009)

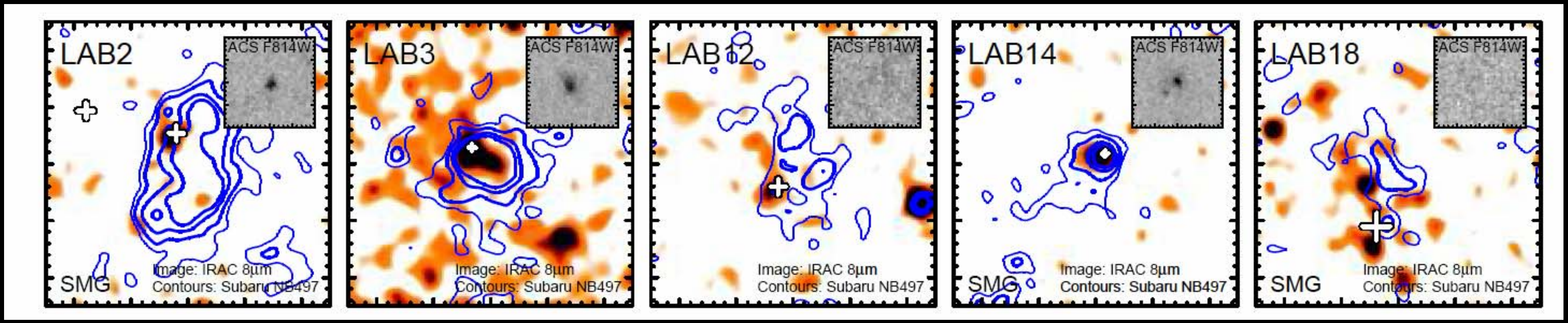

5/29 Blobs at SSA22 /Chandra

Yang et al. (2009)

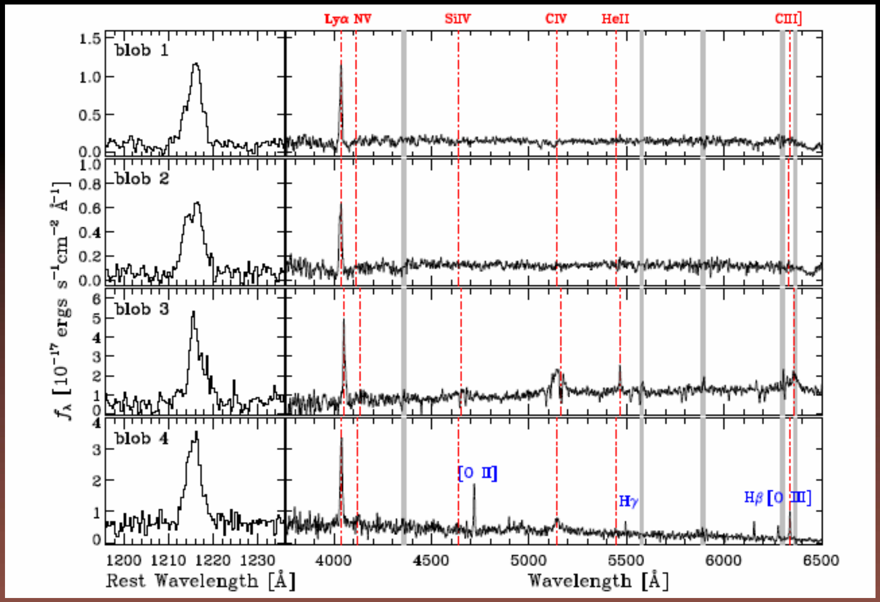

2/4 large blobs show high-ionization lines

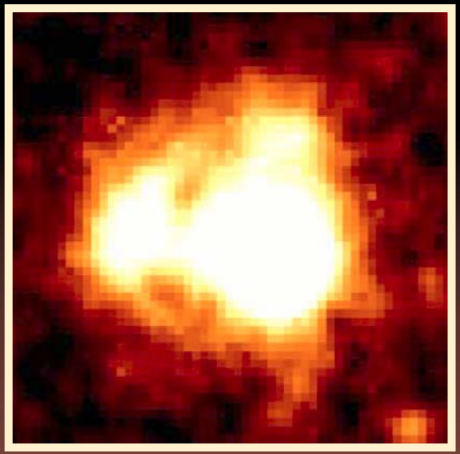

Keel et al. (1999)
X-ray (Chandra) detected
Smail et al. 2003

Dey et al (2004) z=2.83   CIV, HeII, MIPS 24um

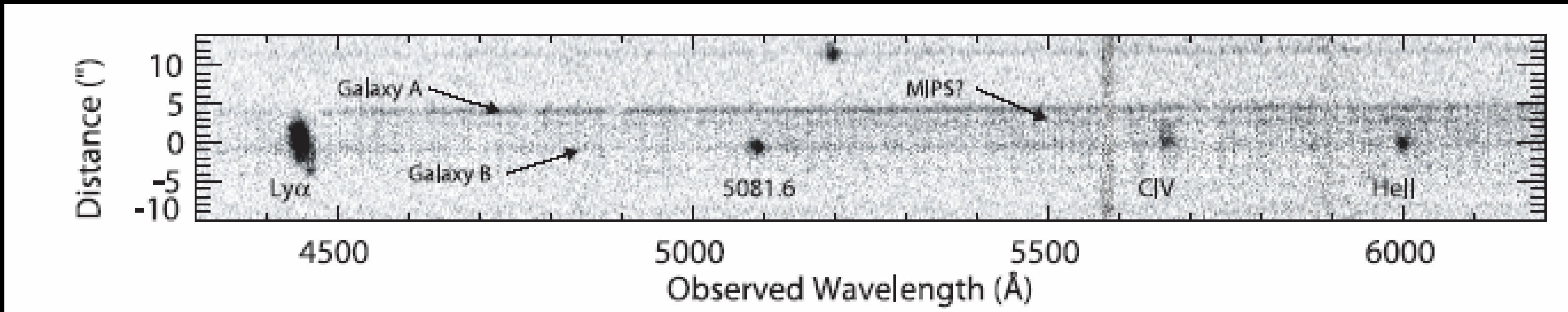

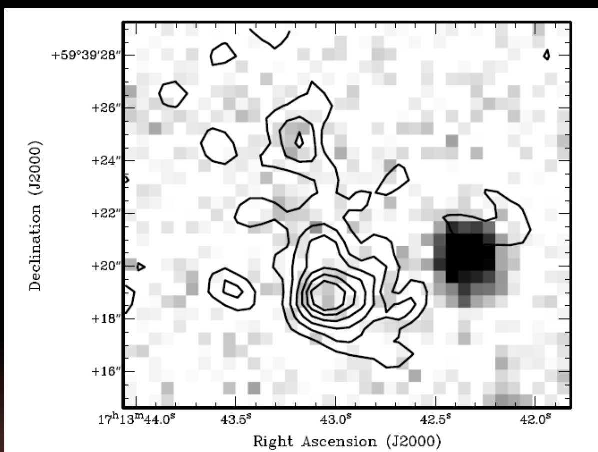

Smith et al. (2009) z=2.85
Radio, opt-MIR SED

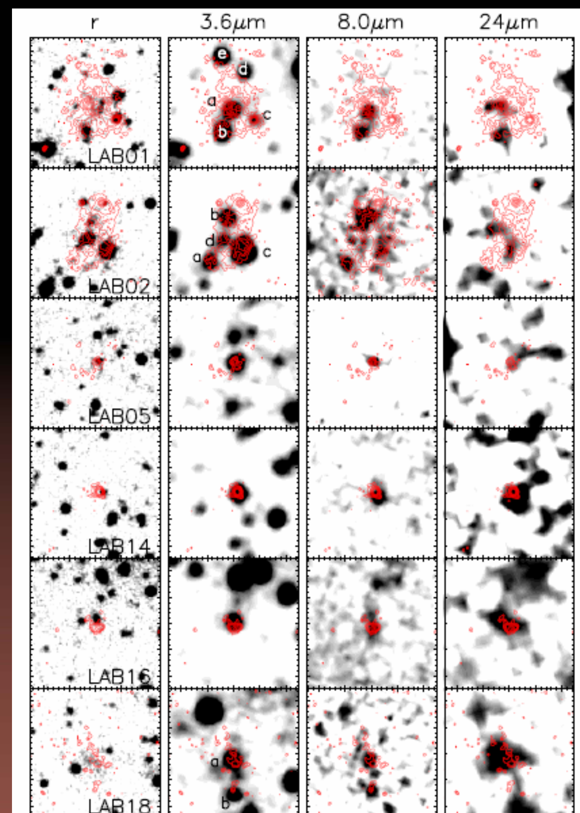

Webb et al. (2009)
IRAC/MIPS SED
SSA22 6/27

AGN among SSA22 z=3.1 Lyα Blobs (35 Matsuda Blobs)

AGN fraction >17% (X-ray) ~20% (MIR),
maybe > 20%

1. Spitzer results Webb et al. (2009), Geach et al. (2006)

2. Chandra results Lehmer et al. (2008), Geach et al. (2009)

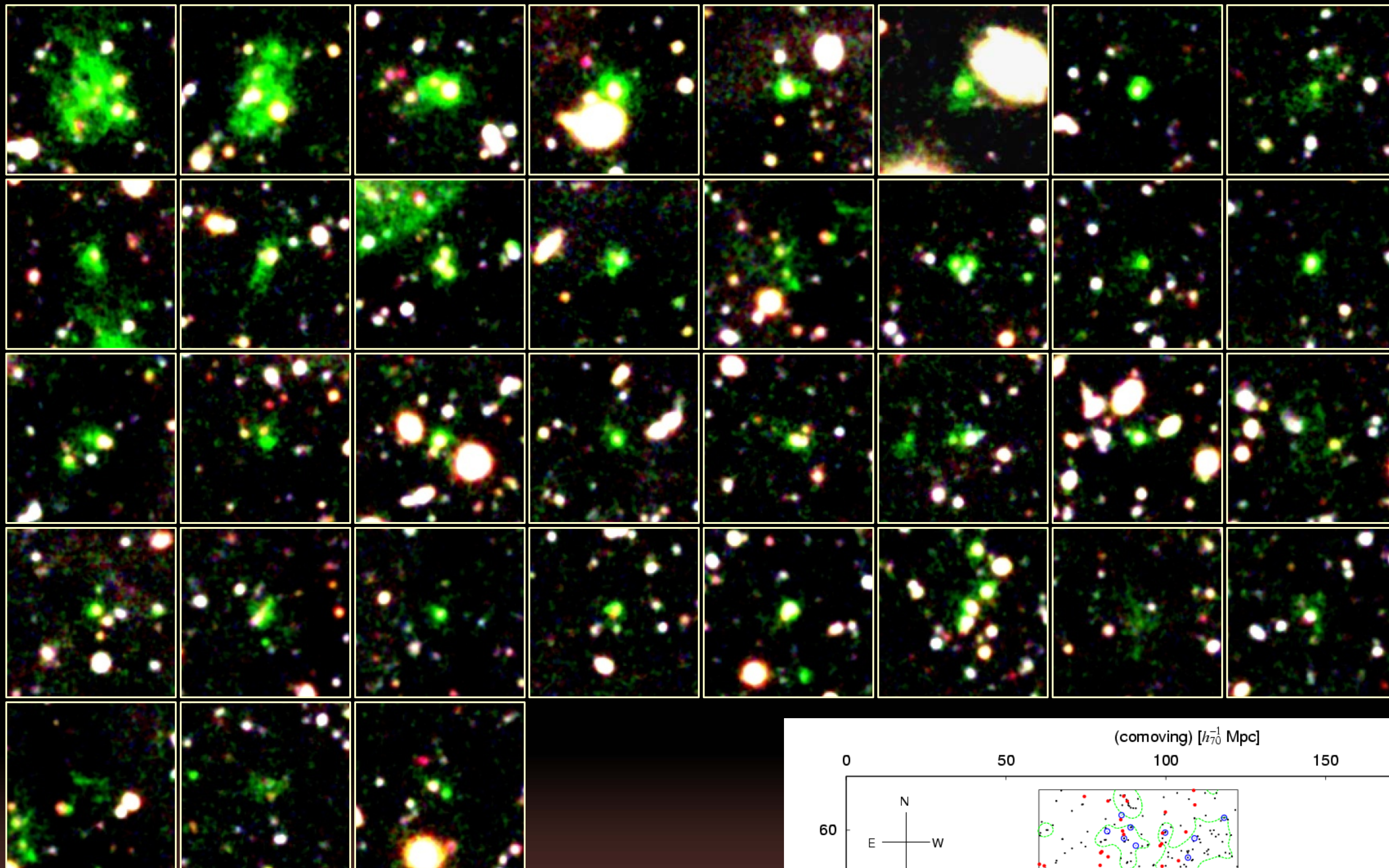

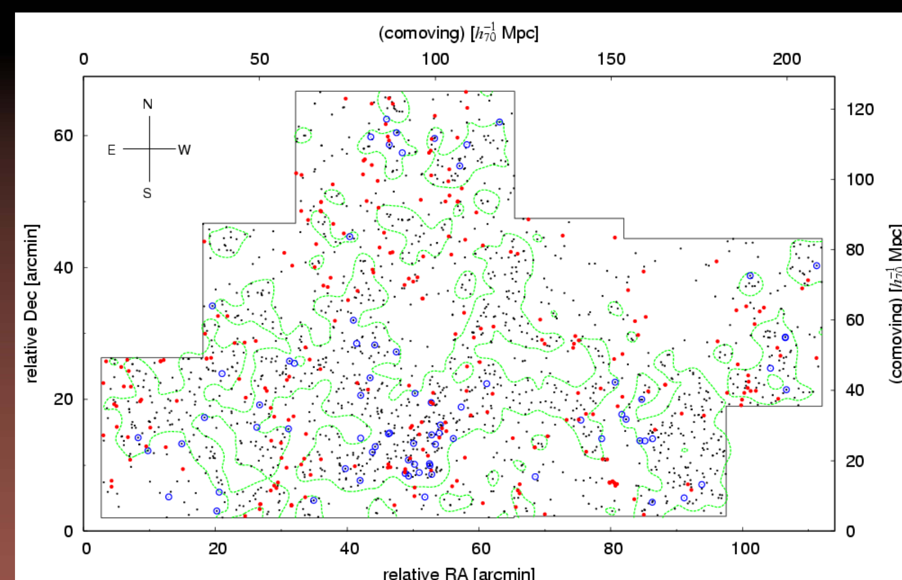
(comoving) [h_{70}^{-1} Mpc]
0
50
100
150
200
N
E
W
S
60
40
20
0
relative Dec [arcmin]
120
100
80
60
40
20
0
(comoving) [h_{70}^{-1} Mpc]
0
20
40
60
80
100
relative RA [arcmin]

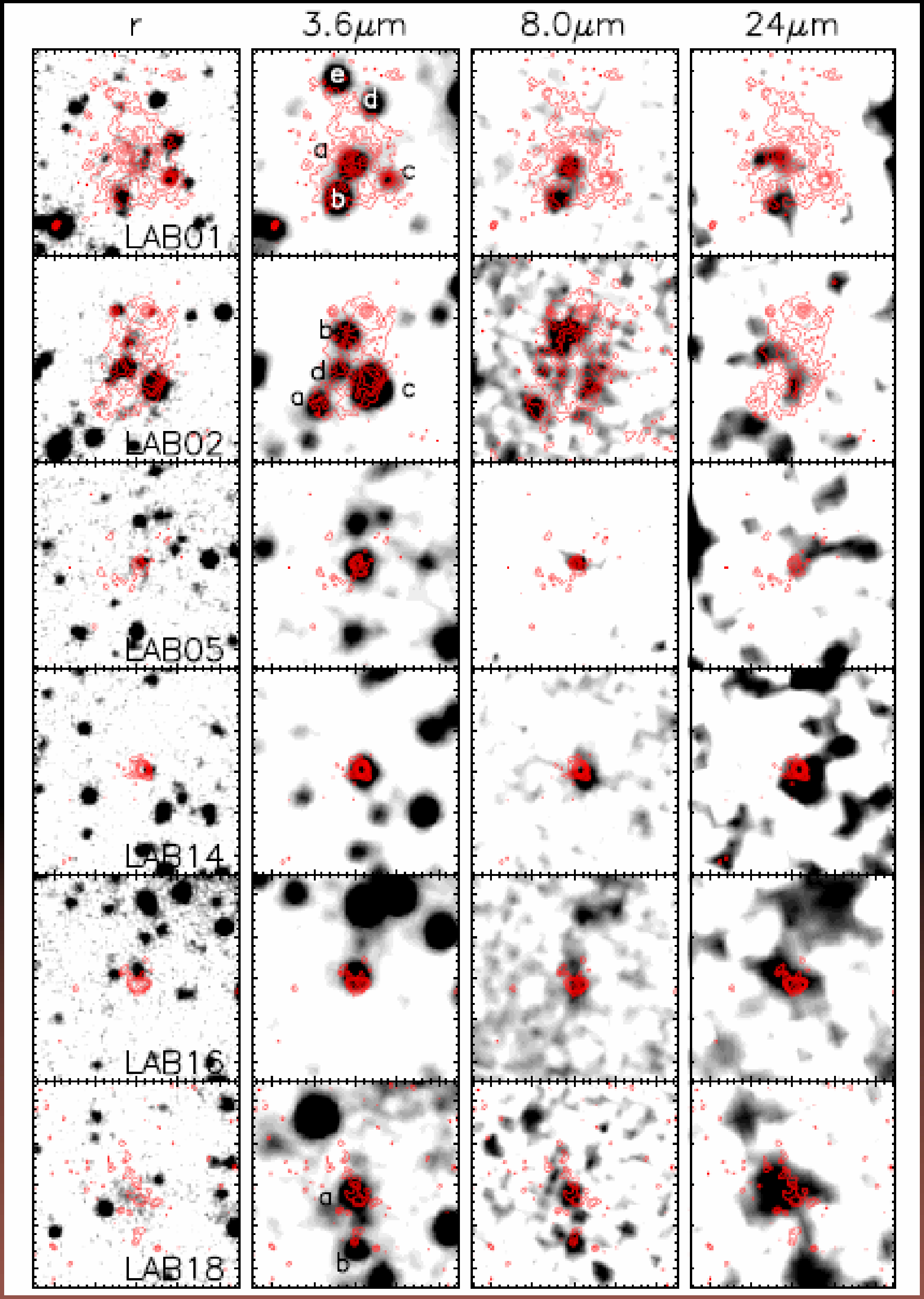

Webb et al. 2009

Spitzer IRAC
8 & 24 μm sources

6/26 Blobs

Lyα Blobs detected in MIR show the IR colors between SMGs and Quasars

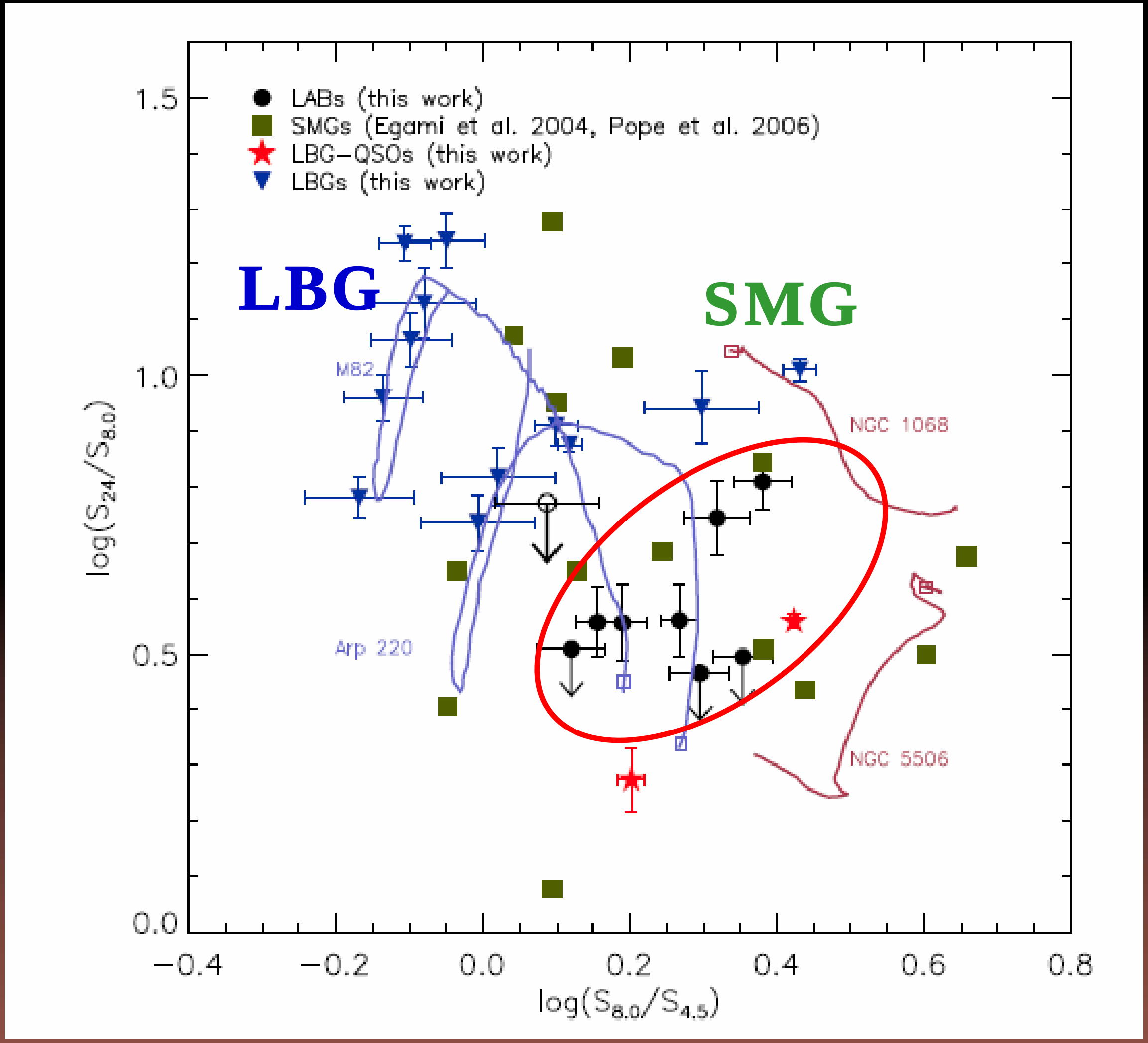

Chandra 400ks observation

Lehmer et al. (2008), Geach et al. (2009)

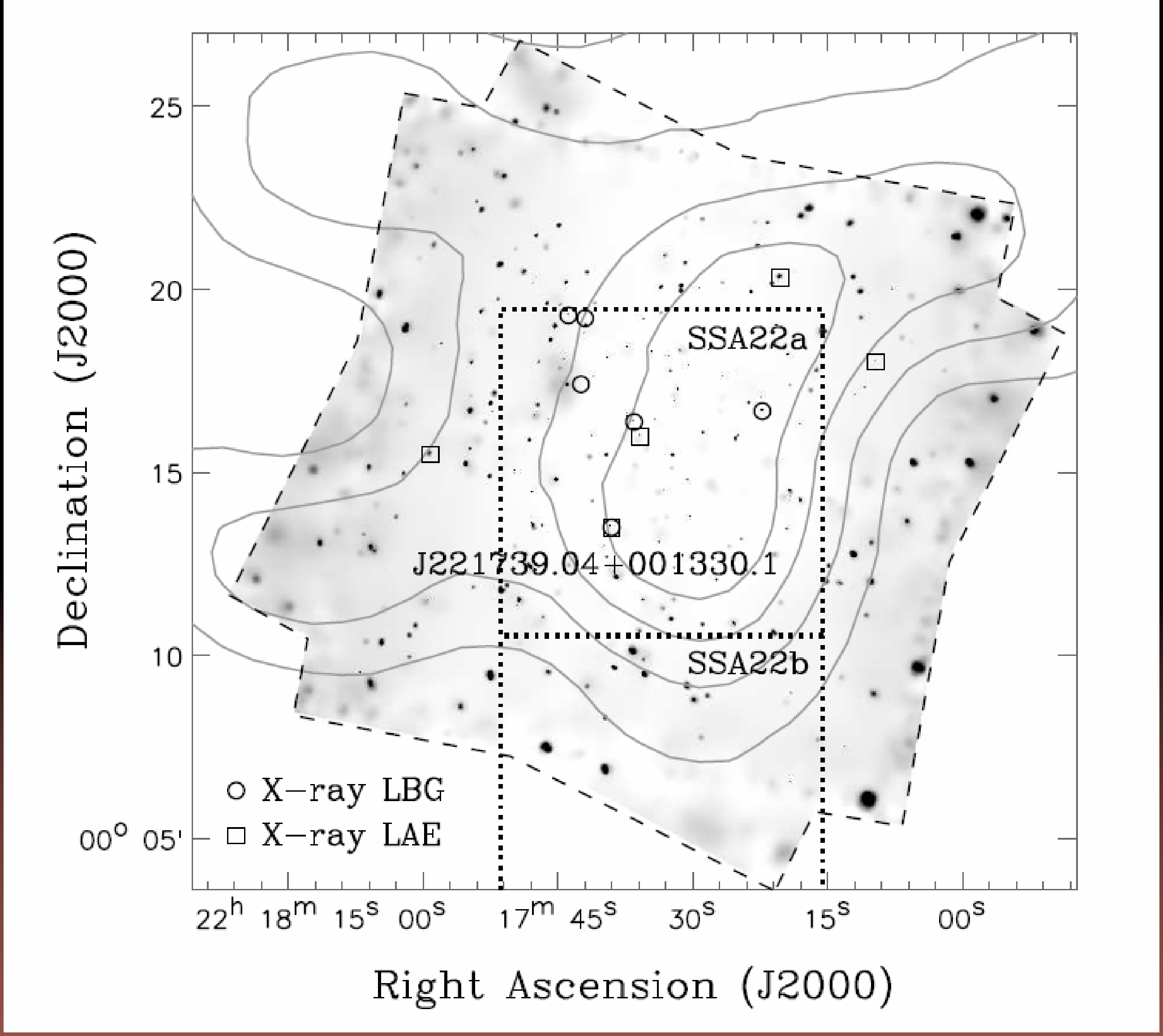

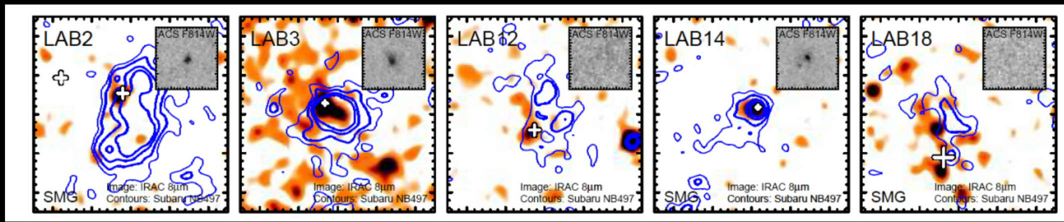

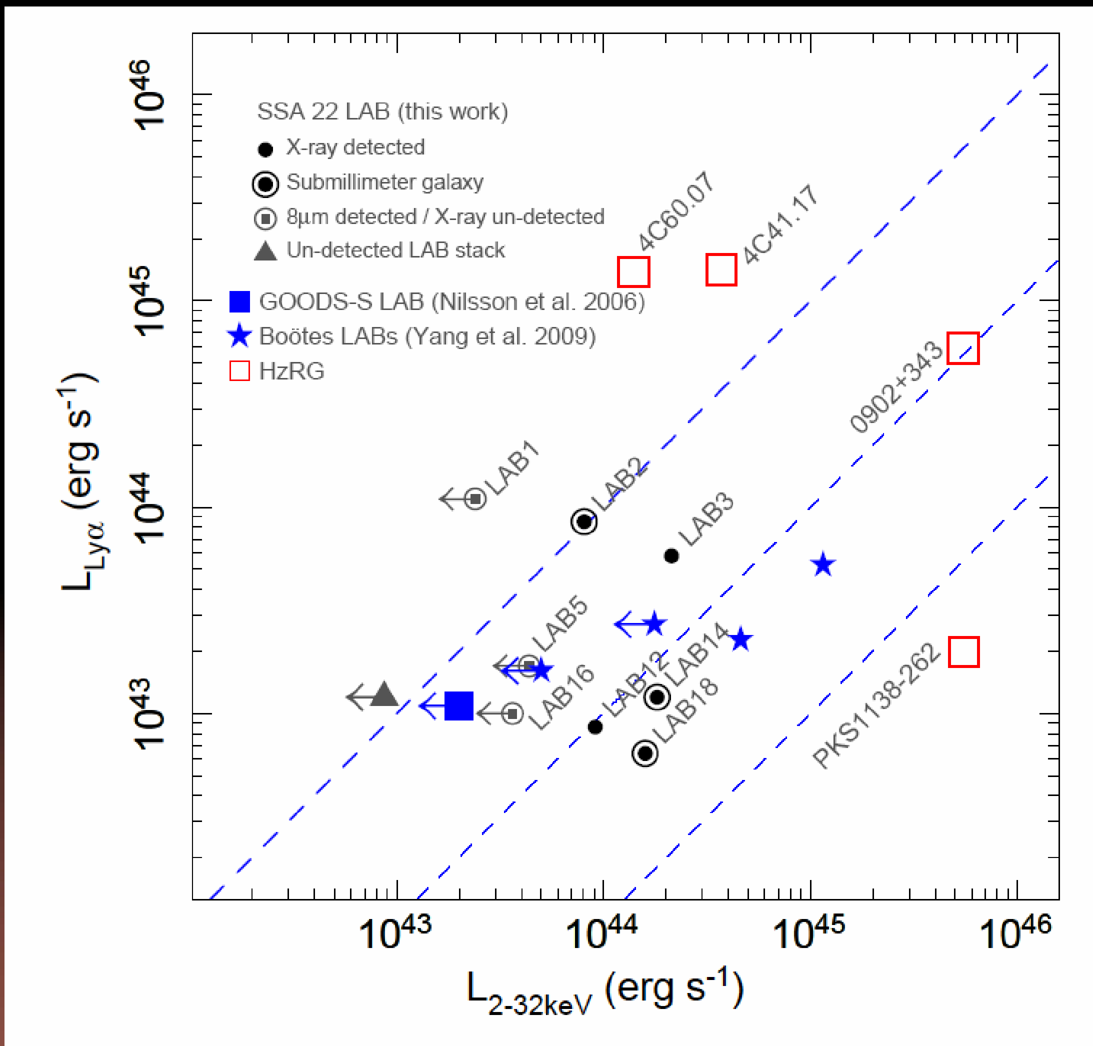

X-ray sources are detected
in 5 Lyα Blobs

@8um source position

Lx ~>L(Lyα)

Γeff < 1
obscured sources
N(H) > 10^{23}cm^{-2}

Case of photoionization by AGN and/or SF UV continuum

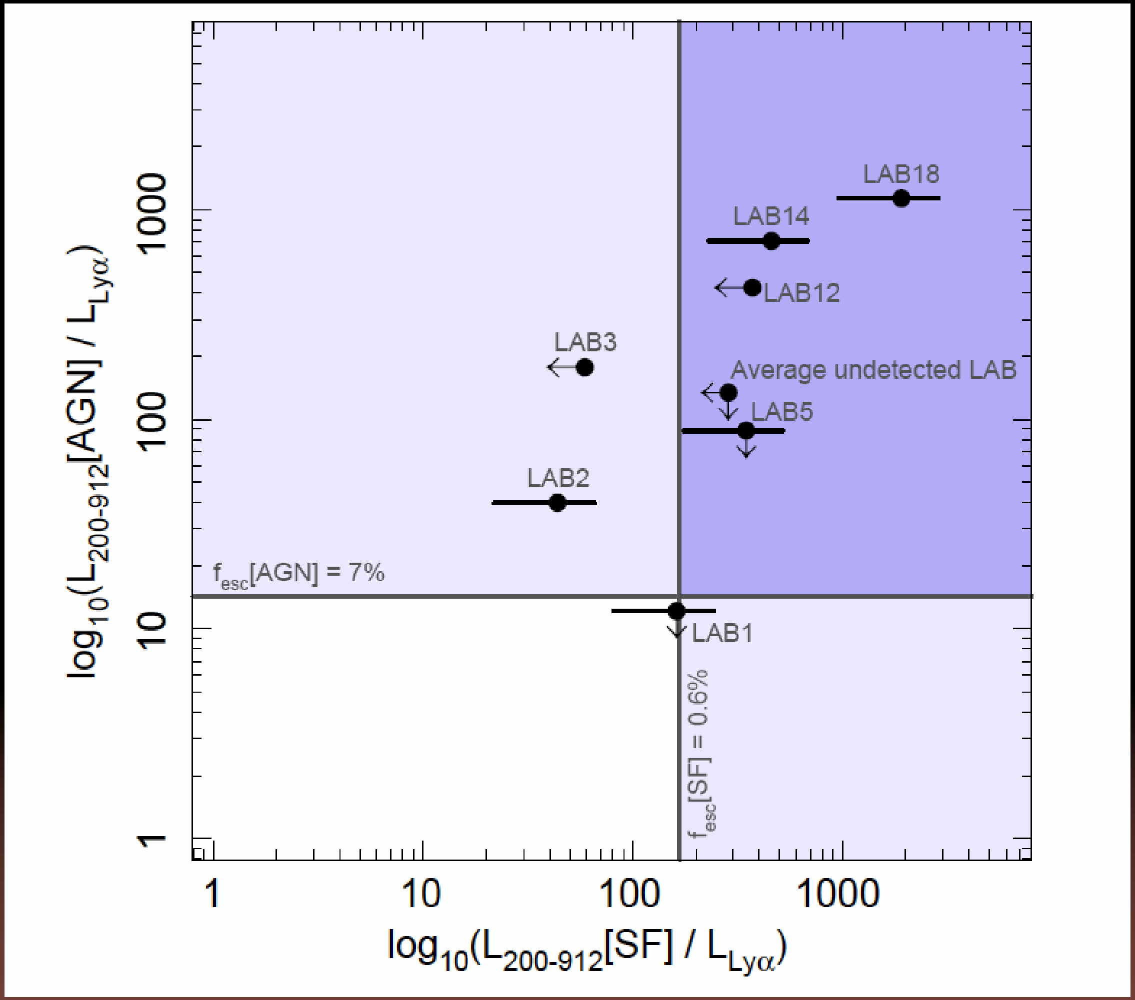

- >15-20% of the Lyα Blobs with 30-150 kpc host AGN with L~10^{43-44} erg/s

➔ AGN contribution, either photoionization and mechanical energy input to the Lyα emission must be there.

- For large blobs (>50kpc), AGN detection rate is high (>50%, TBC), but not all.

- There are overlap with sub-mm sources for the AGN-associated Lyα Blobs. Lyα power source is not unique.

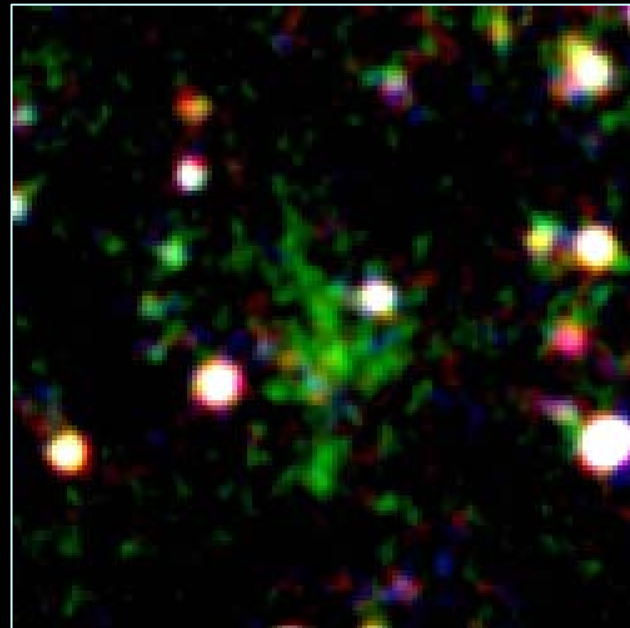

Matsuda, TY, et al. 2004
'LAB 18'

No LBG (UV source)

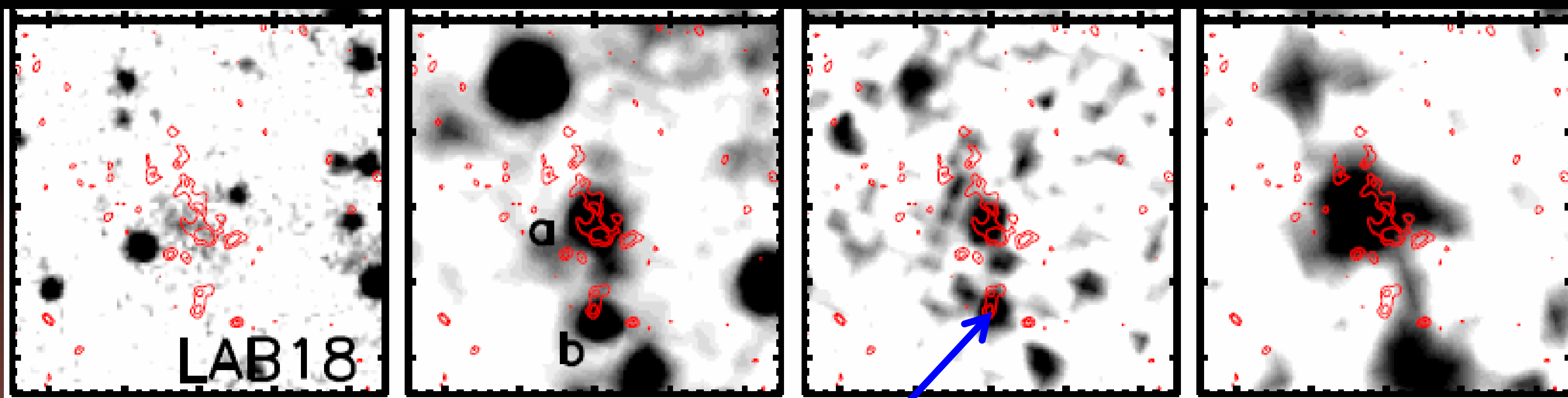

R

3.6um

8um

24um

Chandra source

Webb, TY, et al. (2009)

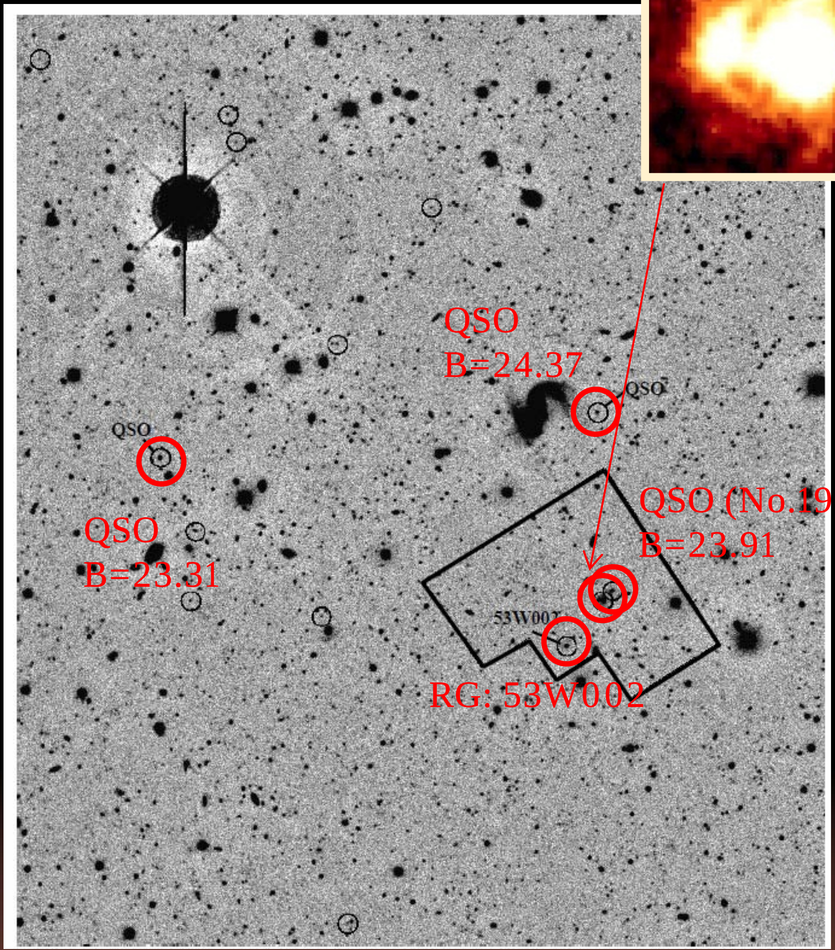

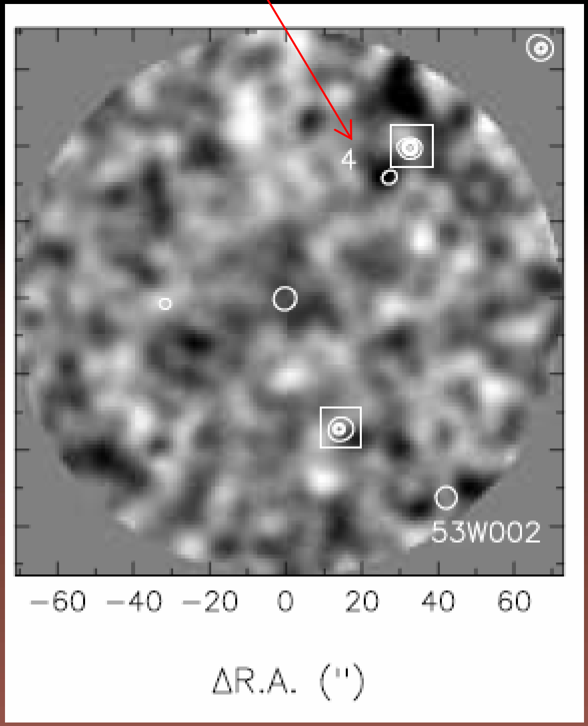

53W002 ‘AGN cluster’ @ z=2.39
Keel et al. 1999

Smail et al. 2003

Gray SCUBA
Contour Chandra

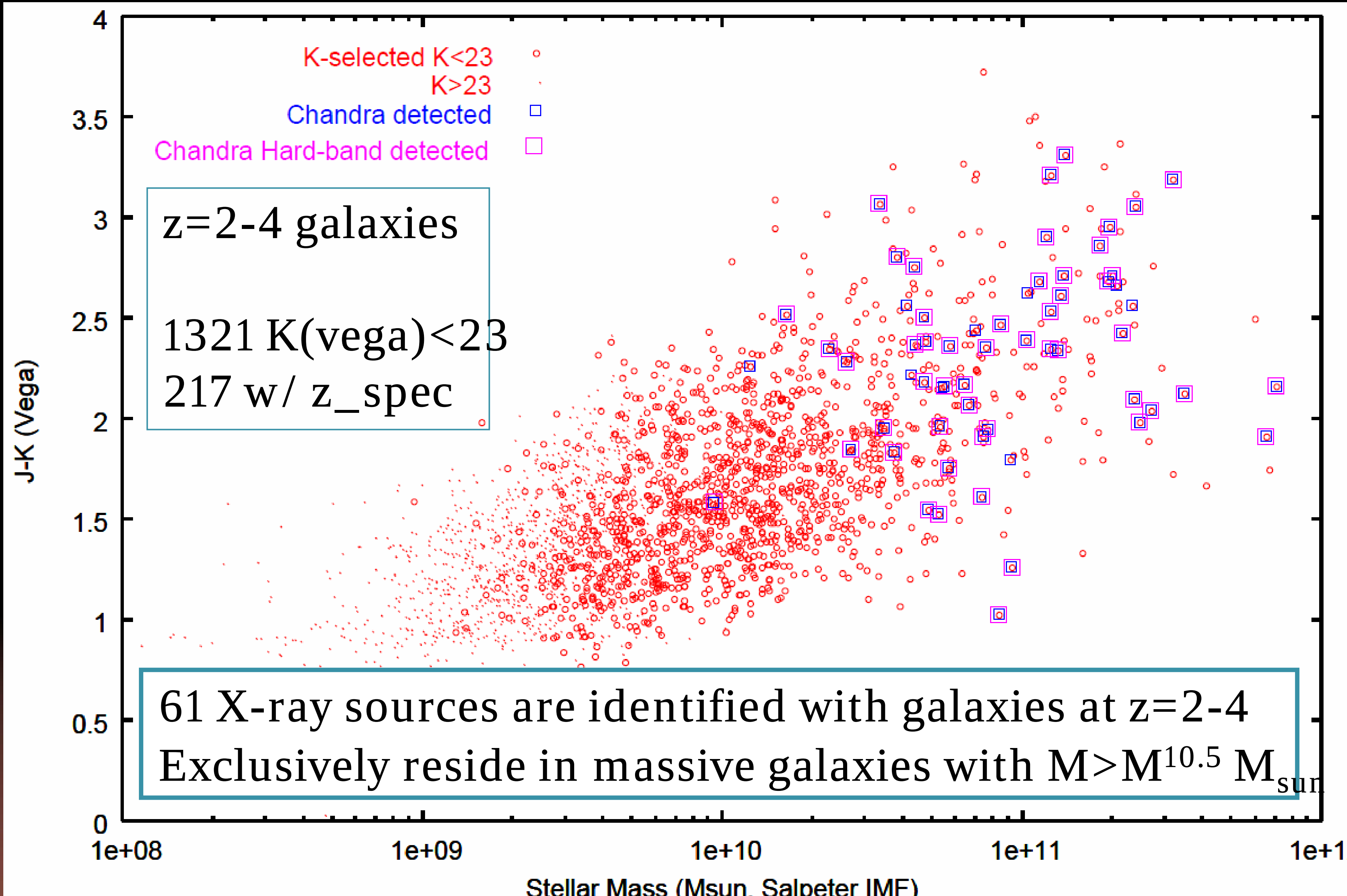

z=2-4 galaxies

1321 K(vega)<23
217 w/ z_spec

61 X-ray sources are identified with galaxies at z=2-4
Exclusively reside in massive galaxies with $M>M^{10.5}\ M_{sun}$

Salpeter IMF

3-2. Extended Lyα Haloes associated with Quasars / Powerful-Radio Galaxies

Extended Lyα Halo Associated with RLQs

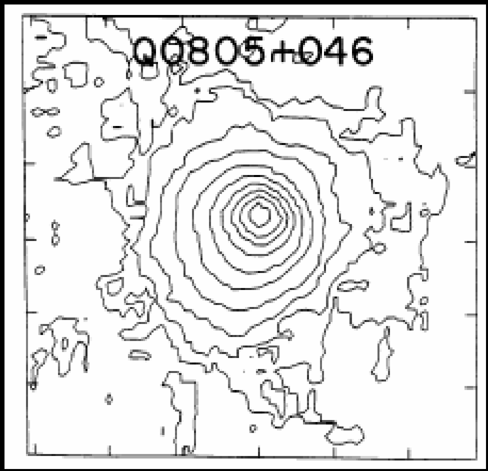

18”x18”

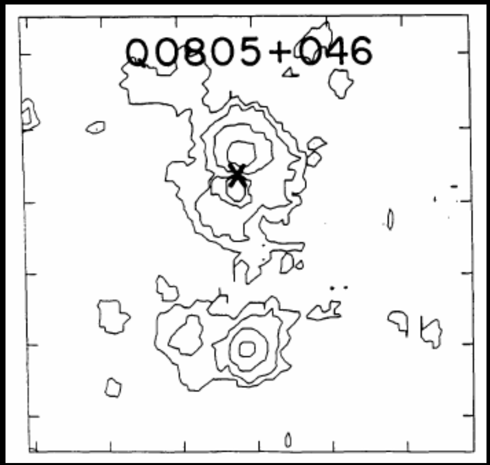

Cont. subtracted

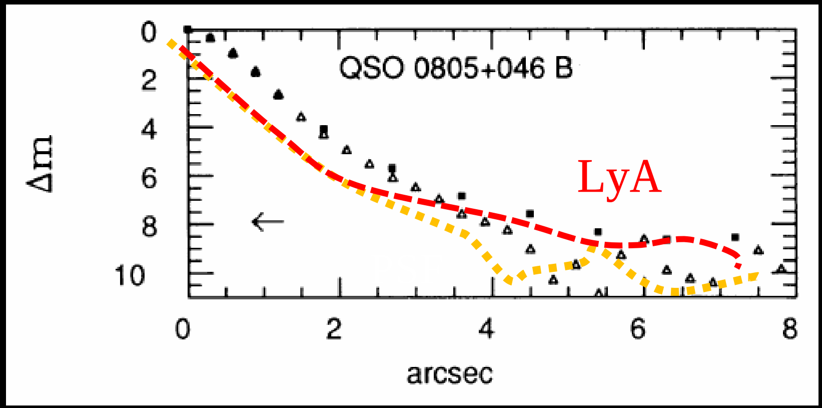

Heckman et al. 1991a,b

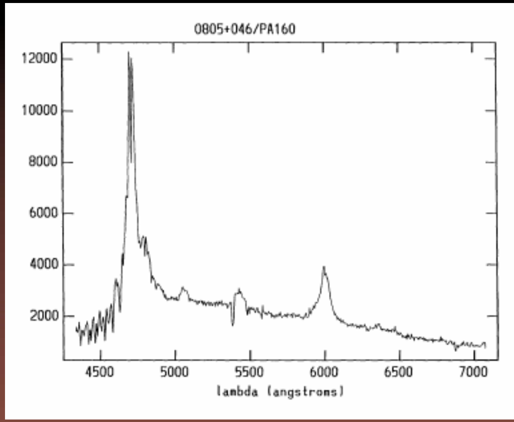

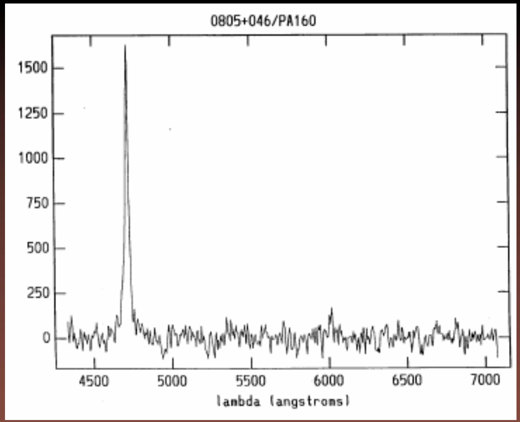

Typically size ~ 100 kpc
L(Lyα) ~ 1.e44 erg/s
Δv ~ 1000 km/s

Extended Lyα Halo Associated with RQQs

Christensen et al. 2006 (PMAS, Calar Alto)

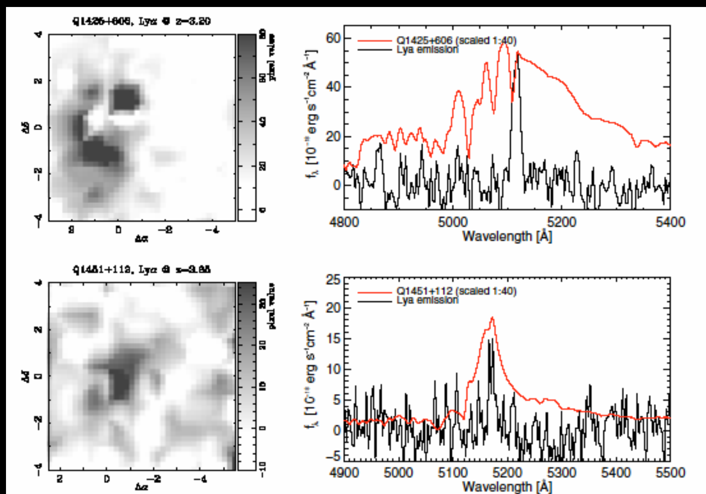

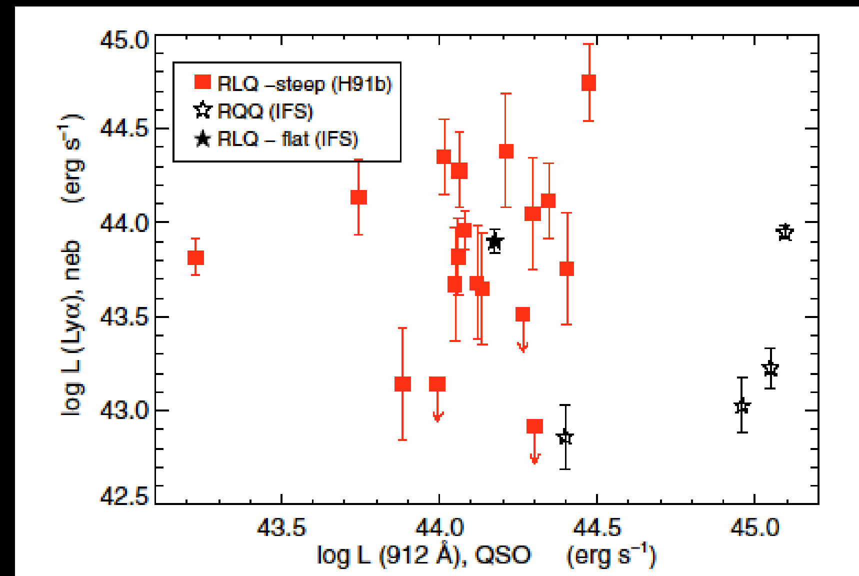

Size 10~60 kpc
Log L(LyA) ~ 43-44 [erg/s]
FWHM ~ 500-1000 km/s

(1) Name	(2) z (Lyα)	(3) V (km s^{-1})	(4) Σ (Lyα) (erg cm^{-2} s^{-1} arcsec^{-2})	(5) size (kpc)	(6) f_{tot} (10^{-16} erg cm^{-2} s^{-1})	(7) log L_{tot} (erg s^{-1})	(8) FWHM (km s^{-1})	(9) ΔV (km s^{-1})
Q0953+4749	4.489			13	0.36 ± 0.17	42.9	1000	1800 ± 200
Q1425+606	3.204	600–200	2×10^{-16}	34	9.8 ± 0.8	43.9	500	100 ± 100
Q1451+122	3.253			15	1.8 ± 0.5	43.2	500	–600 ± 100
Q1759+7539	3.049	200–300	3×10^{-16}	60	9.9 ± 1.6	43.9	450	0 ± 100
Q2233+131	3.301			10	1.1 ± 0.4	43.0	<400	700 ± 100

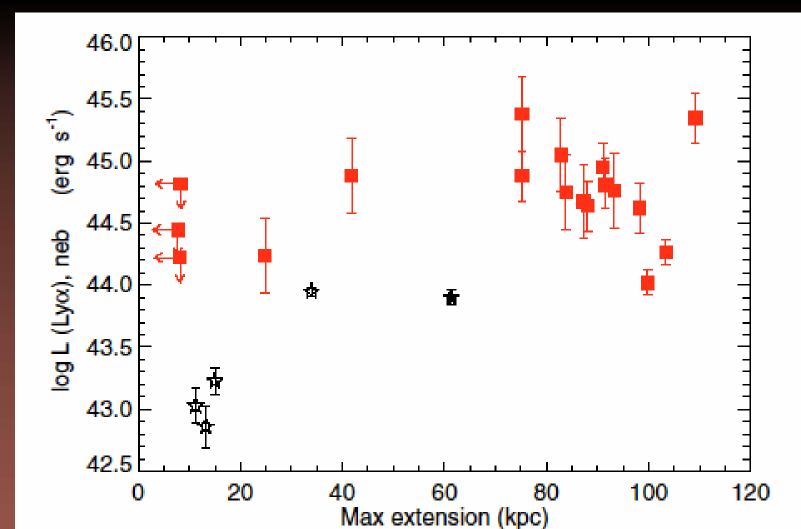

Extended Lyα Halo of Powerful Radio Galaxies

-Typically ~30-100kpc,
-log L(LyA)~44 erg/s

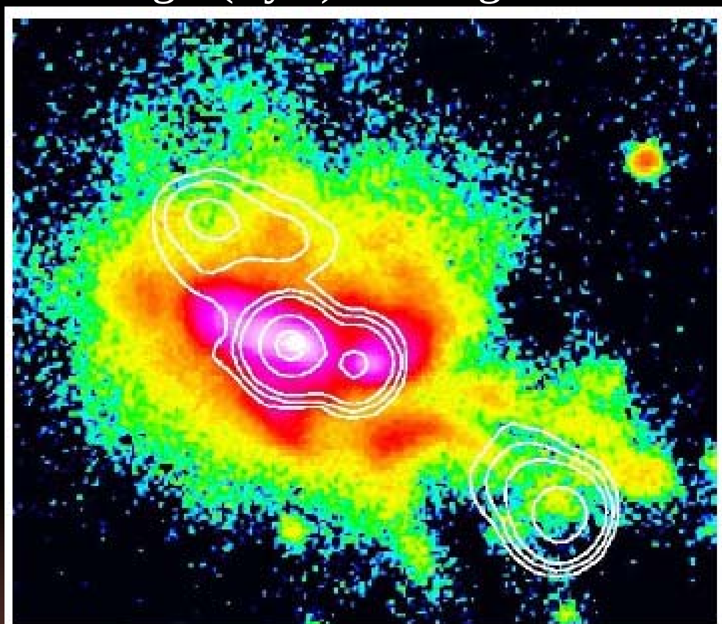

Chambers et al. 1990
van Breugel et al. 2006

- Large Lyα halo (>30kpc) is seen for many HzPRGs (e.g., van Ojik et al. 1997; Venemans et al. 2007)
-PA(LyA) correlates with PA(radio jet) (alignment effect)
- Gas near radio axis:
  metal enriched
  ionized
  (e.g., Reuland et al. 2007)
- Origins of further extended halo (~minor axis of jet) is still uncertain

Venemans et al. 2007

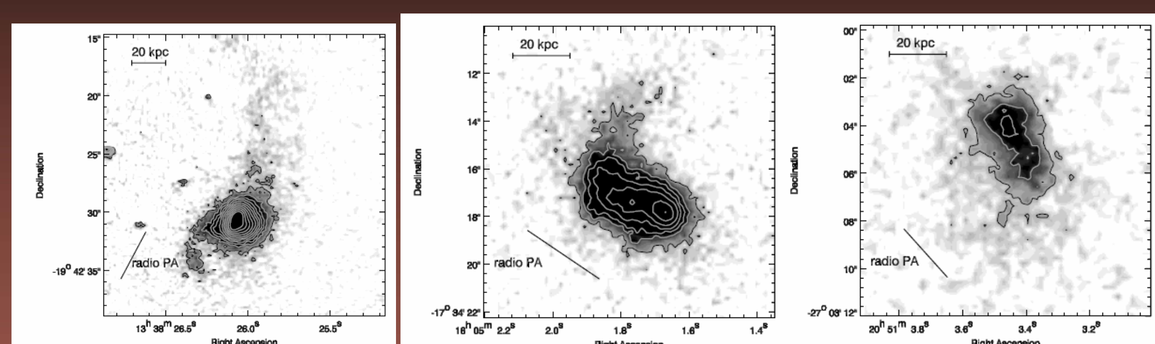

Rest-frame optical lines

4C41.17 Reuland et al. 2007

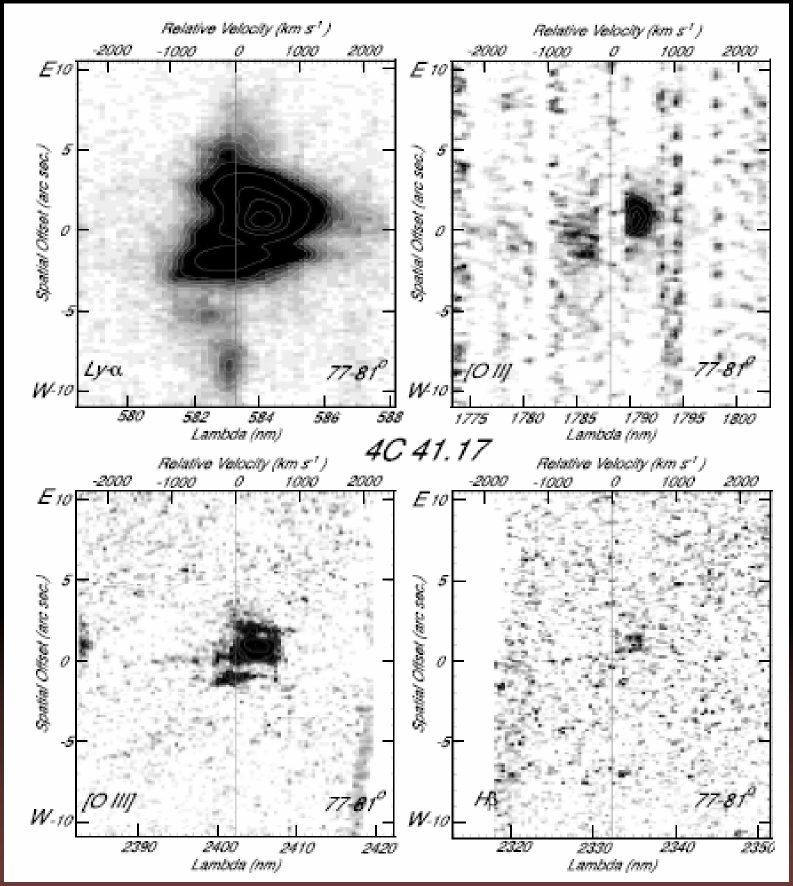

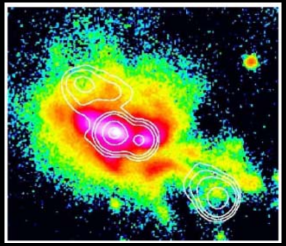

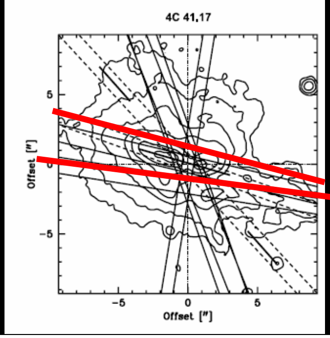

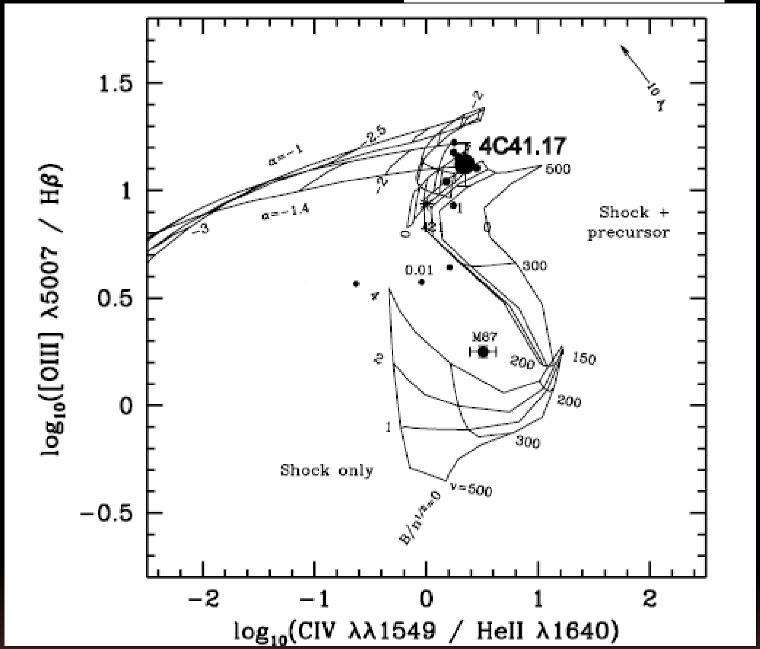

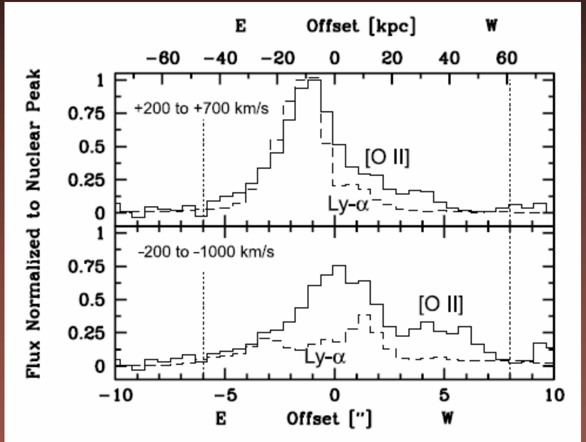

At least inside/near radio-jet axis

- photo-ionized gas
- metal enriched

Fraction of Powerful Radio Galaxies with Giant (>50-100 kpc) Lyα Halo

Table 5. Luminosity, size and position angle (PA) of the Lyα halos surrounding the radio galaxies observed in our VLT program. The position angles of the halos are measured from the Lyα images (Figs. 14–17) and are accurate to ∼10 degrees.

Name	$L_{\mathrm{Ly}\alpha}$ erg s^{-1}	Size kpc×kpc	PA halo deg[a]	PA radio deg[a]
BRL 1602–174	7.5×10^{44}	90 × 55	60	56[b]
MRC 2048–272	6.5×10^{43}	70 × 40	25	42[b]
MRC 1138–262	2.5×10^{45}	250 × 125	74	98[b]
MRC 0052–241	7.5×10^{43}	35 × 30	5	15[b]
MRC 0943–242	2.5×10^{44}	50 × 40	55	74[b]
MRC 0316–257	7.0×10^{43}	35 × 25	55	53[b]
TN J2009–3040	3.0×10^{44}	40 × 40	–[c]	144[b]
TN J1338–1942	4.5×10^{44}	130 × 45	170	152[b]
TN J0924–2201	1.5×10^{43}	10 × 10	90	74[b]

Venemans et al. 2007   1/9 √ab > 100kpc
4/9 √ab > 50kpc

van Ojik et al. 1997   5/18 d > 100kpc
11/18 d > 50kpc

Table 4. Lyα parameters

Source (1)	$\mathrm{FWHM}_{\mathrm{Ly}\alpha}$ ($\mathrm{km\,s^{-1}}$) (2)	H I abs (3)	$D^{20\%}_{\mathrm{Ly}\alpha}$ (kpc) (4)	$D^{\mathrm{tot}}_{\mathrm{Ly}\alpha}$ (kpc) (5)	$\log L_{\mathrm{Ly}\alpha}$ ($\mathrm{erg\,s^{-1}\,cm^{-2}}$) (6)	$M_{\mathrm{Ly}\alpha}$ ($10^8\,M_\odot$) (7)	M(H I) ($10^8\,M_\odot$) (8)	ΔS (kpc) (9)	n_S (10)	w_S (11)
0200+015	1420 ± 75	1	42	72	43.73 ± 02[a]	2.0	3.1	11	1	0.2
0211−122	950 ± 200	1	102	102	43.42 ± 01	2.2	1.6	22	3–4	1.6
0214+183	1200 ± 100	1	48	48	42.78 ± 05[a]	0.8	2.6	6	1	0.5
0355−037	1400 ± 100	0	94	105	43.19 ± 02	1.6		7	1–2	1.0
0417−181	1550 ± 75	1	42	42	43.21 ± 02	1.1	4.9	10	1	0.4
0529−549	1550 ± 75	1	41	45	43.44 ± 02[a]	1.4	1.8	9	2	0.8
0748+134	1300 ± 100	0	45	60	43.50 ± 01	1.6		21	1	0.7
0828+193	1350 ± 150	1	37	103	43.84 ± 01	2.1	0.3	12	3	0.9
0943−242	1575 ± 75	1	15	15	44.07 ± 01	1.4	0.1	3	1	0.4
1243+036	1550 ± 75	0	46	135	44.49 ± 01	7		25	4	1.2
1357+007	1275 ± 75	1	20	45	43.60 ± 03	1.1	0.1	8	2	0.9
1410−001	900 ± 75	0	53	79	44.12 ± 01	3.5		14	2	1.1
1436+157[b]	1100 ± 75	1	51	88	43.70 ± 02[a]	2.1	6.0	3	1–2	0.4
1545−234	900 ± 75	1	32	45	43.56 ± 01	1.6	0.1	13	1–2	0.8
1558−003	950 ± 50	0	46	77	43.85 ± 01	2.4		16	1	0.4
1707+105	670 ± 50	0	97	134	43.62 ± 01	2.7				
2202+128	1150 ± 75	1	37	37	43.67 ± 01	1.7	0.1	9	4–5	2.6
4C41.17	1000 ± 100	0	59	98	44.74 ± 03	6.5		20	3	1.2

[a] measured only from high resolution spectra, which sometimes underestimates the flux.
[b] 1436+157 USS quasar; the parameters are for the narrow line component only.
Note: The size parameter $D^{20\%}_{\mathrm{Ly}\alpha}$ was defined because in the weakest Lyα regions, the most extended detected emission was at ∼ 20% of the Lyα peak flux. For those weakest sources $D^{20\%}_{\mathrm{Ly}\alpha}$ is therefore equal to $D^{\mathrm{tot}}_{\mathrm{Ly}\alpha}$

Typically detection threshold
~ 1.e-18 erg/s/cm2

~10-30% > 100 kpc
~50% > 50 kpc

Presence of large halo is related with overdensity ?

From Venemans et al. 2007

Field	z	N^{a}_{img}	N^{b}_{spec}	N^{c}_{conf}	N^{d}_{none}	$N^{e}_{low\,z}$	N^{f}_{extra}	N^{g}_{tot}	n_{rg}/n^{h}_{field}	σ^{i}_{v} km s^{-1}	M^{j}_{pcl} $10^{14}\,M_{\odot}$
1602	2.04	2	–	–	–	–	–	–	–	–	–
2048	2.06	10	3	2	1	0	1	3	$1.2^{+0.8}_{-0.7}$	–	–
1138	2.16	37	11	11	0	0	4	15	4 ± 2	900 ± 240	3–4
0052	2.86	57	36	35	1	0	2	37	$3.0^{+0.5}_{-0.4}$	980 ± 120	3–4
0943	2.92	65	30	25	4	1	3	28	$3.2^{+0.9}_{-0.7}$	715 ± 105	4–5
0316	3.13	77	30	28	1	1	3	31	$3.3^{+0.5}_{-0.4}$	640 ± 195	3–5
2009	3.16	21	9	9	0	0	2	11	$1.7^{+0.8}_{-0.6}$	515 ± 90	–
1338	4.11	54	36	34	2	0	3	37	$4.8^{+1.1}_{-0.8}$	265 ± 65	6–9
0924	5.20	14	8	6	0	2	0	6	$2.5^{+1.6}_{-1.0}$	305 ± 110	4–9

1138 .. 250kpc x 125kpc
1338 .. 130kpc x 45kpc

The largest Lyα haloes appear in the densest environment of other Lyα emitters?

“Spiderweb” galaxy (MRC1138-262) at z=2.2

Assembly of galaxies and Lyα Halo

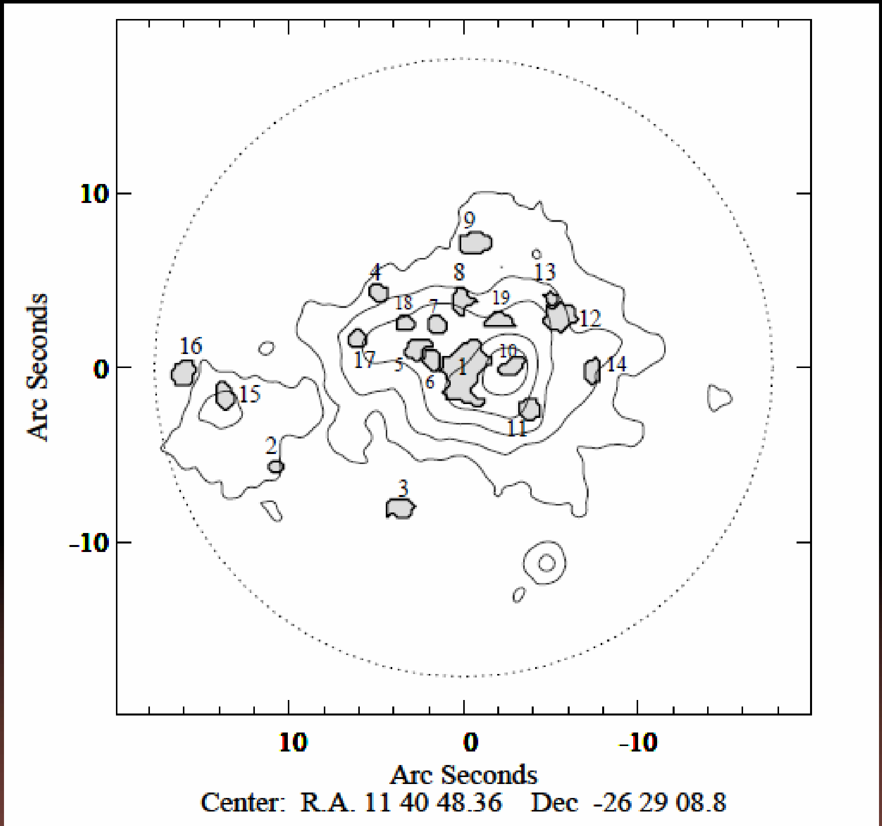

Hatch et al. 2009

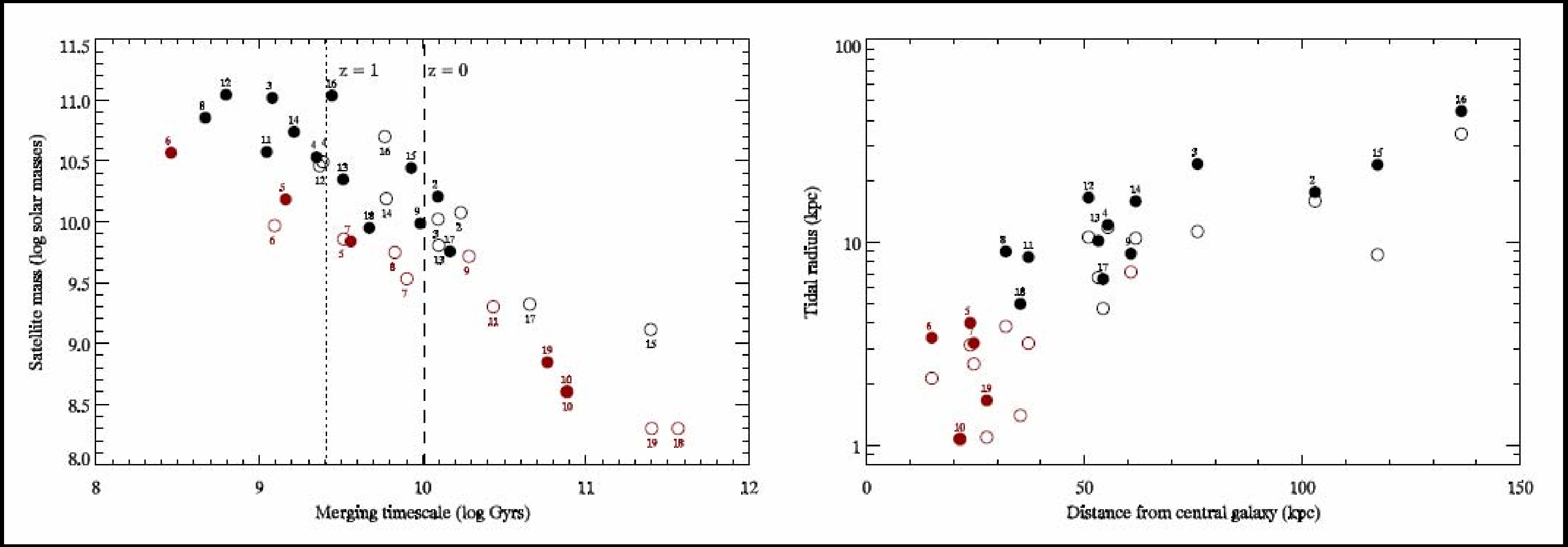

ID	SFR ($M_\odot\ yr^{-1}$)	Mass ($10^9\ M_\odot$)	Mass (upper limit) ($10^9\ M_\odot$)	Detection method
1	15.6 ± 0.7	1100 ± 200	9900^{+300}_{-1300}	Lyα,Hα, BB
2	0.0 ± 0.4	12^{+13}_{-7}	16^{+15}_{-1}	BB
3	2.2 ± 0.5	11 ± 8	105^{+18}_{-54}	Photo-z
4	0.0 ± 0.4	31^{+24}_{-16}	34^{+18}_{-8}	BB
5	5.2 ± 0.5	$7.2^{+0.4}_{-1.4}$	15 ± 3	Lyα
6	4.4 ± 0.4	$9.3^{+5.4}_{-3.9}$	37^{+175}_{-6}	Lyα
7	3.8 ± 0.4	$3.4^{+0.6}_{-0.6}$	$6.9^{+2.6}_{-1.9}$	Lyα
8	1.2 ± 0.5	$5.6^{+4.5}_{-4.1}$	72^{+3}_{-64}	Hα
9	7.2 ± 0.5	$5.2^{+1.5}_{-3.4}$	$9.7^{+64}_{-2.8}$	Lyα
10	4.4 ± 0.4	$0.4^{+0.3}_{-0.1}$	$0.4^{+0.8}_{-0.1}$	Lyα,Hα
11	5.8 ± 0.4	$2.0^{+1.1}_{-1.0}$	38^{+13}_{-32}	Lyα,Hα
12	2.2 ± 0.6	29^{+29}_{-9}	111^{+150}_{-42}	Lyα,Hα, BB
13	0.0 ± 0.4	$6.4^{+6.2}_{-2.9}$	22 ± 9	BB
14	0.4 ± 0.7	16^{+18}_{-5}	55^{+13}_{-10}	BB
15	5.2 ± 0.4	$1.3^{+1.0}_{-0.5}$	28^{+18}_{-25}	Lyα
16	0.7 ± 0.7	50^{+35}_{-20}	110^{+54}_{-31}	BB
17	1.8 ± 0.4	$2.1^{+0.8}_{-0.7}$	6^{+4}_{-2}	Morphology
18	1.8 ± 0.4	$0.2^{+1.0}_{-0.1}$	9^{+8}_{-9}	Morphology
19	1.3 ± 0.5	$0.2^{+1.7}_{-0.1}$	$0.7^{+20}_{-0.2}$	Morphology

Table 1. The mass is derived from fitting the photometry to a single exponentially declining star formation history. The mass upper limit is derived from a two-model fit to the photometry, in which one model is maximally old, i.e., 3 Gyrs and the other is maximally young (1 Myr). Column 5 lists the detection methods by which the galaxy was selected to be in the protocluster. Lyα, Hα are objects which have an excess of line-emission placing them at the same redshift as the radio galaxy, BB indicates galaxies with strong Balmer breaks inferred from large observed J_{110}-H_{160} colours.

< 150 kpc
Merge to the central object
To increase the mass ~2x

SF will be exhausted before the merging?

B20902+34 Radio Galaxy in Giant HI Envelope? Adams et al. (2008)

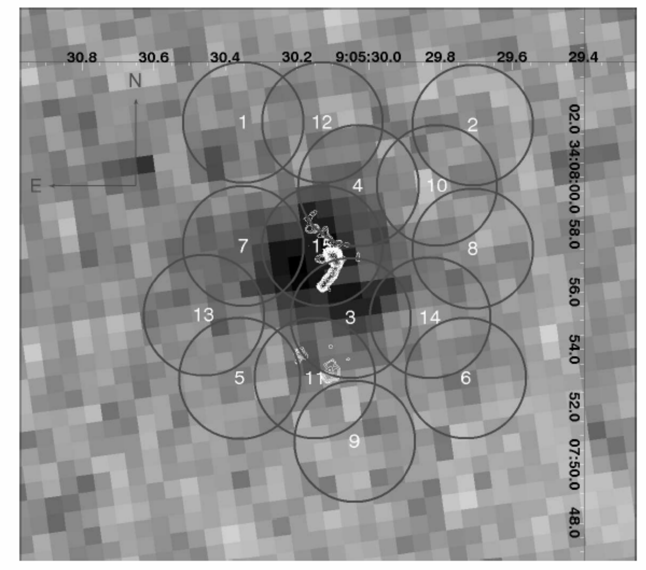

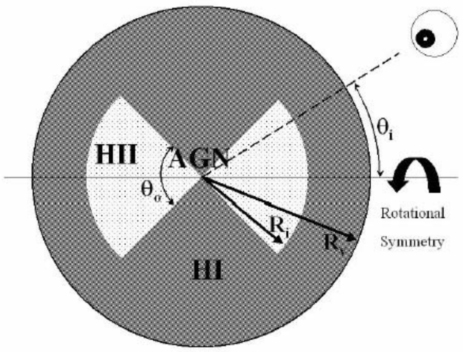

Fig. 2.— The geometry of our simulation. θ_i is the inclination as constrained by Carilli (1995). R_v is the system's virial radius. R_i is the ionization radius of the cones. θ_o is the opening angle of the ionization cones assumed here to be 90°. R_i, R_v, θ_o, and two variables controlling the velocity field are the model's five tunable parameters.

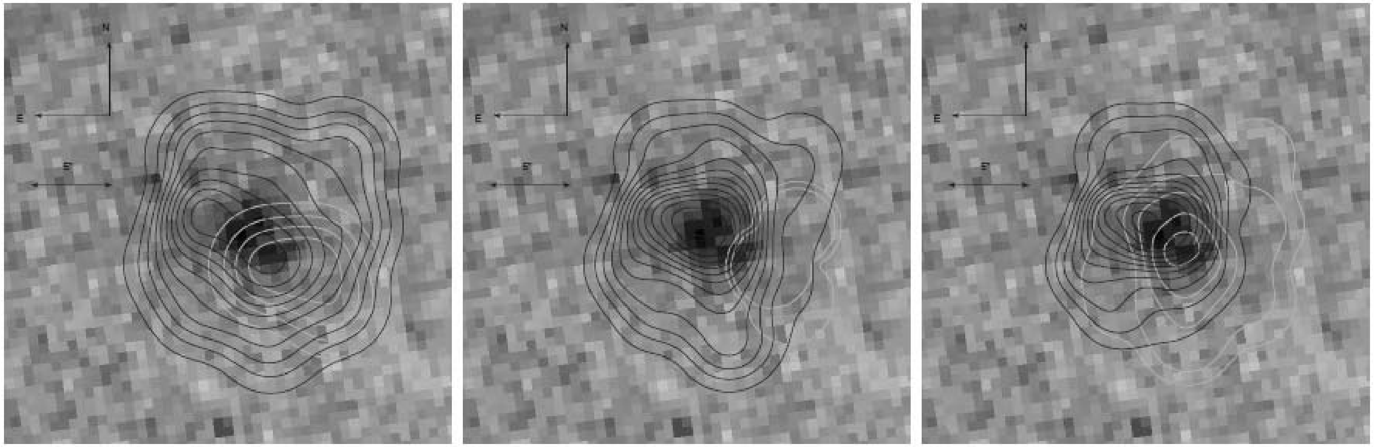

(a) Observed

(b) Simulated, Spectral Decomposition

(c) Simulated, Origin Cone Decomposition

Lyα Blobs and the Halo of Powerful Radio Galaxies How they are related or different?

- Large dimension, A large fraction of the energy comes from the radio jet for the radio galaxies.
  alignment effect / RLQ-RQQ comparison

- Host galaxies:
  PRGs are more massive, central dominant?
  stellar mass of LABs < a few x 10^{11} M_{sun}
  though more sample needed.

- After radio jet turned off, PEG ~ Lyα Blobs?

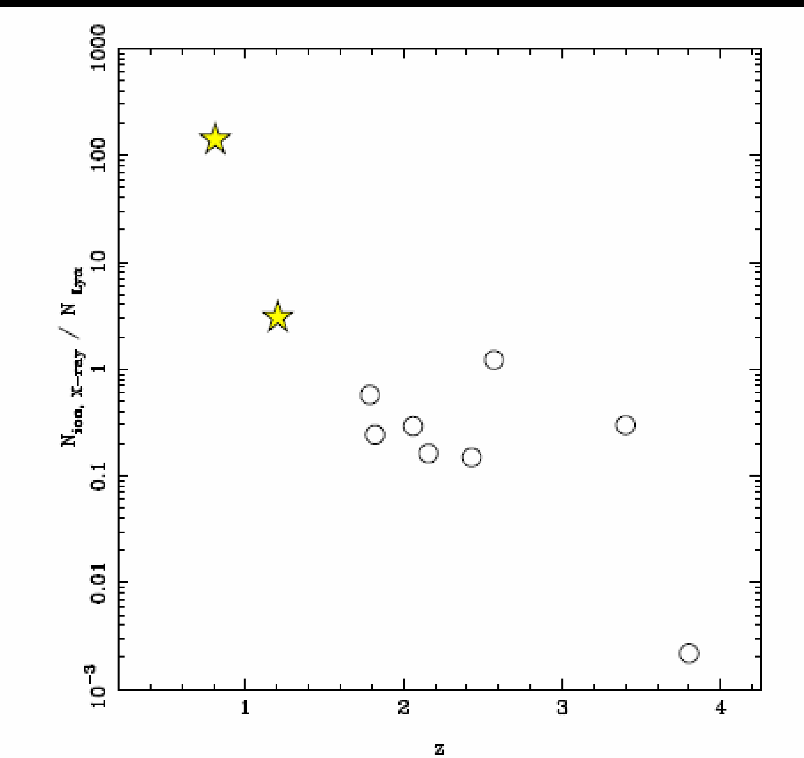

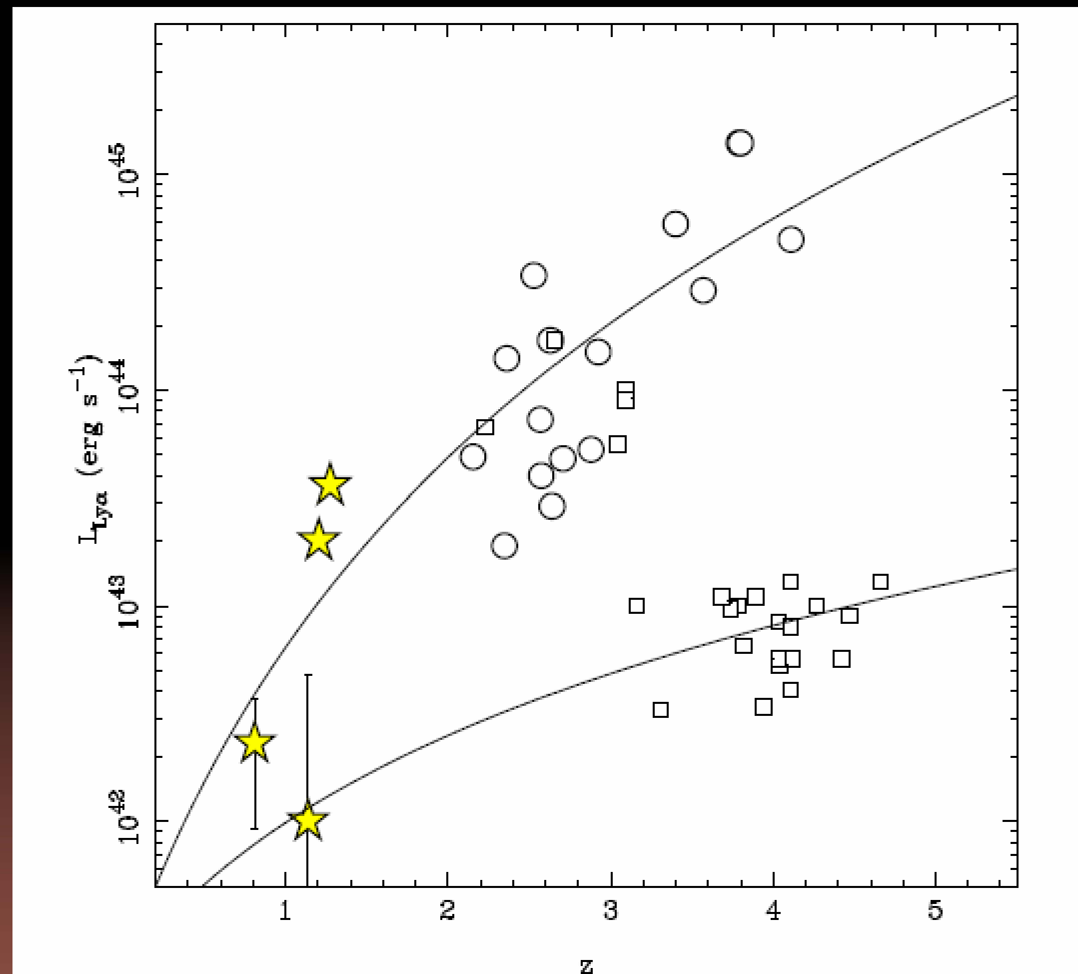

Zirm et al. 2009

4. Summary

- Large Lyα Blobs are associated with massive objects
  ~10^{11}-10^{12} M_{sun}

- A fraction of Lyα Blobs are bright sub-mm sources
  ➔ massive starburst galaxies

- >15-20% of the Lyα Blobs with 30-150 kpc
  host AGN with L~10^{43-44} erg/s .
  The fraction seems even higher for large Blobs.

- Yet, there are objects with no signiture of sufficient
  Starburst and AGN activity to power Lyα emission.

<u>Lyα Blobs are unique objects to study early phase of (massive) galaxy formation , especially their gaseous environment</u>

Backup

Motivation to Search/Study Lyα Blobs

Gaseous Environment of High-Redshift Galaxies

- Gas Bounded in Collapsed Halo
- Infall / Accretion
- Outflow [SNe / AGN feedback]

High-Redshift Lyα Halo and Galaxy Formation

Early Collapse Phase -- virial shock → cooling radiation
Pure Lyα objects ?

Some stars form + Lyα emission from further accreting gas

Major star formation → photo-ionization by massive stars

AGN activity → photo-ionization / jets / feedback

Galactic superwind → shock excitation / ionization

Interaction with cooling flow gas in dense environment
Ionization of HI halo by background UV

What powers extended Lyα emission?

- Photo-ionization
  - Massive Stars
  - Active Galactic Nuclei
  - UV background
- Shock heating/ionization
  - Galactic superwinds
  - AGN radio jet / radiation outflow
- Scattering

Size & Surface Brightness

Emitters with EW_{rest} > 20 A

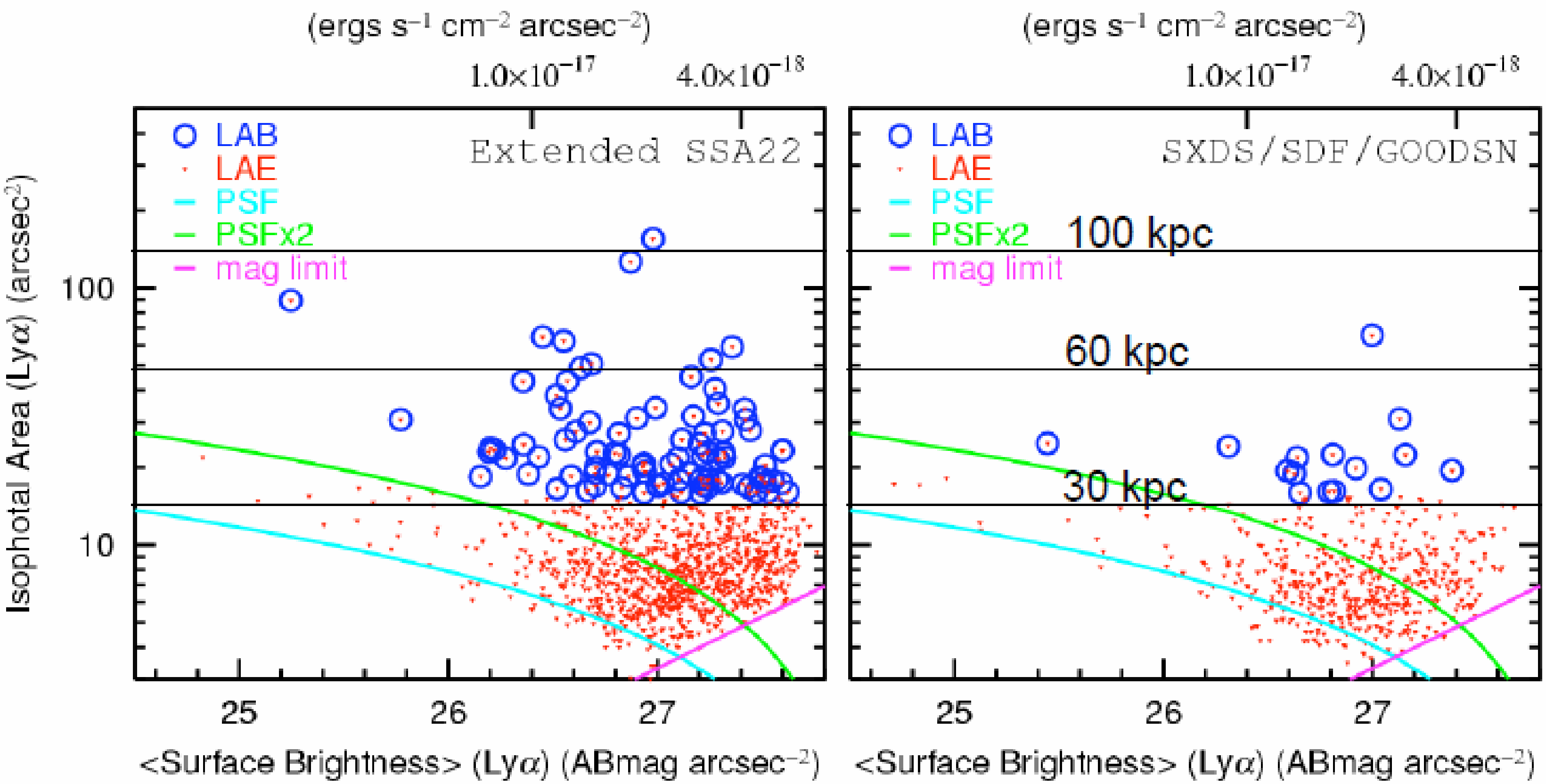

Extended SSA22 (1.4 deg^2)
Proto-cluster & The Surrounding Regions

SXDS/SDF/GOODSN (1.2 deg^2)
Blank Fields

Matsuda, TY, et al. 2008

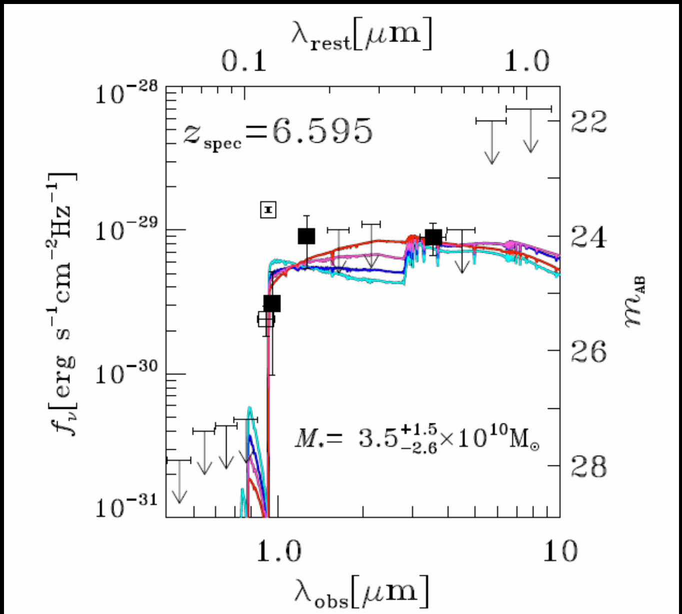
λrest[μm]
0.1
1.0
zspec=6.595
M*= 3.5+1.5−2.6×10^10 M⊙
fν[erg s−1cm−2Hz−1]
mAB
1.0
10
λobs[μm]

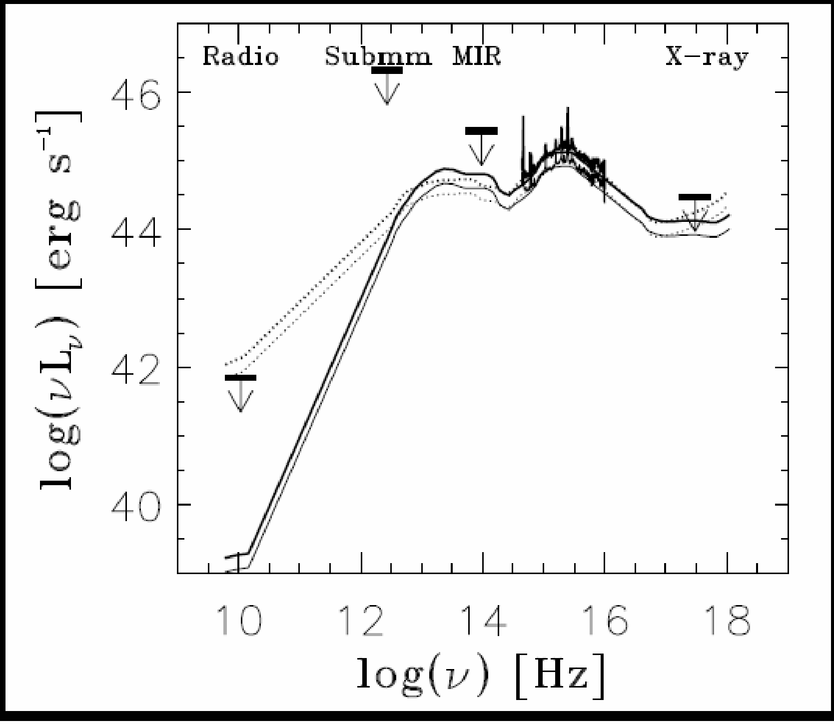
Radio
Submm
MIR
X−ray
log(νLν) [erg s−1]
log(ν) [Hz]

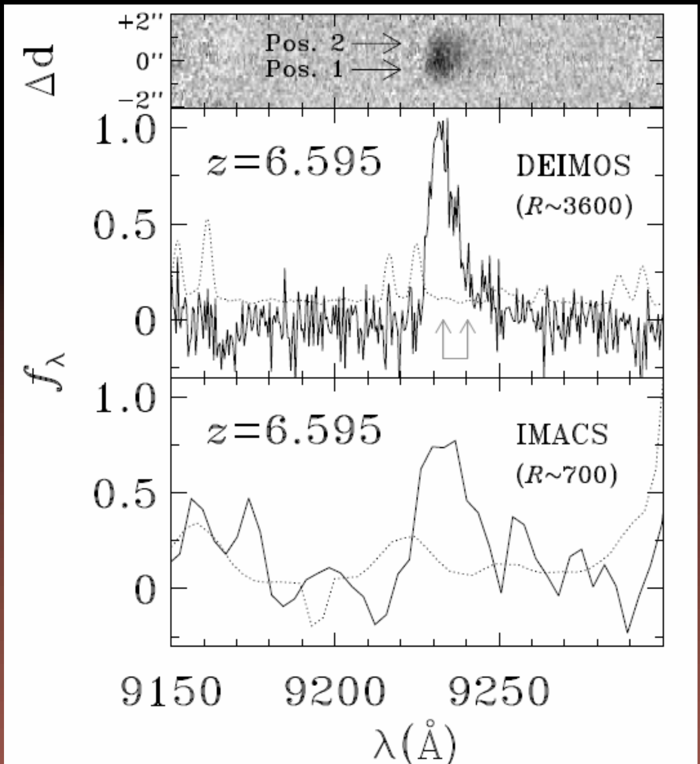
Δd
Pos. 2
Pos. 1
z=6.595
DEIMOS
(R~3600)
z=6.595
IMACS
(R~700)
fλ
λ(Å)

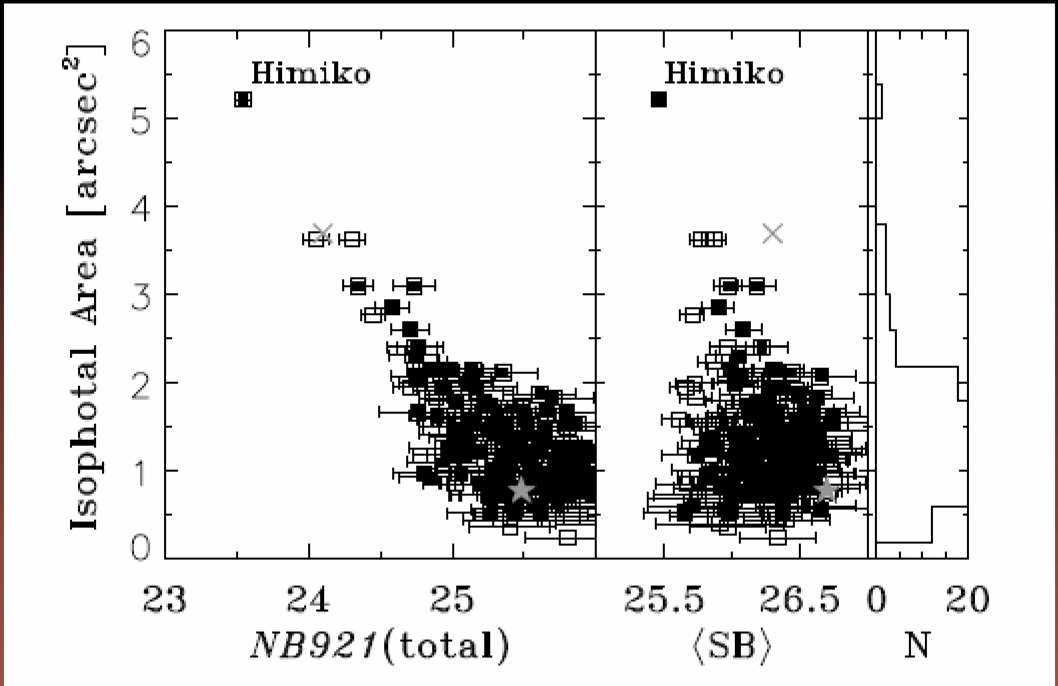
Himiko
Himiko
Isophotal Area [arcsec2]
NB921(total)
⟨SB⟩
N

Lyα Haloes of Lyman Break Galaxies

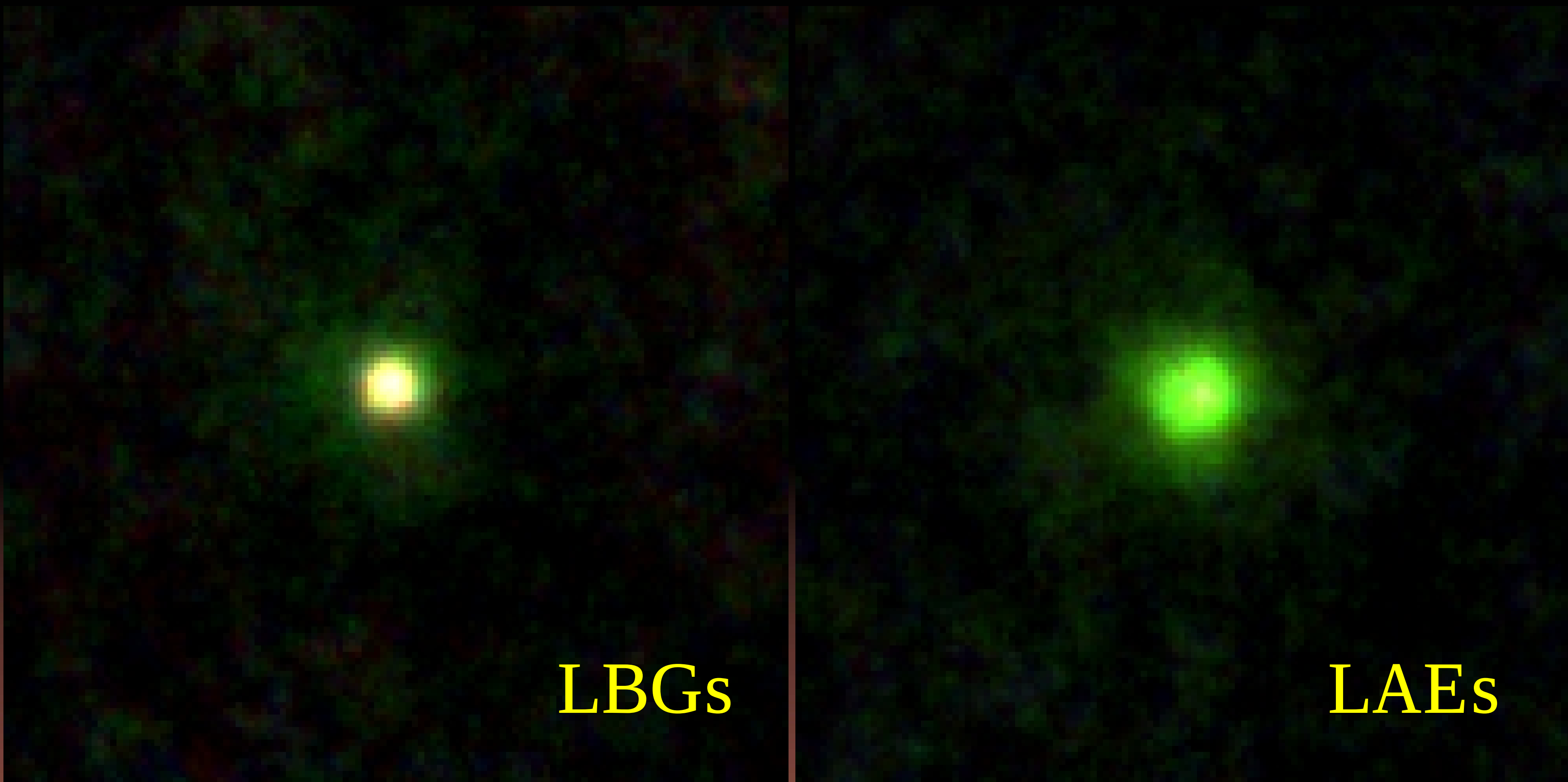

Z=3.1 LBGs and LAEs

Not Lyα Blobs

Lyα Haloes of Lyman Break Galaxies

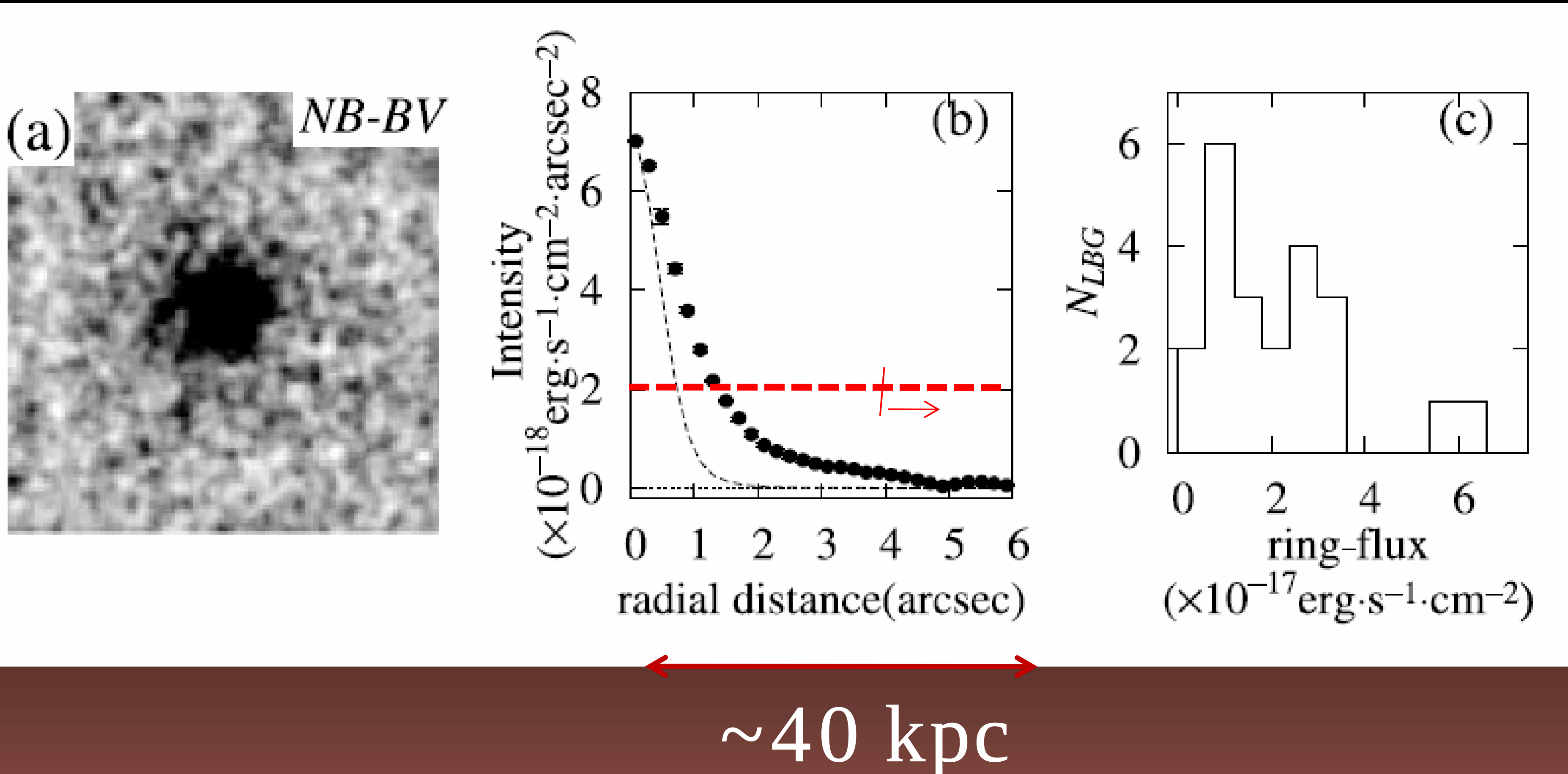

Lyα Haloes of Lyman Break Galaxies

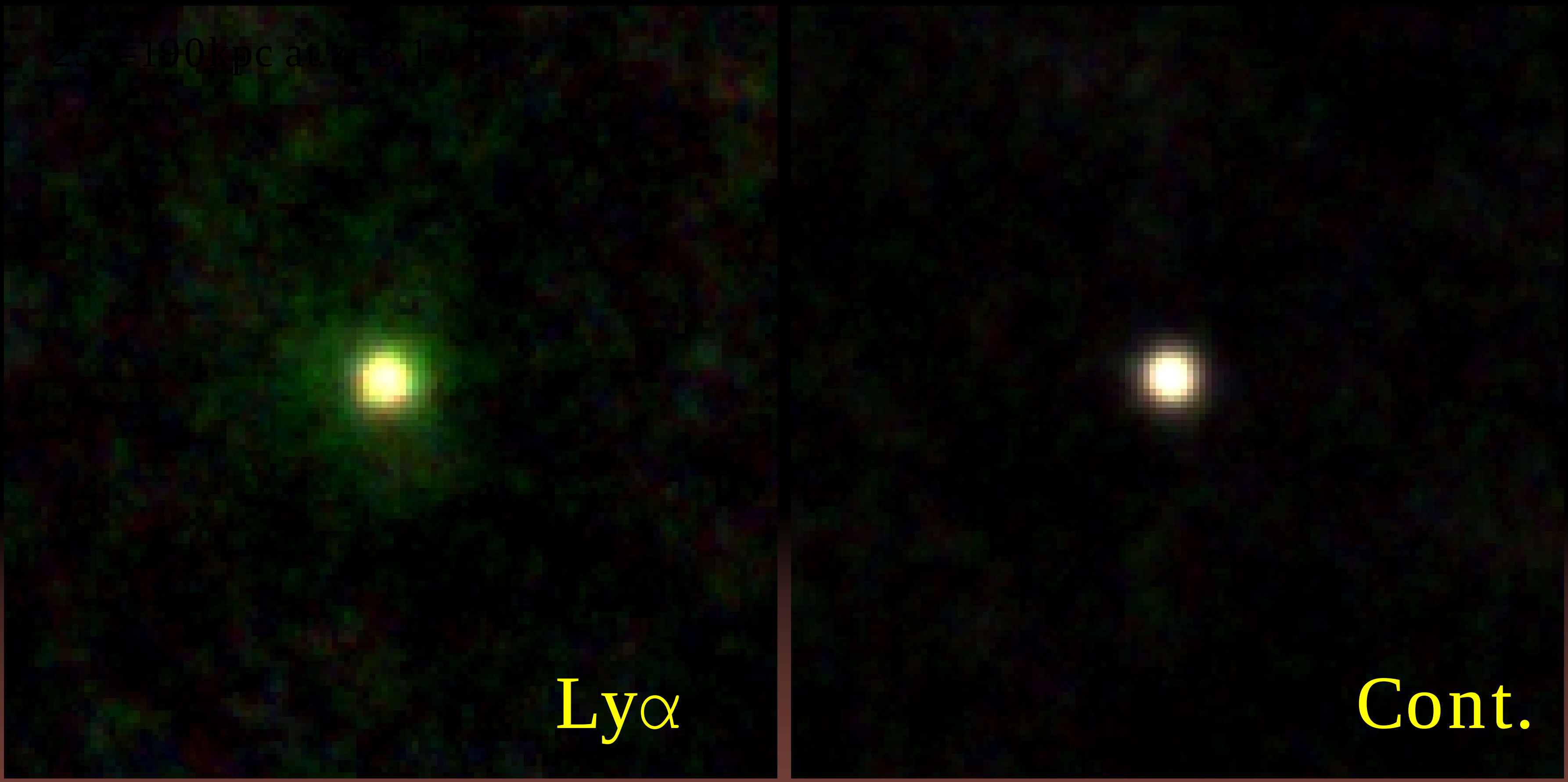

Stack of 22 known LBGs at z~3.1
(which are not detected in our LAE or LAB sample)

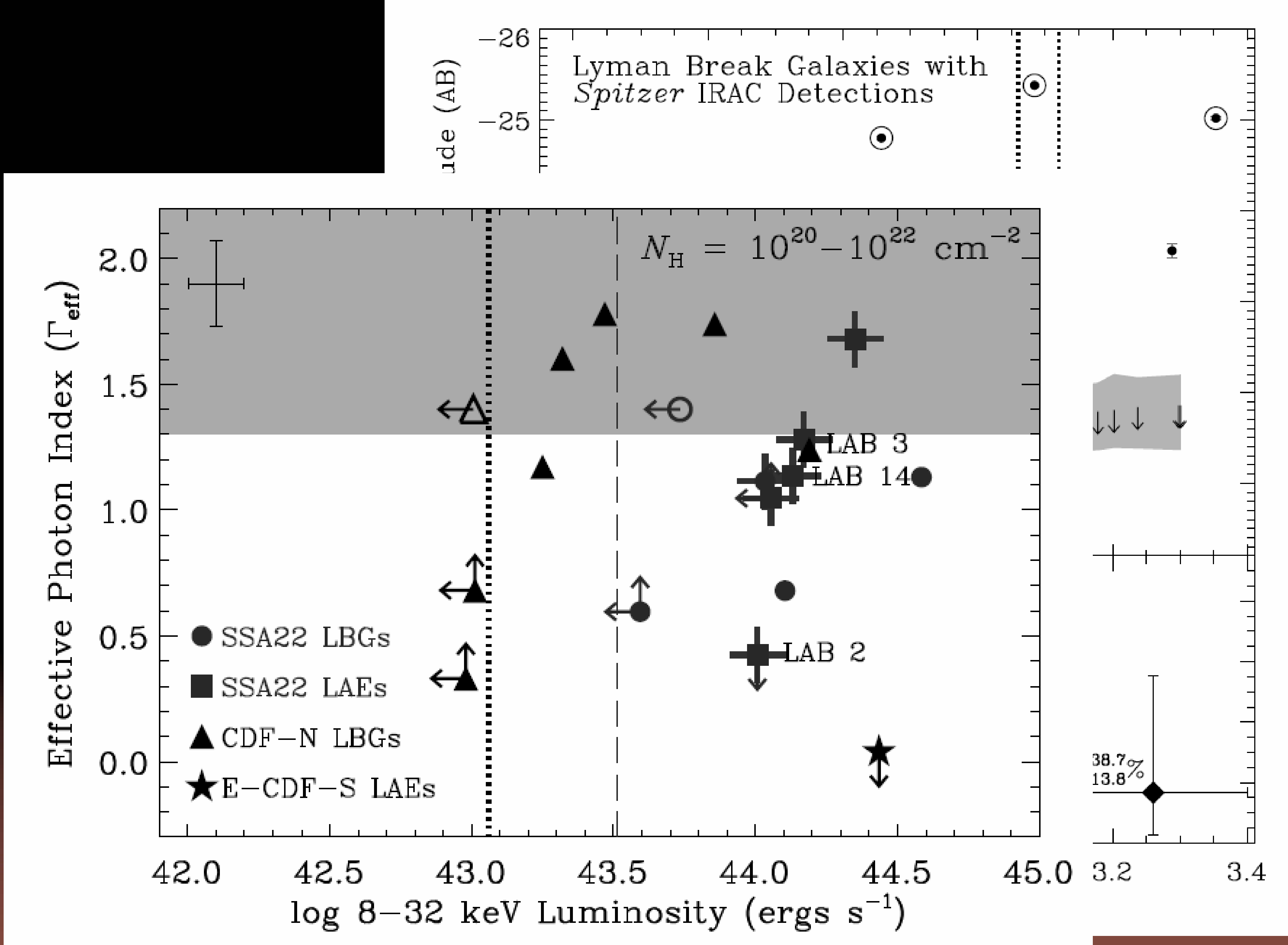
Lyman Break Galaxies with
Spitzer IRAC Detections
N_H = 10^{20}–10^{22} cm^{-2}
Effective Photon Index (Γ_{eff})
log 8–32 keV Luminosity (ergs s^{-1})
LAB 3
LAB 14
LAB 2
SSA22 LBGs
SSA22 LAEs
CDF–N LBGs
E–CDF–S LAEs
38.7%
13.8%

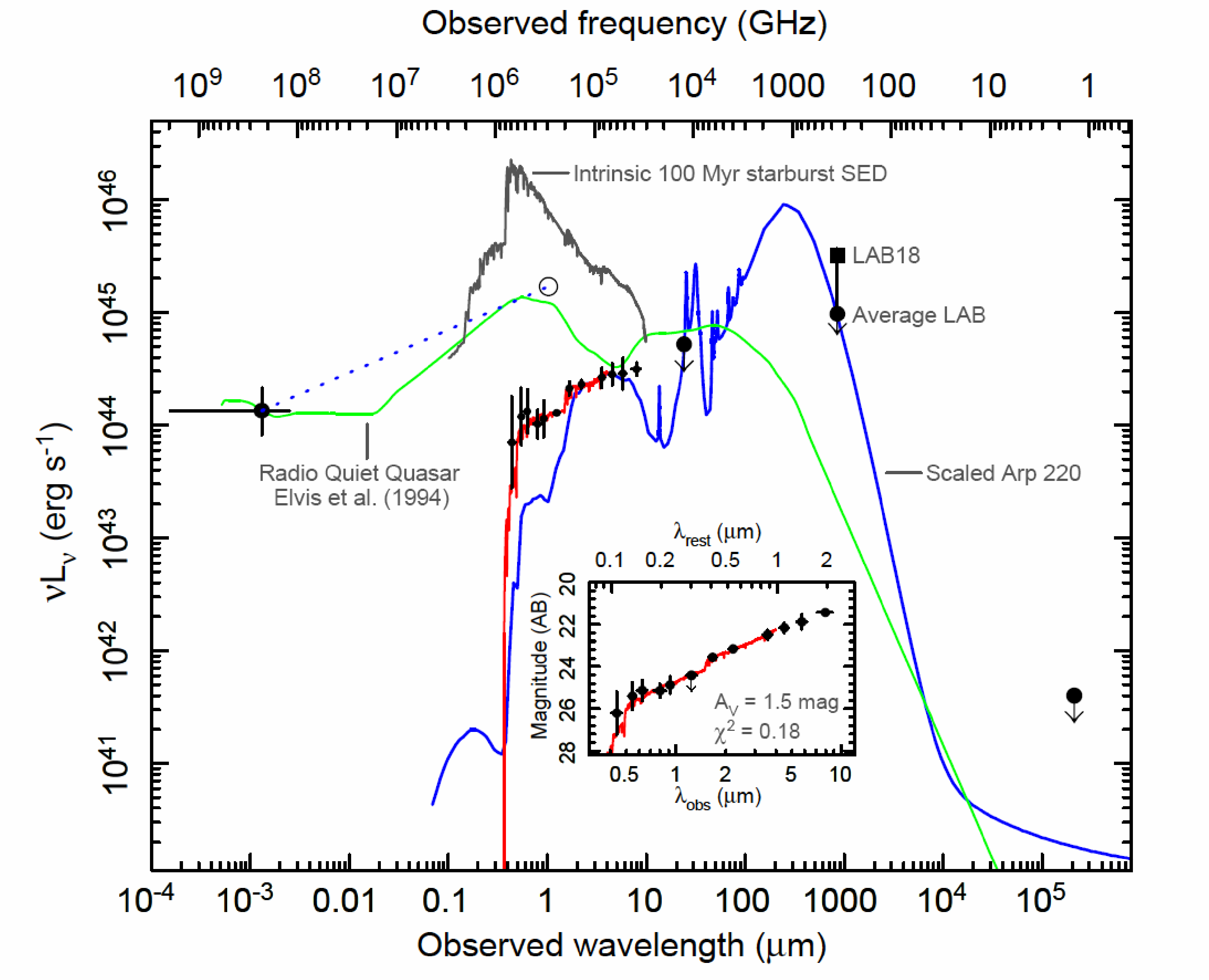

Observed frequency (GHz)
10^9
10^8
10^7
10^6
10^5
10^4
1000
100
10
1
Intrinsic 100 Myr starburst SED
LAB18
Average LAB
Radio Quiet Quasar
Elvis et al. (1994)
Scaled Arp 220
νLν (erg s^-1)
10^46
10^45
10^44
10^43
10^42
10^41
λrest (μm)
0.1 0.2 0.5 1 2
Magnitude (AB)
20 22 24 26 28
AV = 1.5 mag
χ^2 = 0.18
0.5 1 2 5 10
λobs (μm)
10^-4
10^-3
0.01
0.1
1
10
100
1000
10^4
10^5
Observed wavelength (μm)

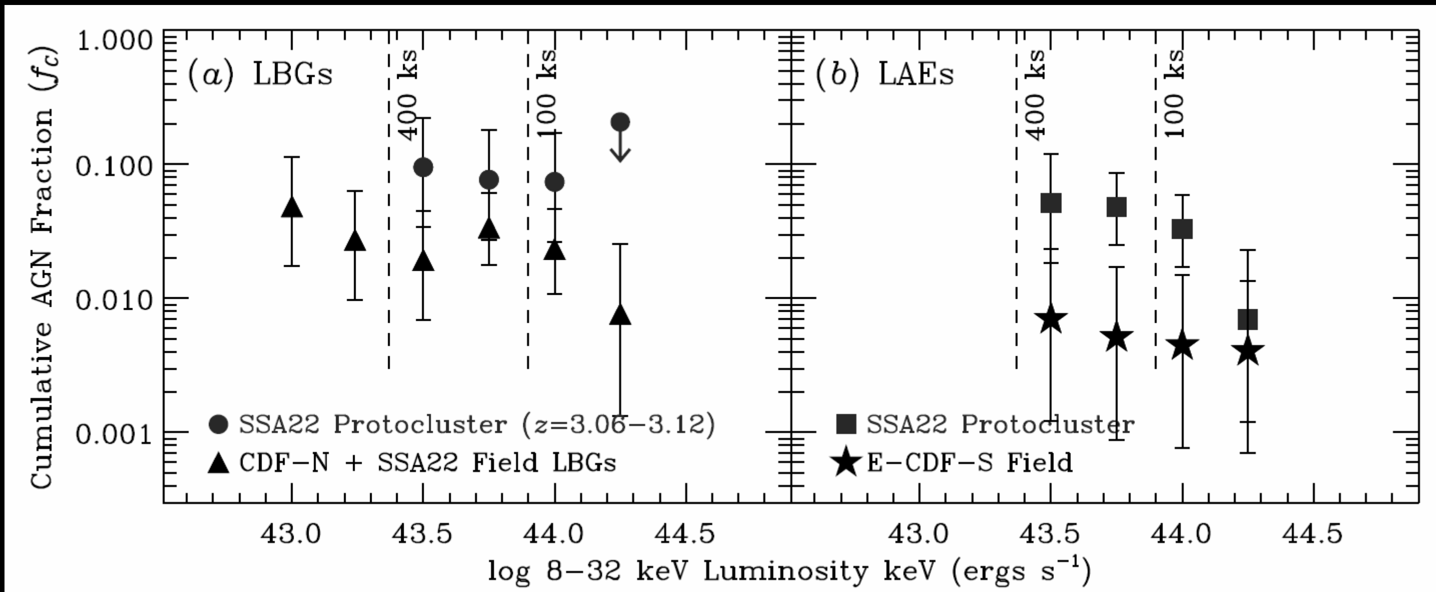

$\log L_{8-32\ \mathrm{keV}}$ (ergs cm^{-2} s^{-1})	SSA22 Protocluster			CDF + SSA22 Field			
	N_{AGN}	N_{gal}	f_C(%)	N_{AGN}	N_{gal}	f_C(%)	Enh[a]
$z \approx 2$–3.4 Lyman Break Galaxies							
43.50	2	21	$9.5^{+12.7}_{-6.1}$	2	103	$1.9^{+2.6}_{-1.3}$	$4.9^{+11.7}_{-3.9}$
43.75	2	26	$7.7^{+10.2}_{-5.0}$	4	118	$3.4^{+2.7}_{-1.6}$	$2.3^{+5.8}_{-1.7}$
44.00	2	27	$7.4^{+9.8}_{-4.8}$	3	128	$2.3^{+2.3}_{-1.3}$	$3.2^{+7.8}_{-2.4}$
44.25	0	27	<20.7	1	130	$0.8^{+1.8}_{-0.6}$	<27.0
$z = 3.1$ Lyα Emitters							
43.50	2	39	$5.1^{+6.8}_{-3.3}$	1	142	$0.7^{+1.6}_{-0.6}$	$7.3^{+17.0}_{-6.2}$
43.75	4	83	$4.8^{+3.8}_{-2.3}$	1	194	$0.5^{+1.2}_{-0.4}$	$9.3^{+16.9}_{-8.7}$
44.00	4	121	$3.3^{+2.6}_{-1.6}$	1	223	$0.4^{+1.0}_{-0.4}$	$7.4^{+13.3}_{-6.9}$
44.25	1	144	$0.7^{+1.6}_{-0.6}$	1	246	$0.4^{+0.9}_{-0.3}$	$1.7^{+5.7}_{-1.3}$

Rest-frame U-V color

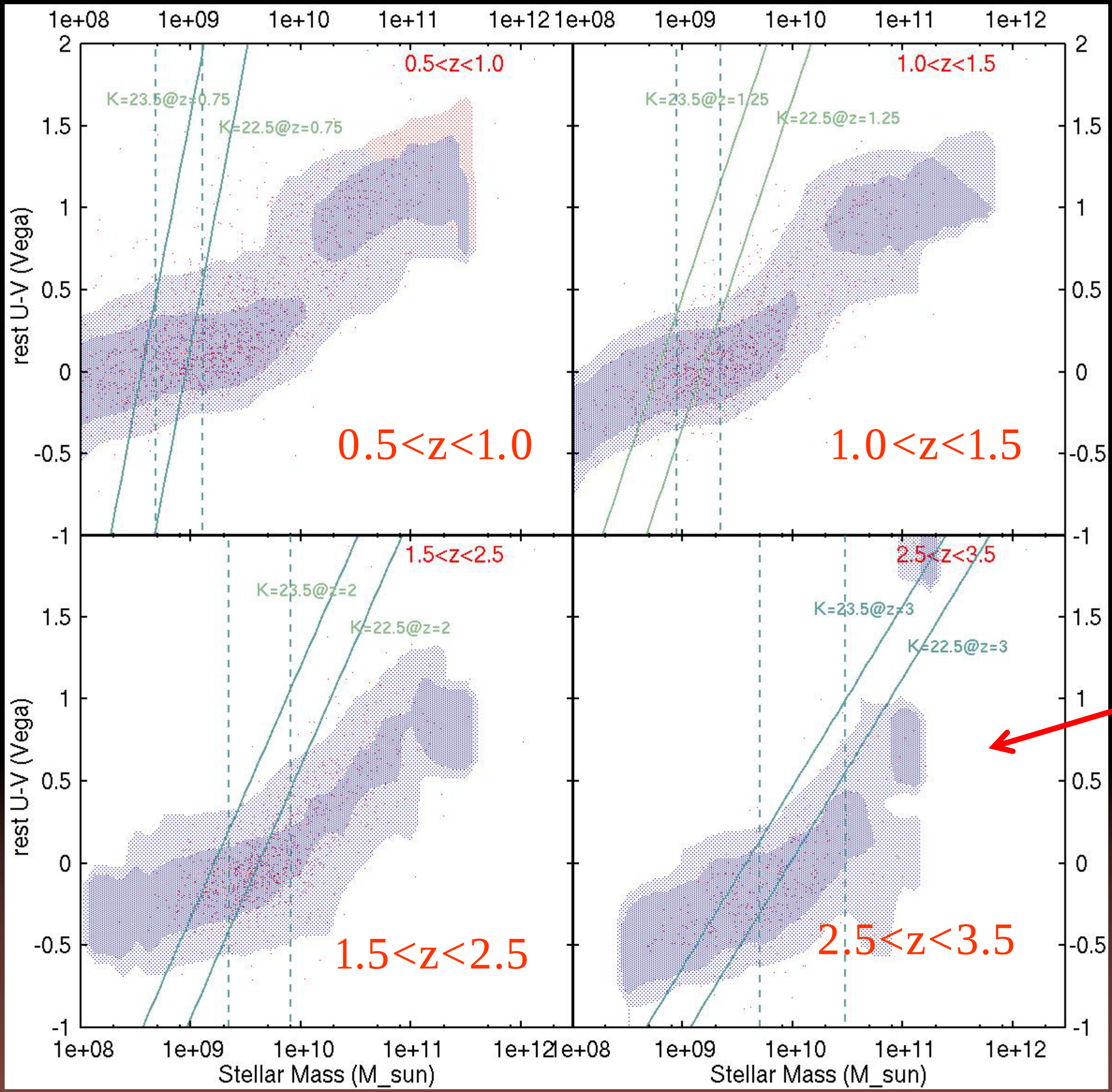

Stellar Mass

Also see, e.g., Kajisawa and Yamada 2005, 2006

Masaru Kajisawa, 2008 April, JAS

Appendix: Lyα Blobs ZOO

SSA22 LAB1 z=3.1 (Steidel et al. 2000; Matsuda, TY, et al. 2004)

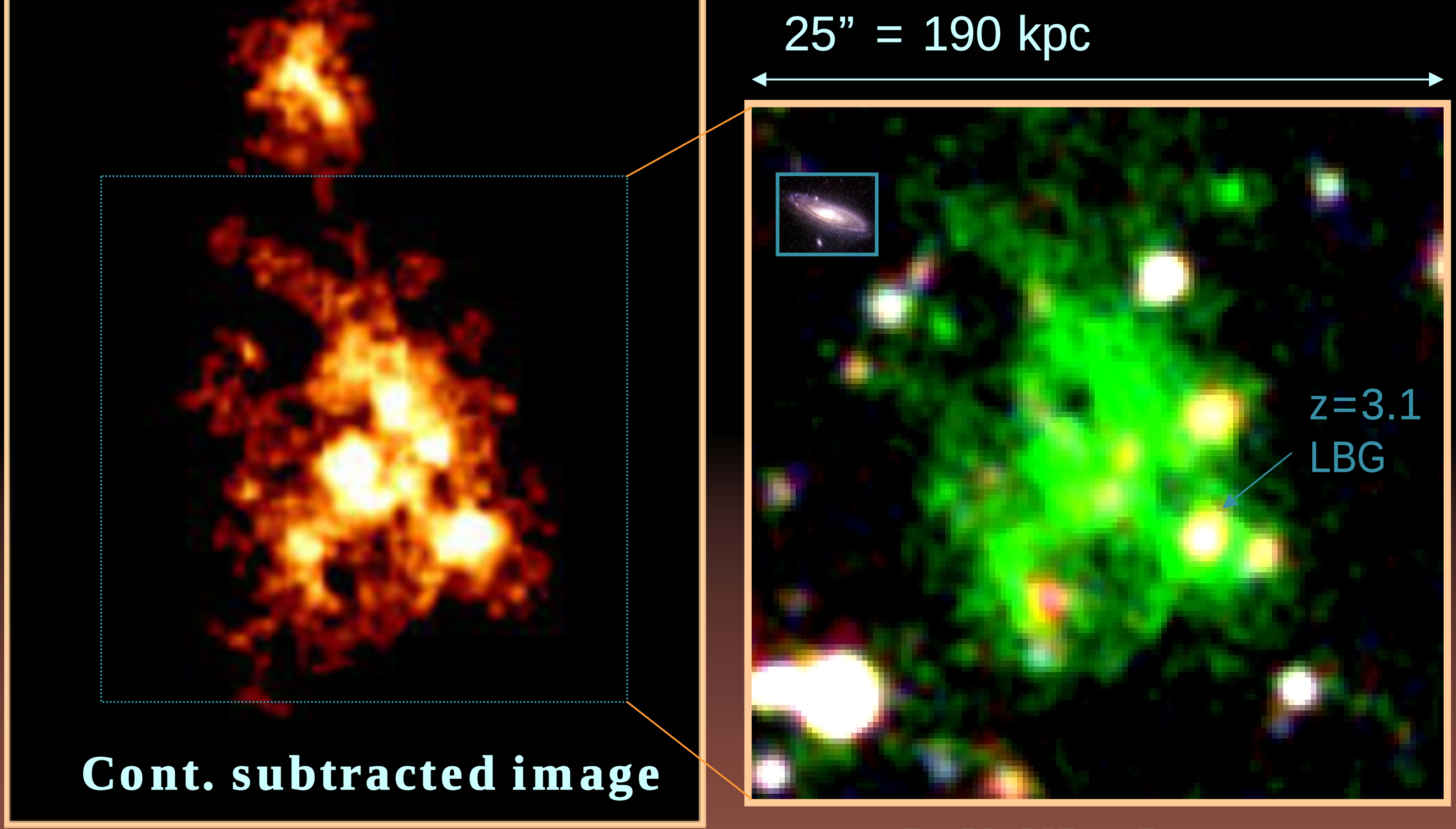

B, V, NB. Lyα= green

SSA22 LAB1 gas motion Δv~2000km/s

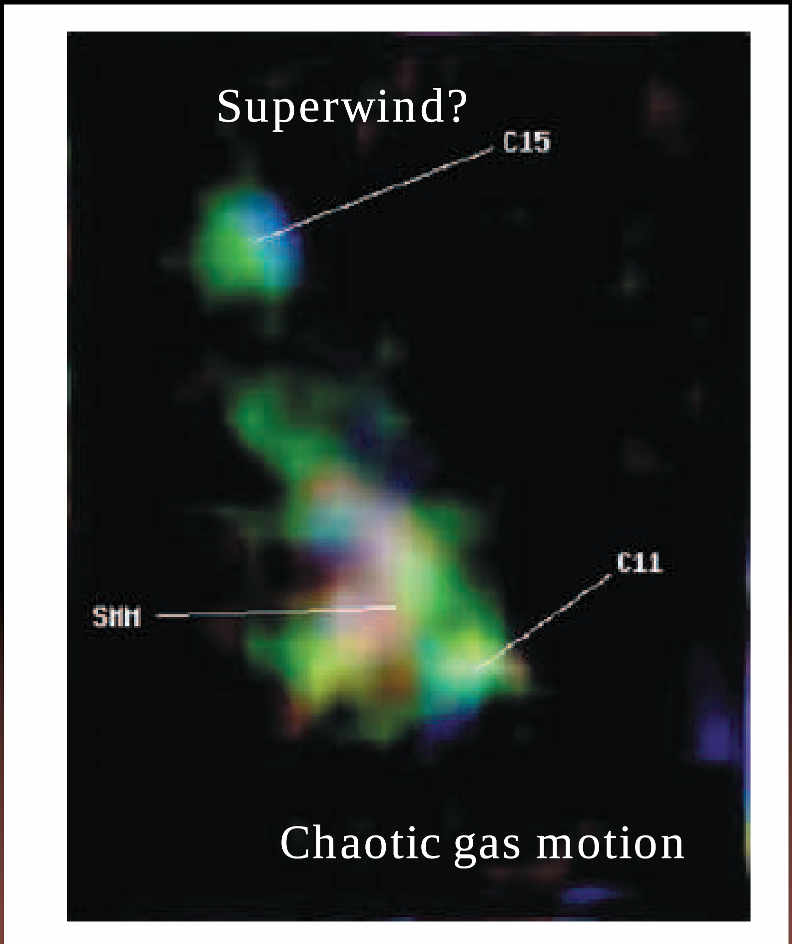

Bower et al. 2004 SAURON

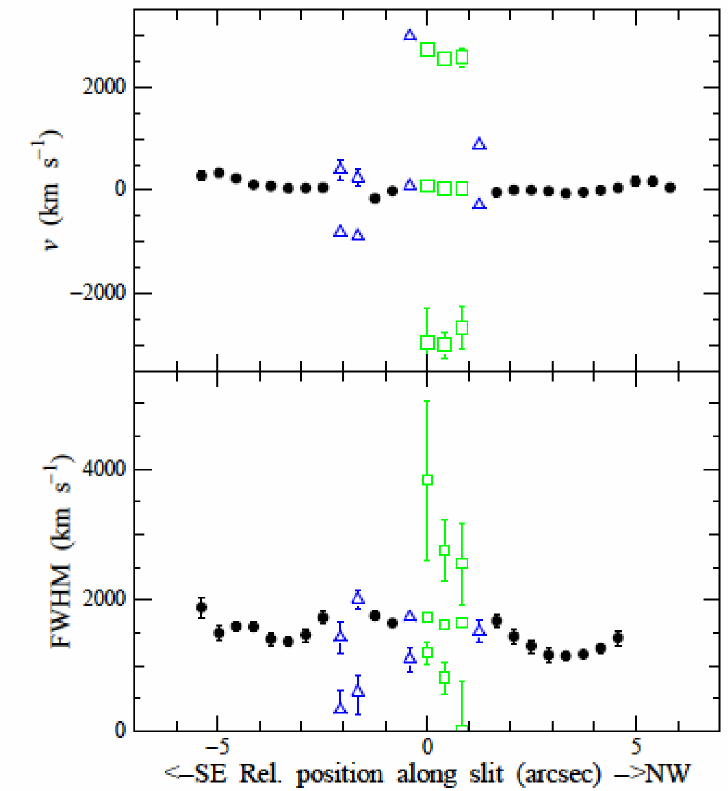

Fig. 4.— The spatial variations of the peak velocities of the Lyα nebula (upper panel) and the FWHMs corrected for the instrumental resolution (lower panel). Data for the triple-peaked regions and the double-peaked regions are shown by open squares and open triangles, respectively. Those for the single-peaked regions are shown by filled circles. Measurement errors are shown by vertical bars.

Ohyama et al. 2003 longslit FOCAS

SSA22 LAB1 sub-mm observations

SCUBA ~18mJy (Chapman et al. 2004)

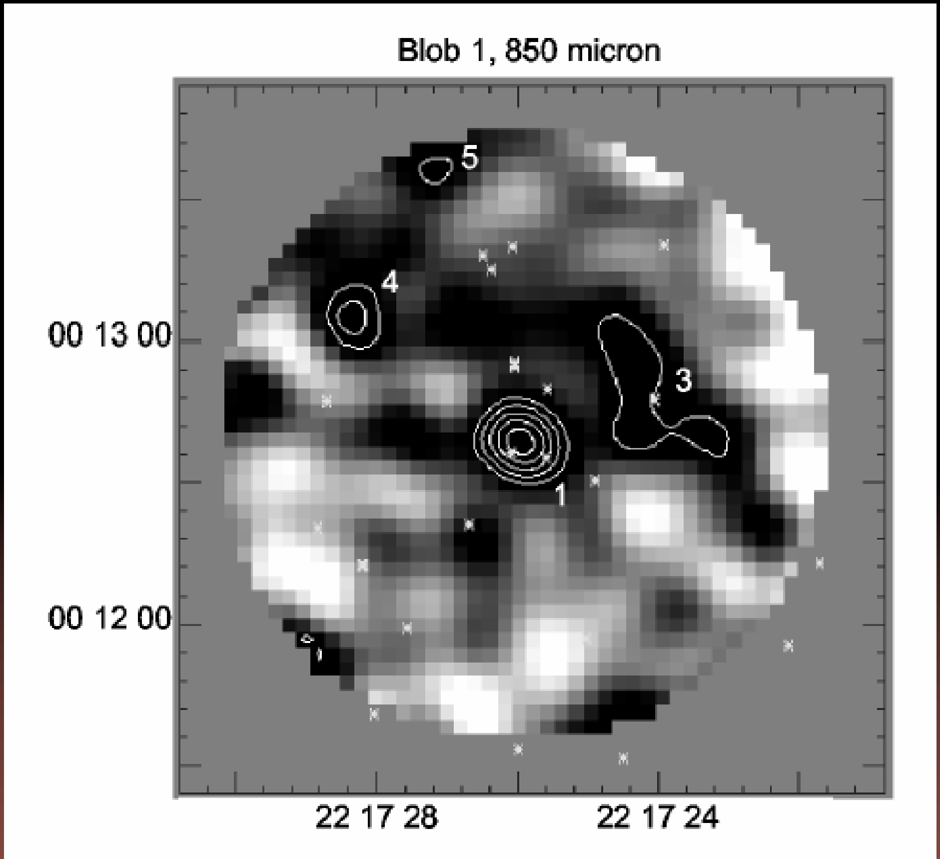

SMA < 4mJy/beam
(Matsuda et al. 2007)

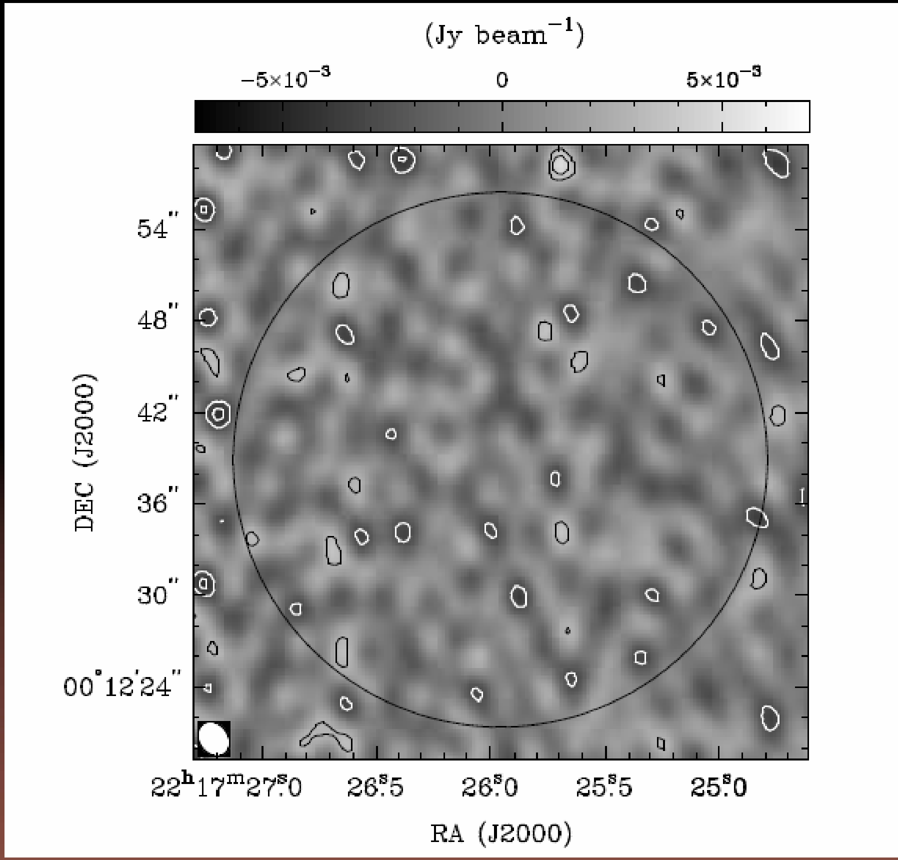

Extended? Θ > 4-5" if Gaussian

SSA22 LAB1

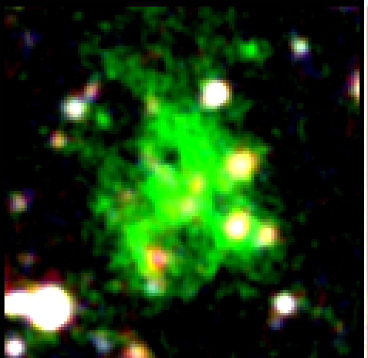

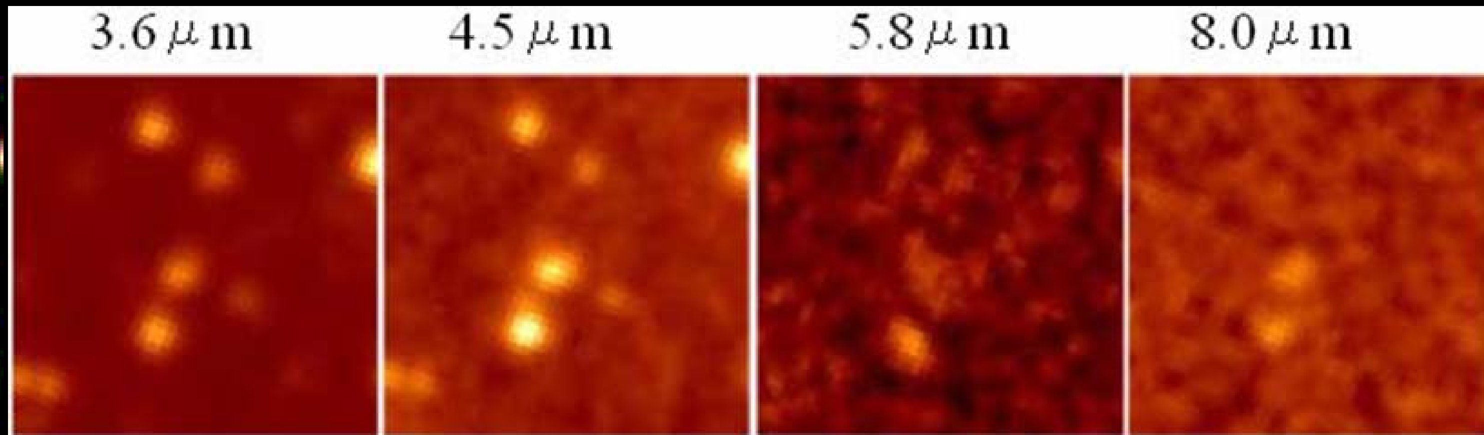

25”

Also see Geach et al. (2006)

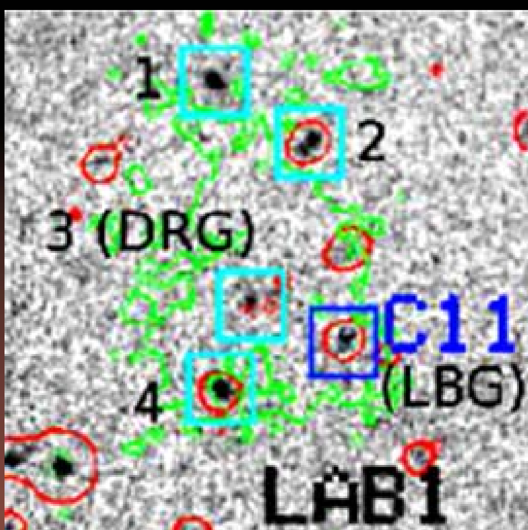

Subaru MOIRCS Ks band

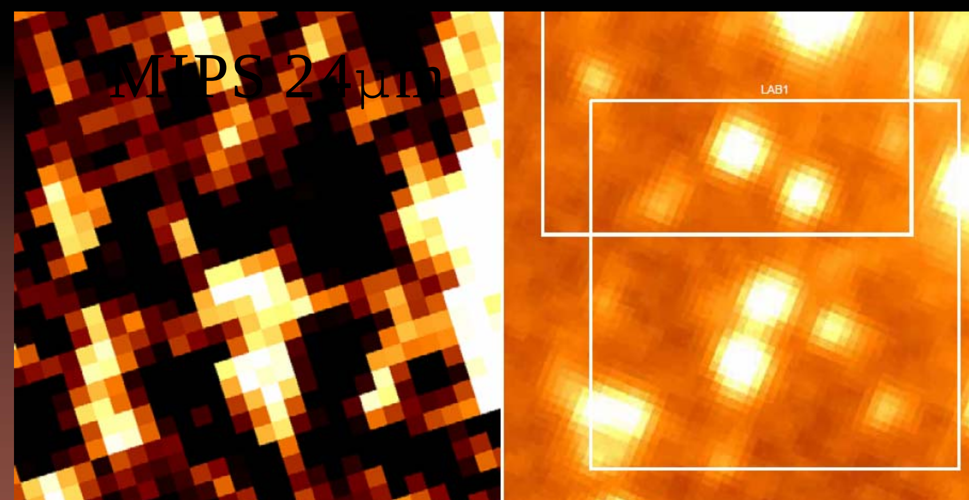

SSA22 LAB1

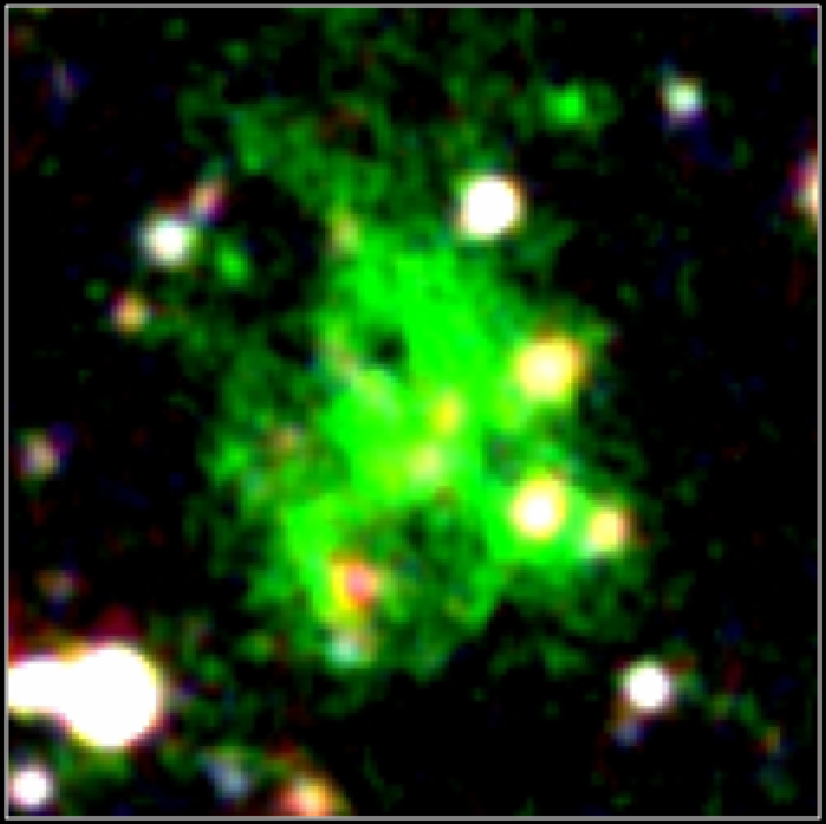

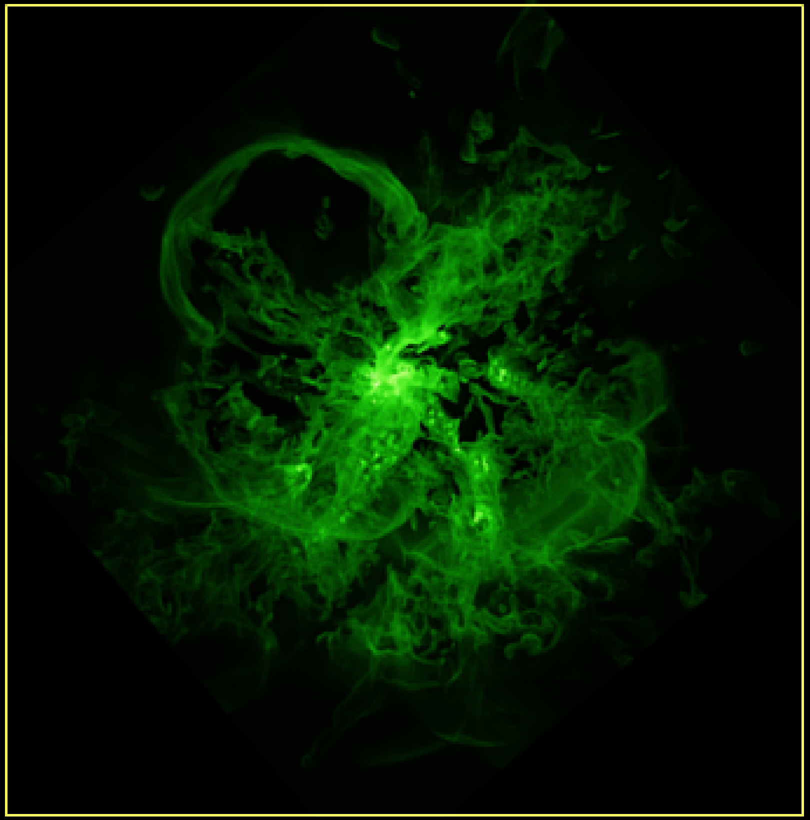

SSA22 LAB2 expanding shell?

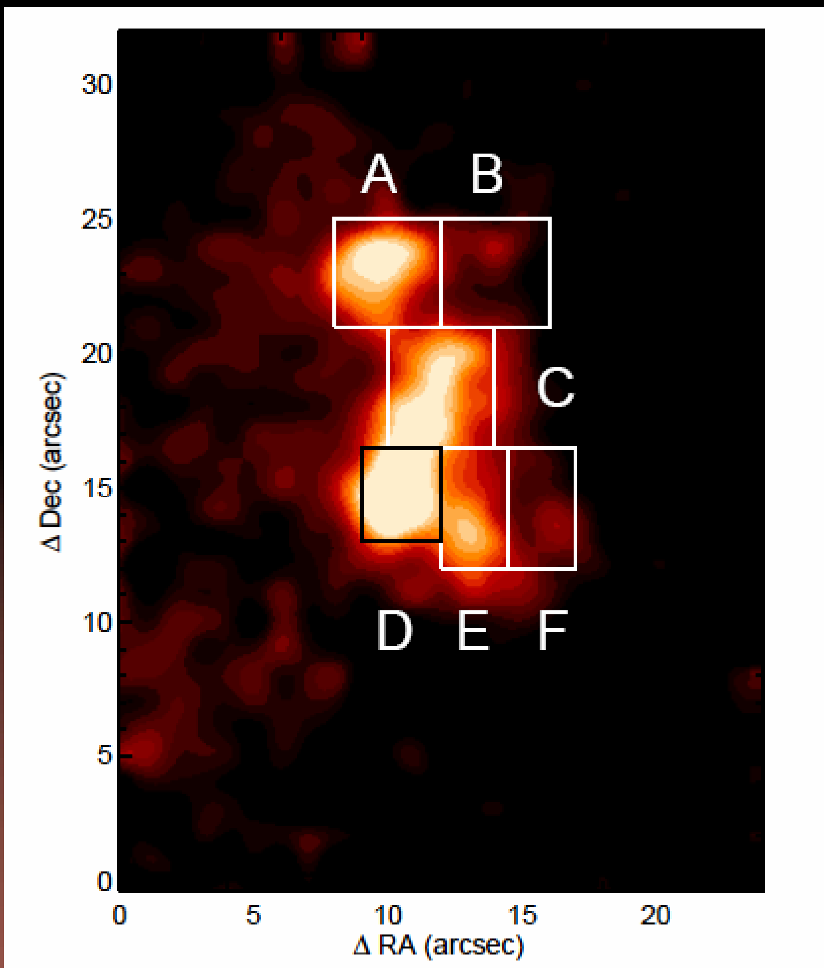

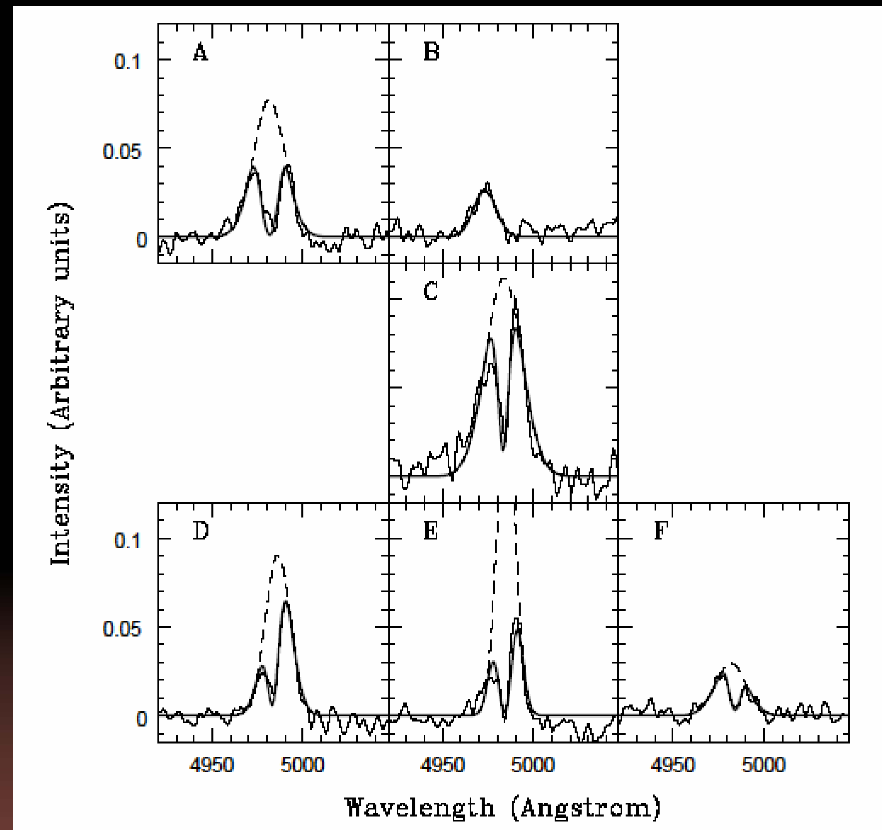

Δv~1000 km/s

Abs➔ HI expanding shell?

Dey et al.'s Blob z=2.656

Discovered in a course of identification of MIPS 24μm (860μJy) sources

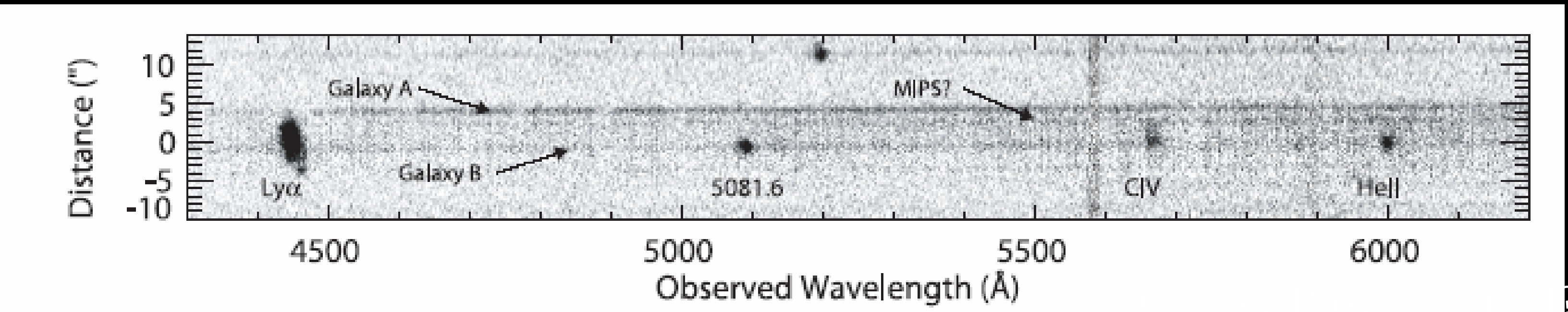

CIV,HeII
@z=2.66

Galaxy B overlapped?

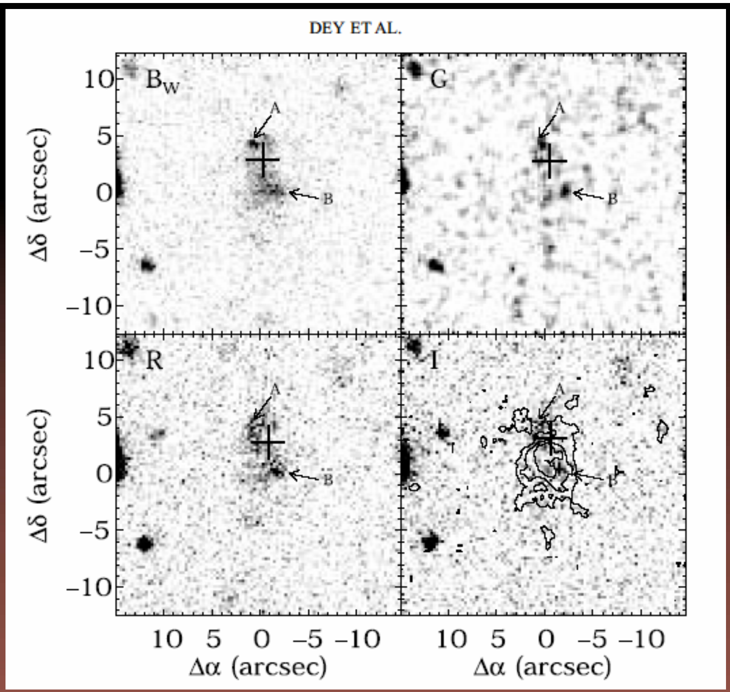

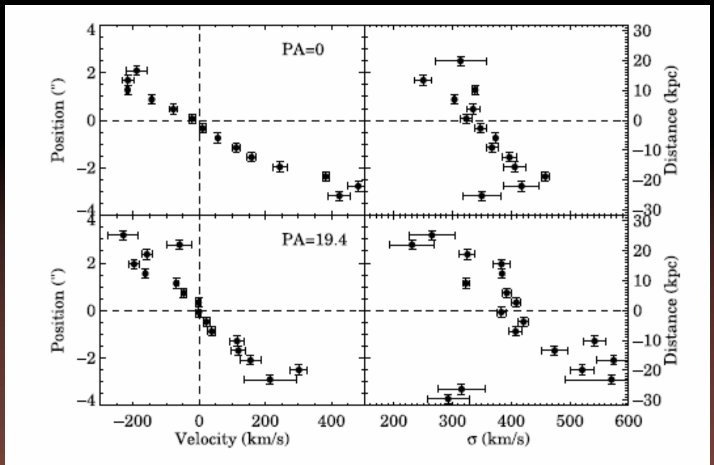

Very systematic gas motion
➔ M(<30kpc) ~6 x 10^{12} $\sin^{-2}i$ M_{sun}

emission (i.e., the same as in Fig. 1). The velocity origin is defined using the wavelength of the He II λ1640 emission line.

Nilsson et al.'s Blob z=3.16

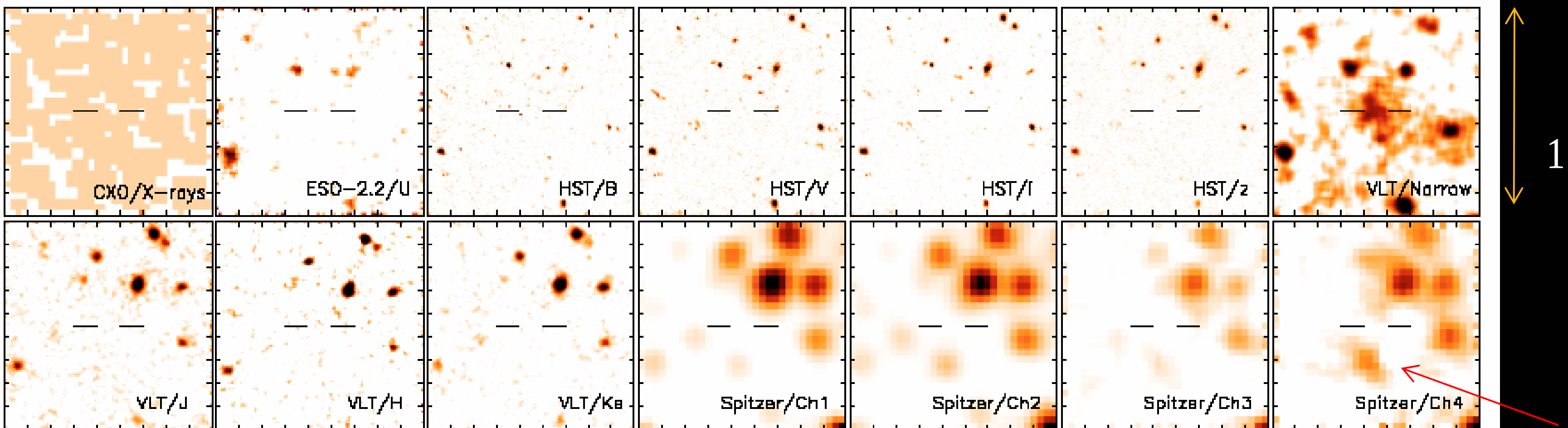

Fig. 2. Thumbnail images of all available multi-wavelength data in the GOODS South field, centred on the Lyα blob. All images are 18″ × 18″.

18”

Red Object?

Not detected
in any other wavelength
… cooling collapsing object?

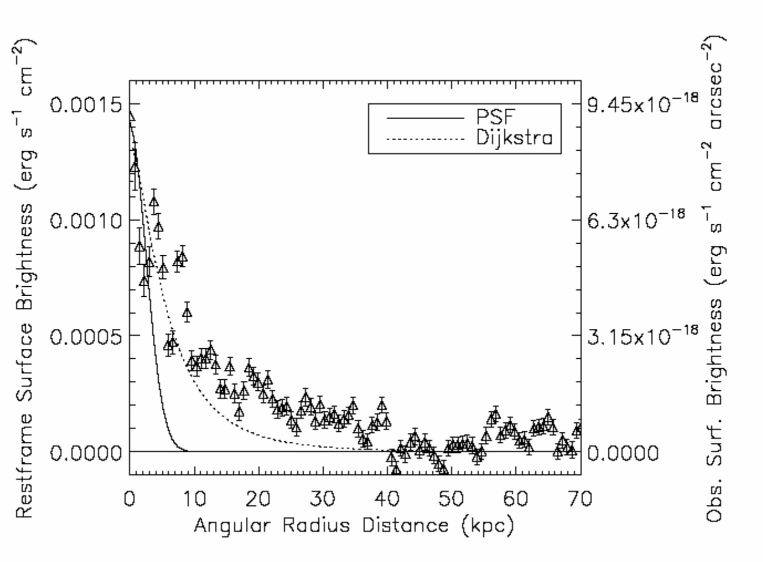

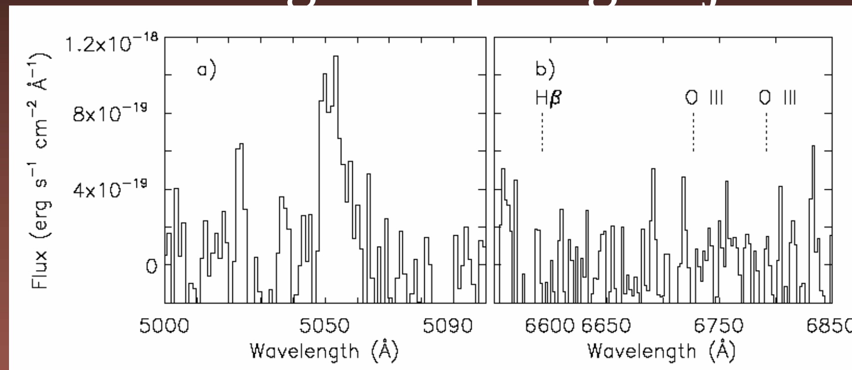

Smith et al.'s Blob z=2.83

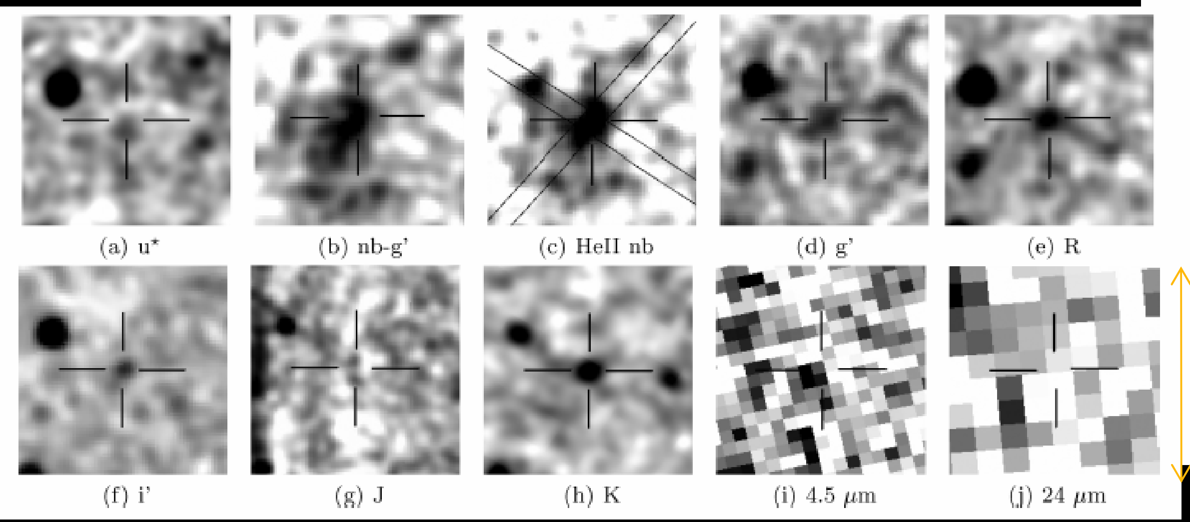

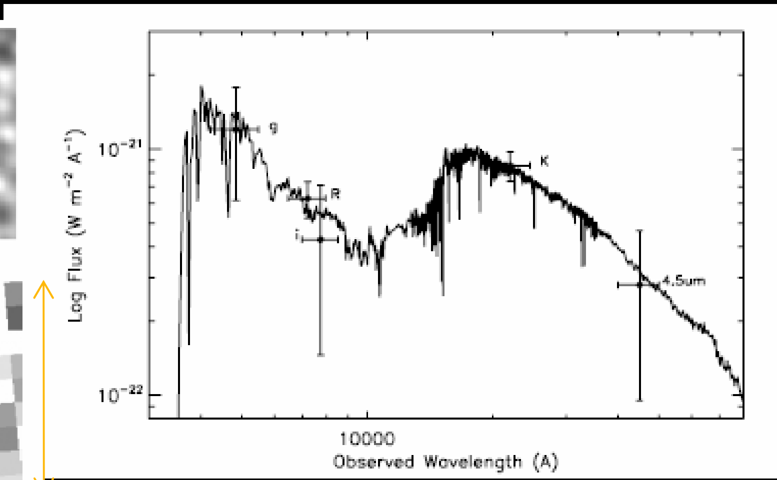

First confirmed LAB in ~15 deg^2
NB survey w/ INT

Cold gas accretion ?
(~Fardel+01, Dijkstra+06)
- SFR(UV,LyA[4”]) ~ 20 M/yr
- Red sharp cut off(?)

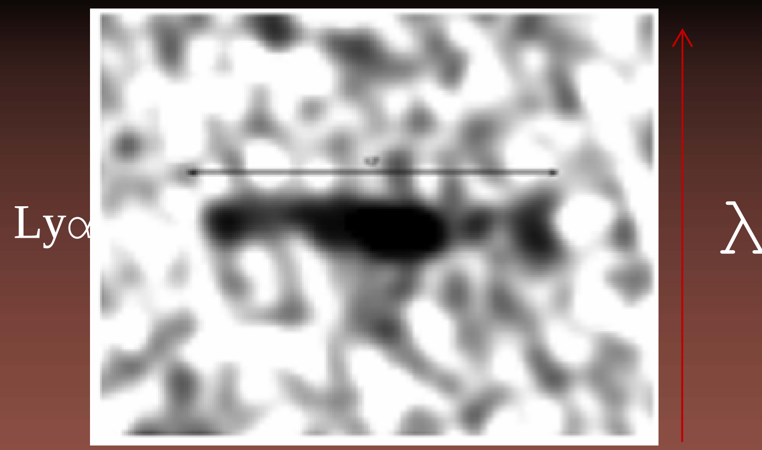

Palunas/Francis LAB z=2.38

PALUNAS ET AL.

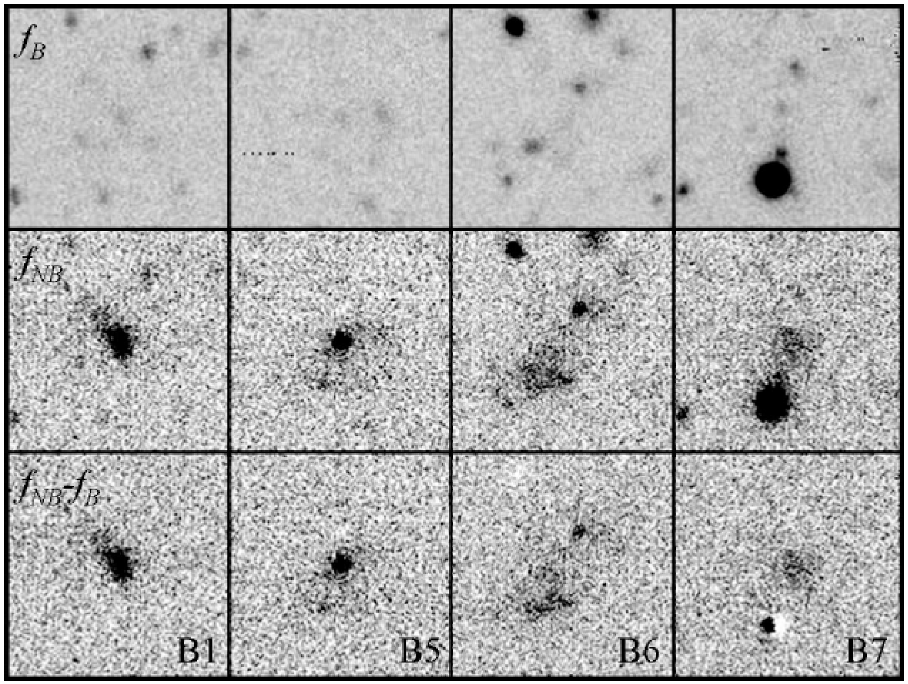

¾ detected by MIPS   Colbert+06

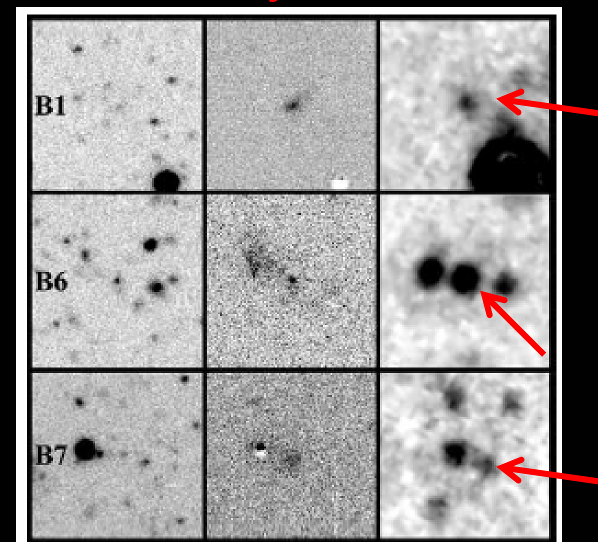

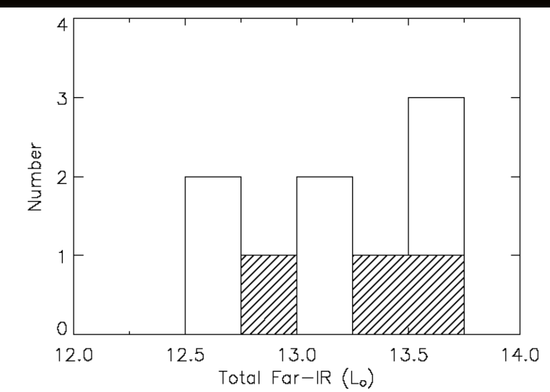

Fig. 2.— Histogram of inferred total far-infrared luminosity for MIPS sources associated with z=2.38 Lyα sources. The three sources potentially associated with the Lyα blobs B6 and B7 are marked with cross-hatching.

Smith et al.'s Blob z=2.85

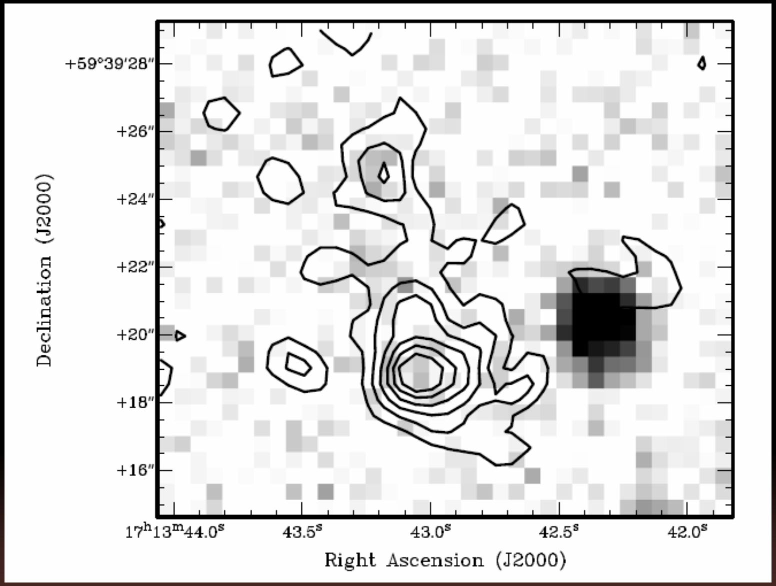

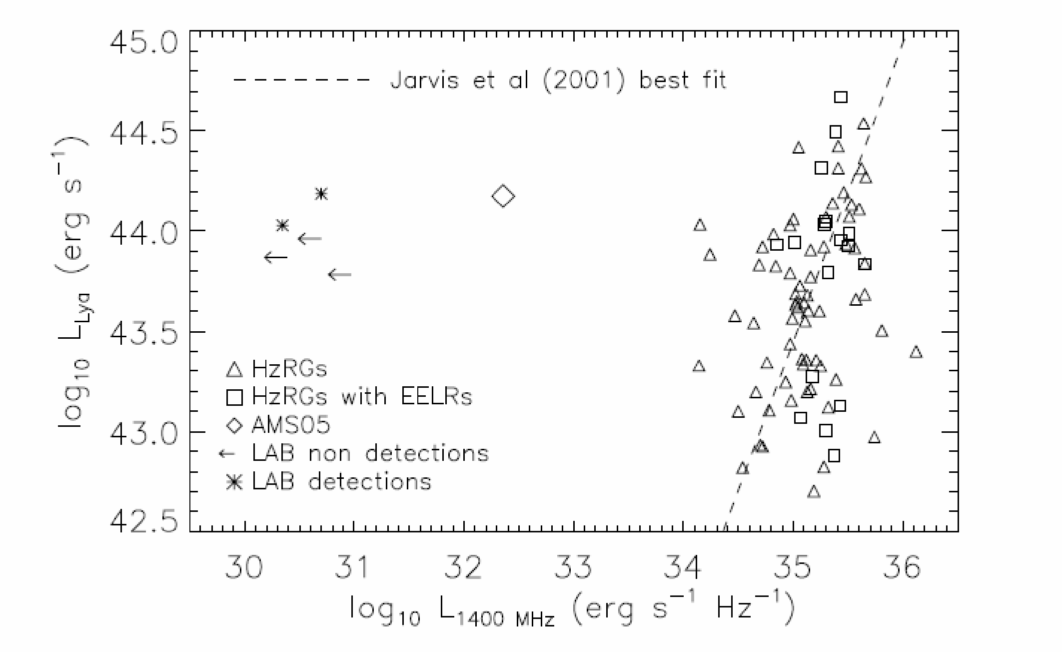

Smith et al. (2009)

Radio detected, but not radio laud

Type-2 QSO

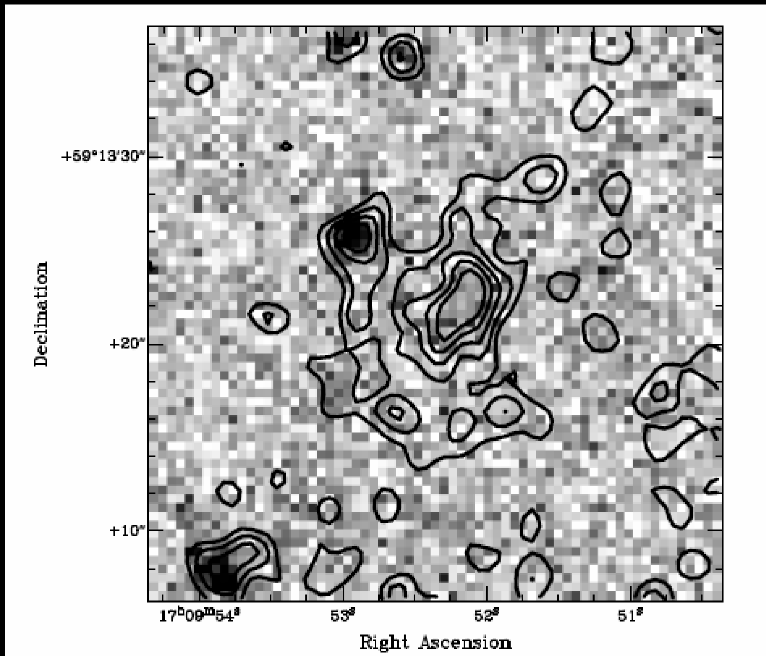
+59°13'30"
+20"
+10"
17h09m54s
53s
52s
51s
Right Ascension
Declination

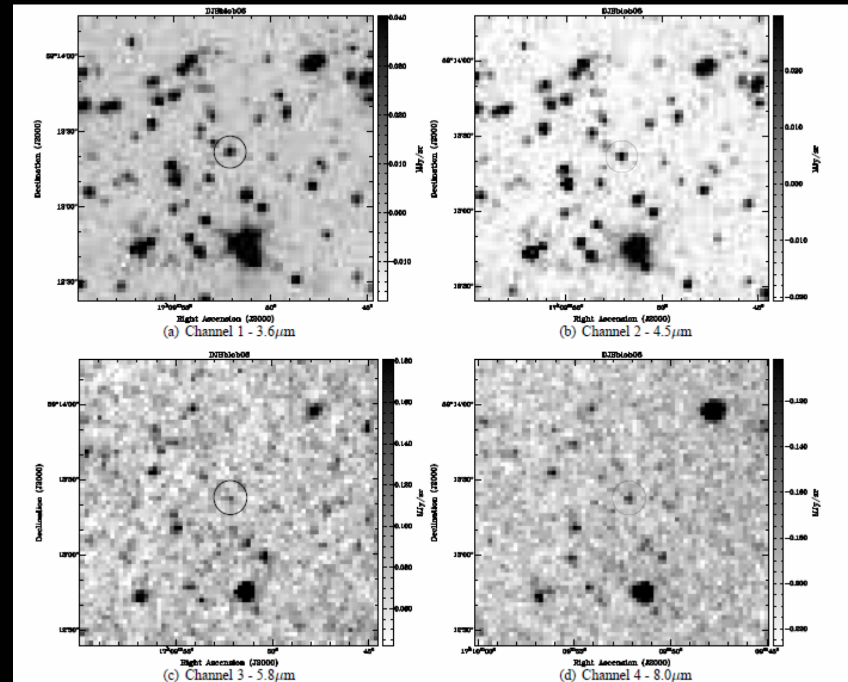
(a) Channel 1 - 3.6μm
(b) Channel 2 - 4.5μm
(c) Channel 3 - 5.8μm
(d) Channel 4 - 8.0μm

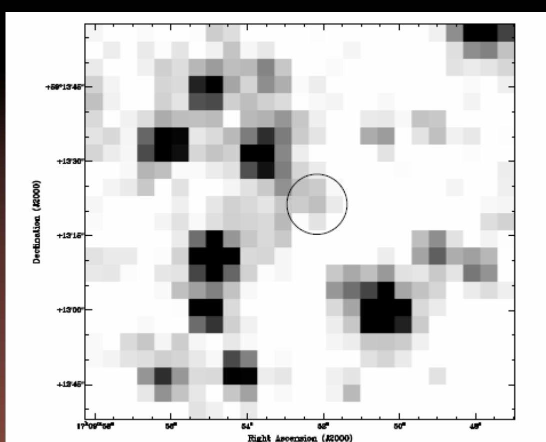

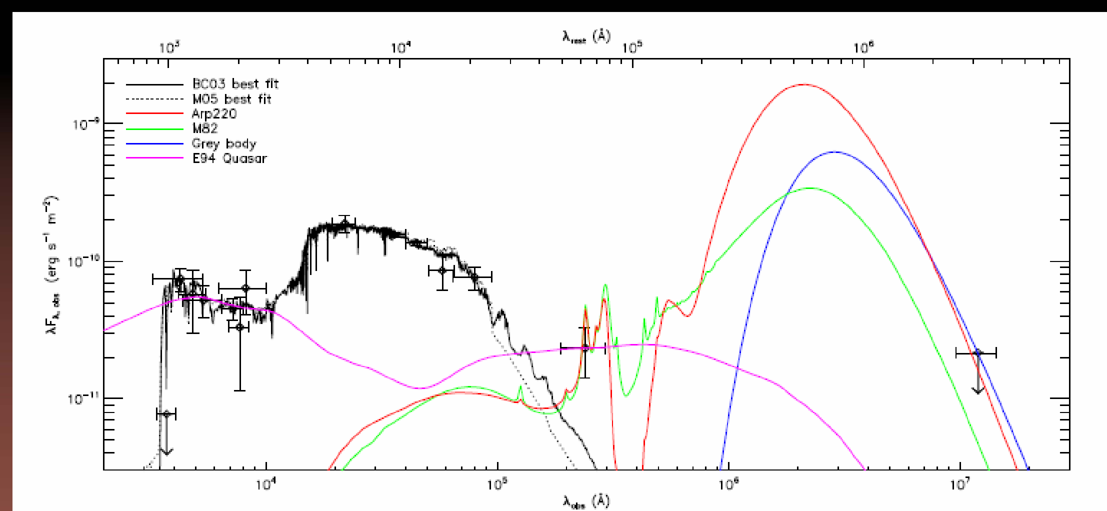
BC03 best fit
M05 best fit
Arp220
M82
Grey body
E94 Quasar